 USGS-OFR-85-540

Uranium-Trend Dating of Quaternary Deposits in the Nevada Test Site Area, Nevada and California

by

J. N. Rosholt, C. A. Bush, W. J. Carr, D. L. Hoover, W C Swadley, and J. R. Dooley, Jr.

U. S. Geological Survey
Lakewood, Colorado
Open-File Report 85-540
1985

Prepared in cooperation with the
Nevada Operations Office
U.S. Department of Energy
(Interagency Agreement DE-AI08-78ET44802)

CONTENTS

TABLES

ILLUSTRATIONS

ABSTRACT

The uranium-trend dating method has been used to estimate the ages of alluvium, colluvium, altered volcanic ash, and eolian deposits in the Nevada Test Site area. For dating of deposits of 5,000 to 800,000 years age, the open-system technique consists of determining a linear trend from analyses of four to ten channel samples collected at different depths in a depositional unit, or in the soil profile formed in a depositional unit. The concentrations of ^{238}U, ^{234}U, ^{230}Th, and ^{232}Th are accurately determined for each sample where analyses are made on subsamples of the less-than-2 mm-size fraction. Isotopic concentrations are determined by alpha spectrometry utilizing radioisotope dilution techniques. The analytical results are plotted as ratios of $(^{238}U-^{230}Th)/^{238}U$ versus $(^{234}U-^{238}U)/^{238}U$. Ideally these data points yield a linear array in which the slope of the line of best fit changes predictably for increasingly older deposits. The rate of change of slope is determined by the half-period of uranium flux, F(0). An empirical model compensates for differing values of F(0) in response to climate and other local and regional environmental factors.

Analyses of deposits of known ages are required to calibrate the empirical model; calibrations were provided by correlations with deposits dated by the radiocarbon and K-Ar methods. Deposits used for calibration are alluvium of mid-Holocene age (5 Ka) in Colorado, loess of Late Wisconsin age (12 Ka) in Minnesota, glacial till and loess of Bull Lake age (150 Ka) near West Yellowstone, Montana, till of Bull Lake age (150 Ka) near Pinedale, Wyoming, and zeolitized volcanic ash from Lake Tecopa, California (Tuff A, 600 Ka, and Tuff B, 740 Ka). Tuff A and Tuff B are the distal facies of the Lava Creek ash and the Bishop ash, respectively. At best, the uranium-trend ages have an estimated accuracy of about ±10 percent for depositional units between 60,000 and 600,000 years old; however, the uncertainty in the slope is strongly dependent on the quality of the linear trend regarding scatter of data points and the length of the line defined by the points.

Analyses of 36 sample suites are included in this report; U-trend dates were determined on 31 of these suites establishing the age ranges for deposition of four major stratigraphic units at the Nevada Test Site. Median ages for these deposits indicate ages of 40 ± 15 Ka for Q2a sediments, 170 ± 40 Ka for Q2b sediments, 270 ' 50 Ka for the younger Q2c stratigraphic unit and 440 ± 60 Ka for the older Q2c unit. Q2s stratigraphic units range in age from about 200 to 500 Ka. Uranium-trend ages of laminar carbonate deposits indicate the time of strong calcium carbonate development rather than the time of deposition of their older host sediments.

INTRODUCTION

Uranium-series disequilibrium dating methods described by Ku and others (1979) used conventional closed system $^{230}Th/^{234}U$ ratios for dating pedogenic carbonates which form rinds on alluvial gravel. These ages provide reasonable estimates of the minimum age of the alluvium. For conventional uranium-series dating (Ku, 1976), a closed system exists throughout the history of a deposit only if there has been no postdepositional migration of ^{238}U or of its daughter products (^{234}U and ^{230}Th). However, open-system conditions impose no restrictions on postdepositional migration of these radioisotopes within and between deposits. Results of other studies of uranium-series disequilibria indicate that uranium commonly exhibits an open-system behavior (Ivanovich and Harmon, 1982).

An open-system variation of uranium-series dating called uranium-trend has been tested extensively over the past decade. A preliminary model for uranium-trend dating was described by Rosholt (1980) with samples collected from a variety of Quaternary deposits including alluvium, eolian sediments, glacial deposits, and zeolitized volcanic ash. A revised model for uranium-trend systematics is described by Rosholt (1985). The empirical model requires time calibration based on analyses of known age deposits; results of these calibrations are included in Rosholt and others (1985). An abbreviated discussion of the mechanisms of uranium migration in surficial deposits is included in this report.

For uranium-trend dating, the distribution of associated uranium-series members in the geochemical environment during and after sedimentation must have been controlled by open-system behavior. Sediments and geochemical precipitates interact with materials carried in water that moves through these deposits. This water usually contains at least small amounts of uranium, and as this uranium decays, it produces a trail of radioactive daughter products that are readily adsorbed on solid matrix material. If the trail of the daughter products, ^{234}U and ^{230}Th, is distributed through the deposits in a predictable pattern, then a model for uranium-trend dating can be developed. The large number of geochemical variables in an open system precludes the definition of a rigorous mathematical model for uranium migration. Instead, an empirical model is used to define the parameters that can reasonably explain the patterns of isotopic distribution. This model requires independent time calibration with known-age deposits and careful evaluation of the stratigraphic relationships of the deposits to be dated.

In the geologic environment, uranium occurs chiefly in two different phases: (1) as a resistate or fixed phase (solids are dominant) where uranium is structurally incorporated in matrix minerals, (2) a mobile phase (water is dominant) which includes the uranium flux that migrates through a deposit. This mobile-phase uranium is responsible for an isotopic fractionation process in the ^{238}U-^{230}Th series (daughter emplacement) that enables the uranium-trend dating technique to work. Another fractionation process is the preferential leaching of ^{234}U from the fixed phase. Many of the deposits analyzed in this study are slightly moist and typically not wet or saturated. Nevertheless, uranium migration occurs, perhaps seasonally, either in solution or on colloids that slowly move through void spaces between mineral grains. In arid and semiarid environments, much of the mobile-phase uranium resides on the surface of dry mineral grains most of the time, and only a small amount of the time it is in solution or in suspension moving through a deposit. As a deposit undergoes interstratal alteration, some uranium isotopes are released from the fixed phase and enter the mobile phase; this process results in another form of isotope fractionation (^{234}U displacement).

Analyses of the isotopic abundances of ^{238}U, ^{234}U, ^{230}Th, and ^{232}Th in a single sample do not establish a meaningful time-related pattern of distribution in an open-system environment. However, analyses of several samples, each of which has slightly different physical properties and slightly different chemical compositions, may provide a useful pattern in the distribution of these isotopes. Analyses of 6 to 8 samples per unit, from a relatively large number of alluvial, colluvial, glacial, and eolian deposits has shown that time-related patterns exist.

The purpose of this investigation is to determine the reliability of an empirical radiometric dating technique (uranium-trend), extending from a few thousand to more than one-half million years, to aid in the geologic study of surficial deposits. This uranium-trend dating method has been applied to the Nevada Test Site region where a major effort is underway to define and date late Cenozoic stratigraphic deposits under the U.S. Department of Energy Nevada Nuclear Waste Storage Investigations project. Numerous trenches excavated in the surficial deposits of the area have provided excellent sites for sampling the deposits (Swadley and Hoover, 1983; Swadley and others, 1984). Stratigraphic units defined by Hoover and others, (1981) were collected for this investigation.

EMPIRICAL MODEL

The very long-lived ^{238}U isotope (half life of 4.5×10^9 years) upon radioactive decay, produced long-lived daughter products, ^{234}U and ^{230}Th. Because the half-life of ^{234}U is 248 Ka, this isotope has a potential as a geochemical tracer in deposits that are as old as 800 Ka. The half-life of ^{230}Th is 75 Ka; because of its daughter-parent relation to ^{234}U, it is a key isotope used in nearly all uranium-series dating models (Ku, 1976). The system equilibrium of the parent material is disturbed during transport, and the attainment of a new, readjusted, system equilibrium starts in the sediment at the time of deposition. Thus, for surficial deposits, the starting point for the uranium-trend clock is the initiation of movement of water through the sediment rather than initiation of soil development, although both of these processes may start at essentially the same time.

The empirical model incorporates a component called uranium flux, F(0). The physical significance of F(0) is not well understood; it is related to the effective concentration of uranium moving through a deposit, which in turn is a function of climate, texture of sediment, and the amount of uranium in the mobile phase. In the model, the effect of this flux on isotopic variations decreases exponentially with time. The following is an oversimplified example of the uranium flux in alluvium. At the time of deposition, large volumes of water pass through the alluvium. However, once the surface becomes geomorphically stable, the sediment compacts and soils subsequently develops; during these phases, the volume of water that passes through the alluvium is significantly less. Both the quantity of water passing through and affecting a deposit, and the concentration of uranium in this water are components of the flux; its magnitude is a function of the concentration of uranium in the mobile phase relative to the concentration of uranium in the fixed phase.

Because of the large number of variables in a system that is completely open with respect to migration of uranium, a rigorous mathematical model based on simple equations for radioactive growth and decay of daughter products cannot be constructed. Instead, an empirical model is based on results obtained from several alluvial, colluvial, glacial, and eolian deposits of different ages. The model requires calibration of both the uranium-trend slope and the uranium-flux factor, F(0), based on analytical results from deposits of known age.

The isotopic composition of several samples from the same deposit, expressed in activity units, is required for solution of the model. The uranium-trend value from which ages are calculated is the slope of the line representing

$$\frac{\Delta(^{234}U - {}^{238}U)}{\Delta(^{234}U - {}^{230}Th)}$$

To accommodate measured isotopic data, the variations are normalized to ^{238}U and the uranium-trend model can be written in the following form,

$$\frac{Y}{X} = \frac{\Delta(^{234}U - {}^{238}U)/{}^{238}U}{\Delta(^{234}U - {}^{230}Th)/{}^{238}U} = \frac{C_1 e^{-\lambda_o t} + C_2 e^{-\lambda_2 t}}{C_3 e^{-\lambda_o t} + C_4 e^{-\lambda_2 t} + C_5 e^{-\lambda_3 t}}$$

$$C_1 = \frac{-\lambda_o\lambda_2}{\lambda_2-\lambda_o}; \qquad C_2 = \frac{\lambda_2\lambda_2}{\lambda_2-\lambda_o}; \qquad C_3 = \frac{3\lambda_o\lambda_2\lambda_3}{(\lambda_2-\lambda_o)(\lambda_3-\lambda_o)};$$

$$C_4 = \frac{3\lambda_2\lambda_2\lambda_3}{(\lambda_o-\lambda_2)(\lambda_3-\lambda_2)} + 2\lambda_2; \qquad C_5 = \frac{3\lambda_2\lambda_3\lambda_3}{(\lambda_o-\lambda_3)(\lambda_2-\lambda_3)} - \lambda_3$$

where (1) λ_o is the decay constant of F(0)=ln 2/[half period of F(0)], (2) λ_2 is the decay constant of ^{234}U, and (3) λ_3 is the decay constant of ^{230}Th. These are equations that define the empirical model and the numerical constants in the coefficients preceding the exponential terms were determined by computer to provide a model with the best fits for deposits of known age. The alternative uranium-trend slope represented by the equation

$$\frac{Y}{X - Y} = \frac{\Delta(^{234}U - {}^{238}U)/{}^{238}U}{\Delta(^{238}U - {}^{230}Th)/{}^{238}U}$$

is used to solve for the age. An example of this uranium-trend plot is shown in Figure 1 where a York fit (Ludwig, 1979) is used to obtain the least squares regression line.

An additional parameter in the uranium-trend plot is the intercept of the slope line on the X-axis, x_i, represented by the equations

$$y = mx + b$$

$$x_i = -b/m$$

where m is the measured slope of the line, b is the intercept on the Y-axis, and x_i is the interecept on the X-axis. The value of x_i is used to obtain time calibration for the uranium-trend model.

A different type of plot is used to determine if all the samples included in the uranium-trend slope describe a reasonable linear array on a thorium plot. This plot serves as a useful criterion to determine if all of the samples are likely to be from the same depositional unit and if any samples contain a significant amount of foreign material.

The thorium plot of the isotopic data can be constructed when the $^{238}U/^{232}Th$ ratios of the samples are plotted on the X-axis versus the $^{230}Th/^{232}Th$ ratios plotted on the Y-axis as shown in Figure 2.

The half period of F(O) and its decay constant, λ_o, are strictly empirical values that allow selection of the proper exponential coefficient in the equation for the uranium-trend model. For deposits of unknown age, a method is required to determine the proper value of λ_o to be used in the equation; this value is determined from a calibration curve based on λ_o values obtained for units of known age. For this calibration, the values of x_i are plotted against the half periods of F(O) as shown on the log-log graph in Figure 3. The calibration curve is defined by the proper λ_o values that yield the known ages for calibration units using the model equation. The x_i values for deposits of known-age are used for calibration. These values are plotted against the half periods of F(O) equivalent to their λ_o values. The solution of the empirical equation, using any given half period of F(O) yields a fan-like array of uranium-trend slopes representing various ages. These slopes rotate counterclockwise from the first to second quadrant of the uranium-trend plots. For deposits whose analyses are included in this paper, the F(O) value is determined from the calibration graph (Fig. 3) using the x_i value measured on the uranium-trend plot of the data for each depositional unit.

Four primary points based on different radiometric dating techniques were used for time calibrations: (1) a radiocarbon age of 12 Ka (Frye, 1973) was used for loess of Late Wisconsin age in Minnesota, (2) an obsidian hydration age of 150 Ka (Pierce, 1979) was used for deposits of Bull Lake age near West Yellowstone, Montana, and in northwestern Wyoming, (3) a K-Ar age of 0.6 Ma was used for calibration of the Lava Creek ash bed, which correlates with the zeolitized ash in Tuff A, Lake Tecopa, California (Izett and others, 1970), and (4) a K-Ar age of 0.73 Ma was used for Bishop ash bed (Dalrymple and others, 1965) which correlates with Tuff B at Lake Tecopa.

GEOLOGIC SETTING

The Nevada Test Site is in the southern part of the Great Basin, an area characterized by north-trending linear mountain ranges that are flanked by extensive alluvial fans and separated by broad alluvial basins. The geographic area including the location of sampling sites for uranium-trend dating is shown in Figure 4. The climate is arid and vegetation is limited to sparse desert plants. Quaternary surficial deposits in the NTS region primarily include alluvial deposits of coarse material, fluvial deposits of sand derived from eolian material, eolian sheets and dunes, and debris flows. Surficial units present in the region are summarized by Swadley and others (1984, Fig. 3).

Late Cenozoic Stratigraphy

The late Tertiary and Quaternary deposits of the study area consist of alluvium, eolian sands, colluvium, lake sediments, and volcanic deposits. These range in age from greater than 3 m.y. old for some of the lake sediments to less than about 150 years old for the youngest alluvial unit (Hoover and others, 1981). Hoover and others (1981) described the stratigraphy of these deposits and defined characteristics by which they can be mapped and correlated across the region on the basis of age, lithology, and depositional environment. The following brief descriptions of the map units are based mainly on their work. The deposits are grouped herein into four major units: (1) late Pliocene and Pleistocene, (2) Pliocene(?) and early Pleistocene, (3) middle and late Pleistocene, and (4) Holocene.

Late Pliocene and Pleistocene Deposits

The oldest surficial deposits investigated are predominantly of late Pliocene age and consist of lacustrine sediments. These lacustrine deposits are mainly unconsolidated to moderately indurated marl and silt that locally contain beds of limestone, sand, and fine-grained volcanic ash. They were deposited in Lake Amargosa, which occupied much of what is now the Amargosa Desert valley (Fig. 4) during the late Pliocene; remnants of the lake probably persisted into the early Quaternary.

The age of the lacustrine deposits is not precisely known; however, an ash bed near the middle of the unit yielded radiometric ages of about 3 Ma (fission-track method; C. W. Naeser, U. S. Geological Survey, written commun., 1980) and 3.8 Ma (K-Ar method on biotite; R. L. Hay, University of California, Berkeley, written commun., 1979). A second ash bed near the top of the unit was dated at 2.1 ± 0.4 Ma by the fission-track method (C. W. Naeser, written commun., 1982). A slightly younger age is suggested for the upper part of the deposits by mammoth remains that are considered to be less than 2 Ma (C. A. Repenning, U. S. Geological Survey, written commun., 1982); these deposits are beyond the range of uranium-trend dating.

Pliocene(?) and Early Pleistocene Deposits

These deposits consist of alluvium that mainly is early Pleistocene but in some areas may be as old as latest Pliocene. Unit QTa, generally older than about 0.74 Ma, is largely coarse debris flows, but talus, colluvium (QTc) and pediment gravel (QTg) are present in some areas. The QTa deposits are commonly eroded and dissected, and normally exhibit strong calcic soils, which locally result in low permeability.

The approximate age of unit QTa is limited by the ages of enclosing units; there are no dated materials within the unit. QTa unconformably overlies lacustrine deposits at several localities in the area (Swadley, 1983), indicating the QTa deposits locally are less than 2 Ma. Unit QTa is overlain by unit Q2e, that locally contains lenses of volcanic ash correlated with the Bishop ash by Izett (1982) on the basis of their similar chemistry. Radiometric dates for samples from the Bishop ash indicate that it is 0.74 Ma old (Izett, 1982). The lower part of unit Q2e is considered approximately 0.74 Ma old on the basis of the correlation with the Bishop ash. A period of erosion and weathering occurred following the deposition of QTa but prior to deposition of Q2e (Hoover and others, 1981), suggesting that QTa deposits may be substantially older than the 0.74 Ma old limit implied by its stratigraphic position below Q2e deposits containing the Bishop ash. Basalt ash deposits in fractures within unit QTa exposed in two fault trenches in eastern Crater Flat are inferred to be approximately 1.2 Ma (Swadley and others, 1984), possibly restricting further the upper limit for the age of unit QTa. One QTa deposit was sampled, analyzed, and found to be beyond the range of the U-trend method.

Middle and Late Pleistocene Deposits

Middle and late Pleistocene deposits (unit Q2) consist of fan alluvium, fluvial and eolian sands, and volcanic ash. These deposits have been subdivided into five mappable units on the basis of relative age and lithology: three alluvial units, Q2c, Q2b, and Q2a (in order of decreasing age); eolian dunes and sand sheets, Q2e, and fluvial sand sheets, Q2s. The lithologies, stratigraphic relations, and soil development of these units are described in more detail by Hoover and others (1981, p. 15).

Unit Q2c consists of fluvial fan deposits and some debris flows. These deposits typically are unconsolidated, poorly to well-sorted, nonbedded to well-bedded, angular to rounded gravel with sand and silt in the matrix. Interbeds of silty sand are locally common. Alluvial fans of Q2c generally are deposited on unit QTa on the middle and upper valley slopes; Q2c also occurs as terrace deposits in larger stream valleys. Eight age determinations were made on fluvial deposits of unit Q2c.

Eolian deposits of unit Q2e occur as dunes and sand sheets in and adjacent to the Amargosa Desert valley. Ramps of fine, well-sorted sand as much as 50 m thick flank many of the hills bordering the Amargosa Desert on the north. Unit Q2e is locally interbedded with the lower part of Q2c and is clearly older than Q2b. One Q2e deposit analyzed for this study was beyond the range of the U-trend method.

The inferred age of 0.74 Ma old for lenses of volcanic ash in the lower part of unit Q2e discussed above is considered the approximate lower age limit for both units Q2e and Q2c. Younger Q2c gravels locally overlie and contain reworked cinders from the Big Dune basalt center 11 km northwest of Lathrop Wells (Fig. 4), which has yielded K-Ar dates ranging from 230,000 to 300,000 years old (Vaniman and others, 1982), indicating the approximate age for the younger part of Q2c deposition.

Fluvial sand sheets of unit Q2s occur along major streams and drainages downstream from dunes. The sheets consist of water-laid fine to medium gravelly sand or stream-reworked windblown sand, and commonly rest on Q2c fans. Three Q2s deposits were dated in this study.

Unit Q2b is similar to Q2c in depositional environment and lithology. It occurs as terrace deposits that are inset in Q2c and underlies lower slope fans. These Q2b fans commonly merge upslope with Q2c fan deposits. Six suites of samples from unit Q2b were dated in this study.

The youngest fluvial part of Q2, unit Q2a, consists of debris flow deposits that are large enough to be mapped at only three localities in this study area. Q2a is poorly sorted, unconsolidated sand- to clay-size material that contains some gravel. Nine age determinations were made on the fluvial part of unit Q2a.

Overlying unit Q2a (and older units) is a thin unit of eolian silt which probably is desert loess. This unit is not present in Holocene deposits (unit Q1) in the study area, indicating a probable age of pre Holocene, but post Q2a (late Pleistocene). Two sample suites were collected and analyzed in this material; only one U-trend age estimate was obtained from these suites.

Holocene Deposits

Unit Q1, Holocene in age, is principally coarse fluvial material and local debris flows in and along present drainages. It has little or no soil development and, mainly on the basis of topography, may be divided locally into as many as three units (Q1a, b, and c). In addition, Q1 contains local eolian deposits (Q1e) and sand sheets (Q1s). No U-trend ages were attempted on Q1 deposits because of the large percentage error limitations inherent in the method for deposits as young as Holocene.

EXPERIMENTAL PROCEDURES

Sample Collection, Preparation, and Chemical Procedures

To obtain a uranium-trend date, several channel samples, about 1 kg each, are collected from a vertical section of each depositional unit. The required number of samples for a reliable trend plot depends on the variation in ratios of uranium and thorium that define the trend line. The minimum number of samples needed is not known until analyses are completed; therefore, subdividing the unit into a larger number of samples usually will increase the likelihood of better defining the uranium-trend line. A minimum of three samples is required, but it is desirable to have 5 to 8 samples in a given sampling unit to determine a reliable slope. It is not always possible to determine, in the field, the exact boundary between depositional units. To help alleviate this problem, collection of a larger number of samples is required to determine the boundary between some depositional units. For soils, sampling by horizon or subhorizon usually is appropriate. Differences in mineralogy and particle size of the sediment also are good field criteria for selecting samples that are likely to have a suitable spread of values to provide a well-defined linear trend. It is preferable to sample a channel through deposits exposed in a trench wall or a relatively fresh, well-exposed, outcrop. Examples of sampled sections are shown in the sketch of collection sites in Yucca Mountain Trench 14 (Fig. 5).

Depositional units at the Nevada Test Site commonly contain pebbles and larger fragments and a subsample of less-than-2 mm size is retained for analysis, pulverized to less-than-0.2 mm size, homogenized, and processed. In deposits where the isotopic composition is similar in each sample, additional data can be obtained by analyzing that part of the unpulverized subsample that is less-than-0.3 mm size. Both <2 mm and <0.3 mm size fractions were analyzed for samples from six localities at the NTS (TSV396, SCF1, SCF2, CF2, YM2 and YM13).

Chemical procedures used for separating uranium and thorium for alpha spectrometry measurements are those described by Rosholt (1985). Spikes of ^{236}U and ^{229}Th are used in the radioisotope-dilution technique to determine the concentrations of uranium and thorium. For defining uranium-trend slopes, a uranium separate is counted four different times in the alpha spectrometer and a thorium separate is counted three different times. The procedure of determining the isotopic abundances of ^{230}Th, ^{234}U, and ^{238}U is described by Rosholt (1984).

DISCUSSION OF RESULTS

Uranium-trend analyses for 28 sample sections at or near the Nevada Test Site, some of which include deposits of more than one age, are included in this report. Site locations are shown on Figure 4, and descriptions of the 37 depositional units analyzed are listed in Table 1. Table 2 contains a generalized description of each sampled unit, including selected soil data and lithologic characteristics, depths below the surface, and uranium and thorium content for each sample. Uranium and thorium concentrations are accurate to within ±2 percent of the reported value. Five sample sequences (SFF, Q2E, SCF1, SCF2, and SCF3) were not datable using the uranium-trend model. Two of the undatable units are eolian sand and the remaining three are fluvial sand. The isotopic ratios required for the plots are listed in Table 3. Also included with the isotopic ratios are error values (2 standard deviation) required for computer calculation of the slope and uncertainty of the slope of the linear regression line. An additional significant figure for these data (Table 3) is retained for the slope calculation to avoid premature arithmetic rounding. Uranium-trend and thorium plots for each deposit listed in Table 2 are shown in Figures 6-34.

Some data were not included in the calculations of uranium-trend age. A few of the units sampled and analyzed at the beginning of this investigation included near-surface materials at depths of less than 8 cm. Data for these near-surface samples have been excluded from the calculation of the linear regression line because of the likelihood of contamination by dust and other foreign material that is significantly younger than the main deposit. In some other cases, samples were excluded from the uranium-trend line if, on the thorium plot, they did not fit the linear array defined by the other samples from the deposit. One reason that a sample may depart from linearity is that it is composed in part or entirely of material from an older or younger deposit. This problem usually is encountered only with the upper or lower sampled part of a deposit. Another reason for the above discrepancies is that the porosity and permeability characteristics of layers within the depositional unit may be sufficiently different so that very different effective uranium fluxes may have occurred in the same deposit. For instance, the effective flux rate is different for an open-work gravel in which the mobile-phase uranium has a short residence time compared to that for a clayey layer through which fluids move more slowly. Assimilation of uranium in a deposit during a late stage of alteration can cause anomalous variations in the isotopic system, such as the incorporation of uraniferous opal. Examples of samples excluded from uranium-trend slope calculations include: Those from the upper horizons in FFPG, S1, RV1-J, S9, CF1, YM13, and YM14; those with anomalous uranium content in TSV-307E and YM14B-2; and sample SCF4-5 that contains a mixture of two different depositional facies in the section. On the basis of the fit of data on the thorium plot, it appears possible to identify samples in the profile that do not belong to the same stratigraphic unit or that have mineralogic or grain-sized components that are not comparable to the whole of the unit.

The uranium-trend model parameters for 33 dated units from NTS are shown in Table 4. These parameters include the values for X-intercept, half period of F(0), uranium-trend slope, and age for each unit. The uncertainty for each age determination listed is one standard deviation, and includes scatter as defined by Ludwig (1979). A unit number for each dated deposit is included in Table 4 and shown on the calibration curve (Fig. 3).

Specific results for each geographic area (Table 1) generally are described below in order of increasing age (Q2a, Q2b, Q2c, QTa). The five samples in unit SFF, collected from a silty, vesicular A horizon in a trench on the edge of Frenchman Flat tend to form a circular array rather than a linear relationship on the U-trend plot (Fig. 6); no U-trend age could be calculated for these samples. A similar eolian sediment with underlying CCa horizon was recollected; 10 samples in section FFPG gave a U-trend age of 30 Ka with large error of ± 30 Ka. The top sample (FFPG-1) was not included in the U-trend slope (Fig. 7) because of possible infiltration of material from the surface. The uppermost sample of 6 samples of the underlying alluvium in the Q2b deposit (S1) also was not included in the U-trend line because of probable infiltration of material from the overlying deposits. Unit S1 yielded a trend line with limited range (Fig. 8) and gives an age of 80 ± 60 Ka. However, an extensive resampling of the alluvium in the trench at Frenchman Flat (represented by units F2 and F3) gave more defined U-trend ages (Figs. 9 and 10) of 200 ± 80 Ka and 190 ± 70 Ka for the upper and lower parts of unit Q2b, respectively.

Units with three different U-trend ages were identified in Rock Valley trench RV1 (Ander and others, 1984, Fig. 8). The upper Q2a units of slope wash (RV1 A-D, Fig. 11) and a buried B horizon (RV1 J-O, Fig. 12) give ages in the 20-50 Ka range. The underlying Q2b unit, represented by the calcareous B horizon (RV1 P-U, Fig. 13), has a U-trend age of 180 ± 40 Ka. The lowest parts of the two RV1 sections consist of the Q2c unit; these deposits gave similar ages of 310 ± 40 Ka (RV1 E-I, Fig. 11) and 270 ± 30 Ka (RV1 V-Z, Fig. 13).

The upper Q2a units sampled in Rock Valley trench RV2 gave U-trend ages of 38 ± 10 Ka (TSV-307, Fig. 14) and 36 ± 20 Ka (RV2-U, Fig. 15); these units are equivalent to the upper units in the nearby Rock Valley trench RV1. The lower gravel alluvium of the Q2c unit in the RV2 section, which was sampled at a greater depth than the RV1 sections, yields an age of 390 ± 100 Ka (RV2-L, Fig. 15).

Initially, only four samples were collected for dating a reddish-brown soil in a sand sheet exposed in a trench near the Jackass Flats Engine Test Stand (ETS, Fig. 4); these samples were insufficient to determine a U-trend age (Fig. 16). Nine samples from a channel through a thicker part of the argillic B horizon in the Q2s sheet sand was resampled; a U-trend slope (Fig. 17) gives an age of 160 Ka with a relatively large error of 90 Ka. This poor U-trend value should be closer to the upper limit of about 250 Ka.

Eight samples of alluvium (S9) were collected from a 1.6 m-thick unit in the upper part of the Jackass Divide trench (JD, Fig. 4). The uranium and thorium isotopic ratios of the upper two samples resemble that of samples from deposits of unit Q2a in other trenches, therefore the values for these two samples were excluded from the U-trend slope of the underlying Q2c unit. The lower six samples yielded an age of 270 ± 50 Ka (Fig. 18); the upper two samples also have a wide divergence from the regression line on the thorium plot of the lower 6 samples. A 1.2 m-thick unit of older alluvium was collected from the lower part of Jackass Divide trench. The 8 samples in this unit provide well defined U-trend and thorium plots (Fig. 19) that indicate an age of 430 ± 40 Ka. This age corresponds to those determined for older deposits of unit Q2c.

A series of 8 samples (SCF1) of pebbly fluvial gravel in unit Q2b was collected in the west trench in South Crater Flat. Both the less-than-2-mm and less-than-0.3 mm size fractions were analyzed in each sample; however, no U-trend age could be calculated from either set of plots (Fig. 20). Another series of 5 samples (SCF3) was recollected from the trench, but a U-trend age could not be calculated for the less-than-2 mm size fraction (Fig. 21). A 0.8 m-thick sequence of 9 samples in fluvial sand and pebble gravel (SCF2) was collected in unit Q2c exposed in the west trench at South Crater Flat. These samples did not provide a U-trend age because of the excessive scatter of the points for both the less-than-2 mm and the less-than-0.3 mm size fractions in all samples (Fig. 22). Eight samples from a 1.2 m-thick section (SCF4) of unit Q2c was recollected from the trench. The upper 4 samples of sandy sediment defined a different trend line than the lower 3 samples of pebbly alluvium; the intermediate sample (SCF4-5) appears to be a mixture of both units (Fig. 23). Uranium-trend ages for the upper and lower parts are 400 and 480 Ka, respectively. These values provide an estimated average age of 440 ± 60 Ka for this Q2c deposit.

A group of 6 samples consisting mainly of calcium carbonate (TSV 396) was collected from trench 1 in Crater Flat. Both the less-than-2-mm and less-than-0.3 mm were analyzed for each subsample. Each size fraction yielded similar ages with an average age of 48 ± 20 Ka as obtained from the U-trend plots shown in Figure 24. These results suggest significant calcium carbonate accumulation and K-horizon development over the past 50 Ka; U-trend ages in this kind of enriched carbonate material reflect the time of strong calcium carbonate development in older sediments.

Eight samples (CF1) of the upper alluvium (Q2a) were collected from trench 3 in Crater Flat. On the thorium plot (Fig. 25), sample CF1-2 diverges from the regression line defined by the remaining samples, therefore it was excluded from the U-trend slope that gives an estimated age of 40 ± 10 Ka. A 25 cm thick buried argillic B horizon in unit Q2b also was collected in this trench (CF6) which yielded a U-trend plot of 5 samples (Fig. 26) with an approximate age of 190 ± 50 Ka. Seven samples (CF2) of alluvium in unit Q2c underlying the argillic B horizon were collected from the trench; both less-than-2 mm and less-than-0.3 mm size fractions gave similar U-trend plots (Fig. 27) and an age of 270 ± 30 Ka.

The YM2 section in Yucca Mountain Trench 2 consists of 4 samples from a thin buried B horizon formed in alluvium (YM2U) and 6 samples from the underlying calcareous gravelly alluvium (YM2L). Plots for the less-than-2-mm and the less-than-0.3 mm size fractions for these deposits are shown in Figure 28. The U-trend age of the upper (Q2a) unit is 47 ± 18 Ka and that of the lower (Q2b) unit is 145 ± 25 Ka.

The YM13 section collected from Yucca Mountain Trench 13 contained deposits of two different ages; an upper Q2a unit (6 samples), and a lower Q2c unit (6 samples). The upper sample in each unit was not included in the U-trend plot because both samples contained admixtures of material from the overlying deposit (Fig. 29). The fractions finer than 2 mm and finer than 0.3 mm were analyzed for each sample in the section. Ages of 35 Ka and 46 Ka for these fractions, respectively, provide an age of about 40 ± 10 Ka for the upper unit (Q2a); and ages of 220 Ka and 250 Ka respectively, provide an age estimate of 240 ± 50 Ka for the lower unit (Q2c).

Two superposed B horizons are exposed in the upper 90 cm of Yucca Mountain Trench 14 (Fig. 5). A 30 cm-thick channel (YM14B) consisting of the lower B horizon only was sampled from the north wall of the trench. Sample YM14B-2 had a higher uranium content than the other samples in this unit, which reflects recent addition of uranium; this sample is not compatible with the other samples in the unit and it was excluded from the U-trend line. The age calculated from the remaining 8 samples representing unit Q2a (Fig. 30) is 38 ± 10 Ka. A 60 cm-thick section (YM14U) containing both the upper and lower B horizons formed in Q2a sand was collected from the south wall in the trench (Fig. 5). The upper sample (YM14-1) is not included in the U-trend slope

(Fig. 31) because it contains material from the overlying sediment. The age obtained from the remaining 8 samples is 90 ± 50 Ka; however, this age is considered to be inaccurate because the section includes two B horizons that may be formed in deposits of different ages. A more reliable U-trend age for the lower 3 samples in the lower B horizon of unit Q2a is 55 ± 20 Ka. A 1.7 m-thick section was collected in the lower Q2c alluvium in the Yucca Mountain Trench 14 (Fig. 5). Three types of Q2c deposits are exposed in the trench; (1) a layer of laminar carbonate in the upper 0.6 m (YM14M, 10-14), (2) a calcareous-sandy sediment in the middle 0.35 m (YM14L, 15-17), and (3) calcite-cemented gravel in the lower 0.75 m (YM14L, 18-22). The U-trend dates for these samples (Fig. 31) suggest that the carbonate accumulation started in the middle part of this section about 270 ± 90 Ka ago. The underlying sandy and gravelly alluvium of unit Q2c has ages of 420 ± 50 Ka and 480 ± 90 Ka, respectively.

A 1.2 m-thick channel in alluvial unit Q2b (CBQ) was collected from the Charlie Brown Quarry northeast of Shoshone, California. The results of the analyses of 8 samples are shown in Figure 32, which gave U-trend age of 160 ± 25 Ka. It unconformably overlies the Tuff A ash bed found in nearby Lake Tecopa (Shepard and Gude, 1968) which has been correlated with the 600 Ka Lava Creek ash (Izett, 1982).

The FHA unit consists of volcanic ash which has been partially altered to clay that was sampled at an outcrop at Fairbanks Hills, Nevada (Fig. 4). A minimum age of 600 Ka was calculated from the poorly defined U-trend plot shown in Figure 33.

Eight samples were collected from an 80 cm-thick channel in a trench on the Eleana Pediment (Fig. 4). The carbonate-cemented alluvium is equivalent to unit QTa but its age is beyond the limits of the dating technique. The U-trend age calculated from the from the measured slope (Fig. 34) yields a minimum age of 800 Ka.

SUMMARY

Uranium-trend dating is a useful method of determining the approximate age of Quaternary deposits in the Nevada Test Site area. The method is the most accurate in the range of 60,000 to 600,000 years. Samples that have a wide spread of data points and minimum scatter about the uranium-trend slope at best may be accurate within ± 10 percent. Relative errors are large near the lower and upper limits of the age range of the method. Age resolution for deposits less than 20,000 years old have errors equal to or greater than the reported age. With respect to the maximum age limit of deposits (greater than 600,000 years), the error usually is greater than 20 percent, thus the limit on the possible maximum age becomes uncertain for ages greater than 700,000 years. Dating of deposits from the Nevada Test Site and in New Mexico (J. N. Rosholt, unpublished data) indicate that age resolution is better for calcareous deposits than for noncalcareous deposits such as carbonate-free till and loess. Poorly sorted alluvial deposits of mixed mineralogy usually yield a better spread of the data points on the uranium-trend plot than do eolian sand or other quartz-rich sand deposits that have little or no soil development.

A tabulation of 31 uranium-trend ages determined on alluvial and fluvial units at NTS are included in Table 5 modified from Swadley and others

(1984). The results are listed according to stratigraphic units defined by Hoover and others (1981). A sample suite (FFPG) containing a loess deposit dated at approximately 30 Ka. The age range in the remaining Q2a deposits of slope wash sand and fluvial gravel is 31 ± 10 to 55 ± 20 Ka. A poor age of sample suite S1 is replaced by results from recollected samples in Frenchman Flat (F2 and F3); thus, the age range of Q2b deposits is considered to be 145 ± 25 to 200 ± 80 Ka. Two groups of Q2c deposits have been found. The younger Q2c stratigraphic unit ranges from 240 ± 50 Ka in the Yucca Mountain area to 310 ± 40 Ka at Rock Valley. The older Q2c stratigraphic unit, sampled in Rock Valley, Jackass Divide, and South Crater flat, has a range of 390 ± 100 to 440 ± 60 Ka. Q2s deposits dated from 160 ± 90 to 480 ± 90 Ka; however, the younger age is a less reliable value with a large error plot and it should be considered as closer to a 250 Ka value. The laminar carbonate (YM14M) reflects the time of strong calcium carbonate development, about 270 ± 90 Ka, rather than the older age of the host fluvial sand in Trench 14.

A histogram showing 30 U-trend age determinations from alluvial units at NTS are shown in Figure 35. Results of the first sampling of Frenchman Flat alluvium (S1) are excluded from the histogram. Median ages for these deposits indicate the following times of widespread depositions: About 40 ± 15 Ka for Q2a sediments, 170 ± 40 Ka for Q2b sediments, 270 ± 50 and 440 ± 60 Ka for younger and older Q2c deposits. These results are reasonably consistent with other age determinations, stratigraphic constraints, and with estimates based on geomorphic evidence. In this geographic area, most of the late to middle Pleistocene sediments appear to have been deposited in these time frames.

REFERENCES CITED

Ander, H. D., Byers, F. M., and Orkild, P. P., 1984, Nevada Test Site field trip guidebook, 1984, Geol. Soc. of America and MacKay School of Mines, University of Nevada-Reno, 1984 Annual Meeting, Reno, p. 1-35.

Dalrymple, G. B., Cox, Allan, and Doell, R. R., 1965, Potassium-argon age and paleomagnetism of the Bishop Tuff, California: Geol. Soc. America Bull., v. 76, p. 665-674.

Frye, J. C., 1978, Pleistocene succession of the central interior United States: Quaternary Research, v. 3, p. 275-283.

Ivanovich, M., and Harmon, R. S., 1982, Uranium Series Disequilibrium: Applications to Environmental Problems, Clarendon Press, Oxford, 571 p.

Izett, G. A., 1982, The Bishop ash bed and some older compositionally similar ash beds in California, Nevada, and Utah: U.S. Geological Survey Open-File Report 82-582, 44 p.

Izett, G. A., Wilcox, R. E., Powers, H. A., and Desborough, G. A., 1970, The Bishop ash bed, a Pleistocene marker bed in the western United States: Quaternary Research, v. 1, p. 122-132.

Ku, T. L., 1976, The uranium-series methods of age determination: Annual Rev. Earth and Planetary Science Letters, v. 4, p. 347-379.

Ku, T. L., Bull, W. B., Freeman, S. T., and Knauss, K. G., 1979, Th^{230}-U^{234} dating of pedogenic carbonates in gravely desert soils of Vidal Valley, Southeastern California: Geol. Soc. America Bull., v. 90, p. 1063-1073.

Ludwig, K. R., 1979, A program in Hewlett-Packard BASIC for X-Y plotting and line-fitting of isotopic and other data: U. S. Geol. Survey Open-File Report, 79-1641, 28 p.

Pierce, K. L., 1979, History and dynamics of glaciation in the northern Yellowstone National Park area: U. S. Geological Survey Prof. Paper 729-F, p. F1-F90.

Rosholt, J. N., 1980, Uranium-trend dating of Quaternary sediments: U. S. Geol. Survey Open-File Report 80-1087, 65 p.

Rosholt, J. N., 1984, Isotope dilution analyses of uranium and thorium in geologic samples using ^{236}2U and ^{229}Th: Nuclear Instr. and Methods, v. 223, p. 572-576.

Rosholt, J. N., 1985, Uranium-trend systematics for dating Quaternary sediments: U.S. Geological Survey Open-File Report 85-298, 34 p.

Rosholt, J. N., Bush, C. A., Shroba, R. R., Pierce, K. L., and Richmond, G. M., 1985, Uranium-trend dating and calibrations for Quaternary sediments: U.S. Geological Survey Open-File Report 85-299, 48 p.

Sheppard, R. A., and Gude, A. J., 1968, Distribution and genesis of authigenic silicate minerals in tuffs of Pleistocene Lake Tecopa, Inyo County, California: U.S. Geological Survey Professional Paper 597, 38 p.

Swadley, W. C., 1983, Map showing surficial geology of the Lathrop Wells quadrangle, Nye County, Nevada: U.S. Geological Survey Miscellaneous Investigations Series Map I-1361, scale 1:48,000.

Swadley, W C, and Hoover, D. L., 1983, Geology of faults exposed in trenches in Crater Flat, Nye County, Nevada: U.S. Geological Survey Open-File Report 83-608, 15 p.

Swadley, W C, Hoover, D. L., Rosholt, J. N., 1984, Preliminary report on late Cenozoic faulting and stratigraphy in the vicinity of Yucca Mountain, Nye County, Nevada: U.S. Geological Survey Open-File Report 84-788, 42 p.

Vaniman, D. T., Crowe, B. M., and Gladney, E. S., 1982, Petrology and geochemistry of Hawaiite lavas from Crater Flat, Nevada: Contributions to Mineralogy and Petrology, v. 80, p. 341-357.

Table 1. Locations, distances from end of trench wall, stratigraphic descriptions, and depths below the surface for all deposits analyzed

Sample Suite (number of samples)	Trench	Location	Material	Stratigraphic Unit	Depth (cm)
SFF	S.W. Frenchman	East Wall	Eolian	Q2a?	2-47
(5)	Flat Trench	13 m north	sediment		
FFPG	36°45.1'N	East Wall	Eolian and	Q2a?	2-22
(10)	115°59.3'W	13 m north	sediment		
S1		East Wall	Alluvium	Q2b	9-85
(6)		23 m north			
F2		East Wall	Buried	Q2b	37-59
(8)		9 m north	B horizon		
F3		East Wall	Pebbly Fan	Q2b	60-170
(12)		9 m north	gravel		
RV1-AD	Rock Valley	West Wall	Slope	Q2a	10-90
(4)	Trench 1	14 m south	wash		
RV1-EI	36°43.4'N	West Wall	Underlying	Q2c	90-190
(5)	116°7.7'W	14 m south	alluvium		
RV1-JO		East Wall	Buried	Q2a	35-58
(6)		12 m north	B horizon		
RV1-PU		East Wall	Calcareous	Q2b	58-81
(6)		23 m north	B horizon		
RV1-VZ		East Wall	K horizon	Q2c	81-100
(6)		23 m north			
TSV-307	Rock Valley	East Wall	Gravel	Q2a	30-170
(7)	Trench 2	20 m north	alluvium		
RV2-U	36°43.5'N	East Wall	Buried	Q2a	50-90
(8)	116°7.4'W	23 m north	B horizon		
RV2-L		East Wall	Gravel	Q2c	120-224
(8)		23 m north	alluvium		
Q2E	Jackass Flats	West Wall	Sand sheet	Q2s	50-110
(4)	Engine Test		deposit		
Q2S	Stand Trench	West Wall	Sand sheet	Q2s	45-135
(9)	36°47.4'N		argillic		
	116°20.0'W		B horizon		
S9	Jackass Divide	West Wall	Upper	Q2c	8-168
(8)	Trench	8.5 m south	alluvium		
JD	36°47.8'N	West Wall	Lower	Q2c	120-240
(8)	116°19.0'W	18.5 m south	alluvium		
SCF1	South Crater Flat	East Wall	Upper	Q2b	23-84
(8)	West Trench	21.5 m north	alluvium		
SCF3	36°43.6'N	East Wall	Upper	Q2b	30-106
(5)	116°33.8'W	24 m north	alluvium		
SCF2		East Wall	Lower	Q2c	23-91
(9)		0.5 m north	alluvium		
SCF4		East Wall	Lower	Q2c	61-181
(8)		3 m north	alluvium		

Table 1. Locations, distances from end of trench wall, stratigraphic descriptions, and depths below the surface for all deposits analyzed (cont'd.)

Sample Suite (number of samples)	Trench	Location	Material	Stratigraphic Unit	Depth (cm)
TSV396 (6)	Crater Flat Trench 1 36°47.3'N 116°30.6'W	North wall about 3 m west of fault zone	Upper carb. enriched zone	---	50-170
CF1 (8)	Crater Flat Trench 3 36°47.0'N 116°30.6'W	South Wall 11.3 m east	Upper alluvium	Q2a	23-84
CF6 (5)		North Wall 24.5 m east	Argillic B horizon	Q2b	54-79
CF2 (7)		South Wall 25.5 m east	Lower alluvium	Q2c	69-157
YM2U (4)	Yucca Mtn. Trench 2 36°51.5'N 116°34.8'W	North Wall 25 m east	Buried B horizon	Q2a	91-142
YM2L (6)		North Wall 25 m east	Gravel alluvium	Q2b	142-231
YM13U (6)	Yucca Mtn. Trench 13 36°52.9'N 116°35.2'W	South Wall 15 m east	Buried B horizon	Q2a	30-107
YM13L (5)		South Wall 15 m east	Gravel alluvium	Q2c	107-182
YM14B (9)	Yucca Mtn. Trench 14 36°50.8'N 116°45.0'W	North Wall 21.5 m west	Lower B horizon below stone line	Q2s	50-77
YM14U (9)		South Wall 24 m west	Upper and lower B horizon	Q2s	30-93
YM14M (5)		North Wall 15 m west	Laminar carbonate K horizon	Q2s	90-146
YM14L (8)		North Wall 15 m west	Cca horizon overlying gravel	Q2s	146-257
CBQ (8)	Charlie Brown Quarry, sho-Shone, CA 35°58.2'N 116°15.2'W	North Wall	Alluvium unconformably overlies Lava Creek ash	Q2b	8-128
FHA (5)	Fairbanks Hills NV 36°31.7'N 116°20.1'W	Outcrop	Altered Volcanic ash	--	0-96
S3 (8)	Eleana Pediment Trench 37°11.0'N 116°5.4'W	South Wall	Gravel carbonate cemented	QTa	10-90

Table 2. Uranium and thorium concentration and Th/U ratio in Quaternary deposits

Sample	Depth (cm)	Description	U (ppm)	Th (ppm)	Th/U
		SFF unit, Frenchman Flat eolian unit			
SFF-1	2-11	All samples analyzed in	2.12	13.07	6.17
SFF-2	11-20	this section of vesicular	1.97	11.56	5.86
SFF-3	20-29	A horizon are silt and	1.66	10.37	6.25
SFF-4	29-38	clay	1.60	9.79	6.11
SFF-5	38-47		1.53	8.84	5.78
		FFPG unit, Frenchman Flat patterned ground eolian unit			
FFPG-1	2-4	All samples analyzed in	2.59	16.43	6.35
FFPG-2	4-6	this section are fine-	2.39	15.56	6.52
FFPG-3	6-8	grained sand, silt and	1.96	11.83	6.04
FFPG-4	8-10	clay.	1.82	11.24	6.19
FFPG-5	10-12		1.71	11.25	6.56
FFPG-6	12-14		1.75	11.02	6.30
FFPG-7	14-16		1.78	11.71	6.57
FFPG-8	16-18		1.72	11.29	6.56
FFPG-9	18-20		1.59	10.70	6.74
FFPG-10	20-22		1.62	11.15	6.87
		S1 unit, Frenchman Flat alluvium			
S1-A	9-20	All samples analyzed in	1.73	10.93	6.31
S1-B	20-33	section are fine- to	1.69	11.33	6.72
S1-C	33-46	medium-grained sand,	1.68	11.52	6.84
S1-D	46-59	silt and clay.	1.55	10.72	6.93
S1-E	59-72		1.47	10.50	7.16
S1-F	72-85		1.43	9.84	6.86
		F2/3 Section, Frenchman Flat alluvium			
F2-1	37-39	Samples in this unit	1.54	7.01	4.57
F2-2	39-42	represent the 3Btca	1.50	6.62	4.40
F2-3	42-44	soil horizon.	1.47	6.34	4.31
F2-4	44-47		1.50	6.03	4.03
F2-5	47-50		1.46	5.85	4.01
F2-6	50-53		1.39	6.13	4.41
F2-7	53-56		1.22	5.80	4.77
F2-8	56-59		1.29	6.00	4.64
F3-1	60-69	Samples in this unit	1.37	5.91	4.30
F3-2	69-78	of pebbly fan gravel	1.40	5.80	4.14
F3-3	78-87	represent the 4Cca.	1.37	5.15	3.75
F3-4	87-96	soil horizon.	1.58	5.58	3.53
F3-5	96-105		1.54	7.44	4.85
F3-6	105-114		1.62	7.01	4.34
F3-7	114-123		1.53	7.15	4.68
F3-8	123-132		1.57	7.41	4.72
F3-9	132-141		1.48	7.79	5.26
F3-10	141-150		1.55	7.26	4.67
F3-11	150-160		1.42	7.22	5.08
F3-12	160-170		1.49	7.18	4.80

Table 2. Uranium and thorium concentration and Th/U ratio in Quaternary deposits, (Cont'd.)

Sample	Depth (cm)	Description	U (ppm)	Th (ppm)	Th/U
RV1 section, (RV1-AD and RV1-EI sample suites) Rock Valley Trench 1					
RV1-A	10-30	Fine to coarse sand	2.18	13.02	5.97
RV1-B	30-50	Fine to coarse sand	2.63	12.58	4.79
RV1-C	50-70	Caliche-rich portion	4.95	8.13	1.64
RV1-D	70-90	Fine to coarse sand	2.83	9.52	3.36
RV1-E	90-110	All samples analyzed in unit are fine to coarse sand.	2.46	10.06	4.09
RV1-F	110-130		2.13	9.16	4.29
RV1-G	130-150		2.25	9.96	4.43
RV1-H	150-170		2.13	9.79	4.60
RV1-I	170-190		2.25	10.06	4.47
RV1 Section (RV1-JO, RV1-PU, and RV1-VZ sample suites) Rock Valley Trench 1					
RV1-J	35-58	Samples in this unit represent a buried B horizon	1.99	13.51	6.79
RV1-K	38-42		1.88	12.69	6.76
RV1-L	42-46		1.78	12.53	7.06
RV1-M	46-50		1.82	13.00	7.15
RV1-N	50-54		1.70	12.67	7.43
RV1-O	54-58		1.87	12.61	6.75
RV1-P	58-62	Samples in this unit represent the calcareous B horizon	2.22	11.99	5.40
RV1-Q	62-66		2.15	12.06	5.60
RV1-R	66-69		2.06	12.59	6.11
RV1-S	69-73		1.97	12.09	6.13
RV1-T	73-77		2.05	11.99	5.86
RV1-U	77-81		2.11	11.82	5.61
RV1-V	81-85	Samples in this unit represent he K horizon	2.57	10.46	4.08
RV1-W	85-89		2.27	10.11	4.45
RV1-X	89-92		2.25	9.58	4.25
RV1-Y	92-96		2.61	9.22	3.53
RV1-Z	96-100		2.85	8.25	2.90
TSV 307 unit, Rock Valley Trench 2					
307-A	30-50	Fine to coarse sand with profile extending across orange B zone in Q2 alluvium.	2.00	11.76	5.87
307-B	50-70		2.10	12.70	6.05
307-C	70-90		2.01	12.76	6.36
307-D	90-110		2.05	11.34	5.52
307-E	110-130	Caliche horizon	3.23	13.96	4.32
307-F	130-150	Upper part of lower Q2 alluvium.	2.64	8.49	3.22
307-G	150-170		2.40	7.16	2.99

Table 2. Uranium and thorium concentration and Th/U ratio in Quaternary deposits, (cont'd)

Sample	Depth (cm)	Description	U (ppm)	Th (ppm)	Th/U
		RV2 section, Rock Valley Trench 2			
RV2-1	50-55	Samples in this unit	2.15	13.16	6.11
RV2-2	55-60	represent the 2Bt horizon	1.99	12.53	6.29
RV2-3	60-65		1.97	12.77	6.48
RV2-4	65-70		1.92	12.75	6.65
RV2-5	65-70		1.82	12.67	6.96
RV2-6	75-70		1.88	12.74	6.77
RV2-7	80-85		1.86	11.99	6.46
RV2-8	85-90		2.02	11.81	5.84
RV2-9	120-133	This unit is poorly sorted,	2.16	9.84	4.53
RV2-10	133-146	nonbedded, sandy gravel	2.28	9.64	4.22
RV2-11	146-159		2.47	9.80	3.97
RV2-12	159-172		2.24	10.07	4.53
RV2-13	172-185		2.77	9.79	3.54
RV2-14	185-198		2.52	9.39	3.73
RV2-15	198-211		2.70	9.60	3.54
RV2-16	211-224		2.33	9.66	4.15
		Q2E unit, eolian sand, Jackass Flats Engine Test Stand Trench			
Q2E-1	50-65	All samples in this unit	1.90	12.39	6.53
Q2E-2	65-80	are reddish-brown oxidized	1.83	12.01	6.58
Q2E-3	80-95	medium to coarse sand.	1.84	11.65	6.34
Q2E-4	95-110		2.21	11.81	5.36
		Q2S unit, sand section, Jackass Flats Engine Test Stand Trench			
Q2S-1	45-55	All samples in this unit	1.74	10.90	6.27
Q2S-2	55-65	are reddish-brown oxidized	1.71	11.07	6.48
Q2S-3	65-75	medium to coarse sand	1.69	10.57	6.26
Q2S-4	75-85		1.68	10.20	6.06
Q2S-5	85-95		1.72	10.59	6.16
Q2S-6	95-105		1.68	10.20	6.06
Q2S-7	105-115		1.90	11.01	5.79
Q2S-8	115-125		1.91	11.11	5.82
Q2S-9	125-135		2.13	11.82	5.55
		S9 unit, Jackass Divide Trench, upper part			
S9-A	8-28	All samples analyzed in this	2.24	15.14	6.75
S9-B	28-48	section are fine to	2.10	13.55	6.47
S9-C	48-68	coarse sand with	2.41	13.67	5.68
S9-D	68-88	some silt and clay.	2.52	12.39	4.92
S9-E	88-108		3.07	9.83	3.21
S9-F	108-128		2.75	12.62	4.59
S9-G	128-148		3.18	13.04	4.11
S9-H	148-168		2.93	13.19	4.51

Table 2. Uranium and thorium concentration and Th/U ratio in Quaternary deposits, (cont'd.)

Sample	Depth (cm)	Description	U (ppm)	Th (ppm)	Th/U
		JD unit, Jackass Divide Trench, lower part			
JD-1	120-135	All samples analyzed in this section are fine to coarse sand with some silt and clay.	3.24	10.39	3.21
JD-2	135-150		3.11	12.05	3.87
JD-3	150-165		3.68	11.65	3.17
JD-4	165-180		3.33	12.04	3.62
JD-5	180-195		2.91	12.10	4.15
JD-6	195-210		2.97	12.92	4.35
JD-7	210-225		3.30	12.67	3.84
JD-8	225-240		3.69	12.94	3.51
		SCF1 unit, upper alluvium in South Crater Flat West Trench			
SCF1m-1	23-30	Fluvial sandy pebble deposit. All samples in this part were less than 2 mm fraction.	2.63	15.68	5.95
SCF1m-2	30-38		2.76	15.06	5.46
SCF1m-3	38-46		2.86	15.46	5.41
SCF1m-4	46-53		2.58	14.76	5.73
SCF1m-5	53-61		2.61	13.77	5.28
SCF1m-6	61-69		2.62	13.95	5.32
SCF1m-7	69-76		2.69	14.24	5.29
SCF1m-8	76-84		2.69	14.38	5.34
SCF1f-1	23-30	Same horizons as above, less than 0.25 mm fraction.	2.52	15.26	6.06
SCF1f-2	30-38		2.61	14.83	5.69
SCF1f-3	38-46		2.57	15.17	5.89
SCF1f-4	46-53		2.59	15.64	6.05
SCF1f-5	53-61		2.69	16.27	6.05
SCF1f-6	61-69		2.58	14.65	5.68
SCF1f-7	69-76		2.53	14.84	5.85
SCF1f-8	76-84		2.39	15.42	6.45
		SCF2 unit, lower alluvium in South Crater Flat West Trench			
SCF2m-1	23-30	Sandy pebble deposit with samples 1-5 mainly sand, 6-9 mainly pebble, less than 2 mm fraction.	3.77	14.22	3.78
SCF2m-2	30-38		4.50	13.83	3.08
SCF2m-3	38-46		4.31	12.29	2.85
SCF2m-4	46-53		4.55	9.26	2.03
SCF2m-5	53-61		4.08	10.27	2.52
SCF2m-6	61-69		3.58	14.38	4.02
SCF2m-7	69-76		3.72	15.43	4.15
SCF2m-8	76-84		4.47	15.60	3.49
SCF2m-9	84-91		4.51	14.68	3.26
SCF2f-1	23-30	Same fluvial deposit as above, less than 0.25 mm fraction.	3.67	13.82	3.76
SCF2f-2	30-38		4.55	12.72	2.80
SCF2f-3	38-46		4.42	11.29	2.56
SCF2f-4	46-53		4.48	8.92	1.99
SCF2f-5	53-61		4.25	9.21	2.17
SCF2f-6	61-69		4.13	13.71	3.32
SCF2f-7	69-76		4.76	15.31	3.22
SCF2f-8	76-84		6.36	16.13	2.54
SCF2f-9	84-91		4.77	14.41	3.03

Table 2. Uranium and thorium concentration and Th/U ratio in Quaternary deposits, (cont'd.)

Sample	Depth (cm)	Description	U (ppm)	Th (ppm)	Th/U
		SCF3 unit, upper aluvium in South Crater Flat West Trench			
SCF3-1	30-46	Sandy pebble, mainly	2.58	15.01	5.82
SCF3-2	46-61	pebble deposit on	2.73	15.54	5.69
SCF3-3	61-76	Q2b terrace.	2.79	15.09	5.41
SCF3-4	76-91		2.75	15.30	5.56
SCF3-5	91-106		2.80	15,25	5.45
		SCF4 unit, lower alluvium in South Crater Flat West Trench			
SCF4-1	61-76	Fluvial sand and	3.61	13.15	3.64
SCF4-2	76-91	pebble deposit with	3.40	13.15	3.87
SCF4-3	91-106	top half more sandy	3.28	13.82	4.21
SCF4-4	106-121	and bottom half	3.01	12.41	4.12
SCF4-5	121-136	more pebbly. Unit	3.51	13.34	3.80
SCF4-6	136-151	is more sandy than	3.95	14.06	3.56
SCF4-7	151-166	equivalent SCF2	3.69	14.88	4.03
SCF4-8	166-181	section.	3.67	12.76	3.48
		S3 unit, Eleana pediment			
S3-A	10-20	All samples analyzed	2.90	8.50	2.93
S3-B	20-30	in this section were	2.42	10.50	4.34
S3-C	30-40	medium to coarse sand,	3.57	8.62	2.42
S3-D	40-50	with caliche.	2.42	8.78	3.63
S3-E	50-60		2.25	8.83	3.92
S3-F	60-70		2.46	8.59	3.50
S3-G	70-80		2.33	8.37	3.59
S3-H	80-90		2.29	8.67	3.78
		TSV 396 unit, upper carbonate enriched zone in Crater Flat Trench 1			
396m-A	50-70	K-horizon gravel, moderately	4.07	14.86	3.65
396m-B	70-90	cemented with Stage III to	4.66	13.12	2.82
396m-C	90-110	Stage IV caliche. All	3.75	13.79	3.68
396m-D	110-130	samples less than 2 mm	5.55	10.84	1.95
396m-E	130-150	fraction	6.73	11.54	1.71
396m-F	150-170		7.28	8.39	1.15
396f-A	50-70	Same horizons as above;	4.11	14.07	3.42
396f-B	70-90	all samples less than	4.57	12.05	2.64
396f-C	90-110	0.3 mm fraction	3.82	13.15	3.45
396f-D	110-130		5.46	11.54	2.12
396f-E	130-150		6.69	11.26	1.68
396f-F	150-170		7.16	8.36	1.17

Table 2. Uranium and thorium concentration and Th/U ratio in Quaternary deposits, (cont'd.)

Sample	Depth (cm)	Description	U (ppm)	Th (ppm)	Th/U
		CF1 unit, alluvium in Crater Flat Trench 3			
CF1-1	23-30	All samples in this unit of	2.16	14.56	6.75
CF1-2	30-38	sandy, pebble-cobble fluvial	2.20	13.80	6.28
CF1-3	38-46	deposit were less than	2.32	14.52	6.26
CF1-4	46-53	0.33 mm fraction. No	2.50	14.66	5.87
CF1-5	53-61	bedding or poor bedding	2.47	14.70	5.95
CF1-6	61-69	is in the deposit.	2.46	14.37	5.85
CF1-7	69-76		2.35	14.17	6.04
CF1-8	76-84		2.31	13.98	6.05
		CF6 unit, older argillic B-horizon soil in Crater Flat Trench 3			
CF6-1	54-59	All samples of sandy clay	2.65	16.10	6.07
CF6-2	59-64	were less than 2 mm	2.70	16.61	6.14
CF6-3	64-69	fraction.	2.24	13.68	6.12
CF6-4	69-74		2.51	14.46	5.76
CF6-5	74-79		2.59	15.75	6.08
		CF2 unit, lower alluvium in Crater Flat Trench 3			
CF2m-1	69-81	All samples in this unit	3.83	14.14	3.70
CF2m-2	81-94	of pebble to boulder beds	4.23	12.83	3.04
CF2m-3	94-107	with poor bedding were	3.91	13.22	3.78
CF2m-4	107-119	less than 2 mm fraction.	3.23	14.22	4.40
CF2m-5	119-132		3.28	13.76	4.19
CF2m-6	132-145		3.29	14.69	4.47
CF2m-7	145-157		3.28	12.96	3.95
CF2f-1	69-81	Same unit as above with	3.54	12.85	3.63
CF2f-2	81-94	samples less than 0.25 mm	4.31	12.22	2.83
CF2f-3	94-107	fraction.	3.79	11.71	3.09
CF2f-4	107-119		3.43	12.33	3.59
CF2f-5	119-132		2.90	12.99	4.47
CF2f-6	132-145		2.81	14.48	5.16
CF2f-7	145-157		2.85	11.95	4.19
		YM2 section, alluvium in Yucca Mountain Trench 2			
Upper unit					
YM2m-1	91-104	B horizon at top, grading	2.42	16.26	6.71
YM2m-2	104-117	into pebble-gravel at	2.35	16.75	7.12
YM2m-3	117-130	base. Samples were less	2.21	17.44	7.88
YM2m-4	130-142	than 2 mm fraction.	2.72	16.50	6.06
YM2f-1	91-104	Same horizons as	2.23	14.87	6.67
YM2f-2	104-117	above. Less than	2.17	15.38	7.09
YM2f-3	117-130	0.3 mm fraction.	2.08	16.29	7.84
YM2f-4	130-142		2.53	14.59	5.76

Table 2. Uranium and thorium concentration and Th/U ratio in Quaternary deposits, (cont'd.)

Sample	Depth (cm)	Description	U (ppm)	Th (ppm)	Th/U
Lower unit					
YM2m-5	142-155	Mostly gravel, underlain by 1.4 m of similar gravel. Samples were less than 2 mm fraction.	3.83	15.87	4.15
YM2m-6	155-170		3.31	17.14	5.18
YM2m-7	170-185		3.43	16.69	4.86
YM2m-8	185-201		3.54	13.76	3.89
YM2m-9	201-216		4.12	15.06	3.66
YM2m-10	216-231		3.43	12.24	3.56
YM2f-5	142-155	Same horizons as above. Less than 0.3 mm fraction.	3.68	15.16	4.11
YM2f-6	155-170		3.09	14.44	4.67
YM2f-7	170-185		3.39	13.40	3.95
YM2f-8	185-201		3.46	11.98	3.46
YM2f-9	201-216		4.06	12.41	3.06
YM2f-10	216-231		3.64	12.40	3.41
		YM13 section, alluvium in Yucca Mountain Trench 13			
Upper part					
YM13m-1	30-38	B horizon at top, grading into pebble-gravel at base. Samples were less than 2 mm fraction.	2.18	15.28	7.00
YM13m-2	38-51		1.93	19.34	10.00
YM13m-3	51-64		1.97	17.97	9.14
YM13m-4	64-76		1.97	18.22	9.25
YM13m-5	76-91		2.54	17.06	6.72
YM13m-6	91-107		3.29	15.20	4.62
YM13f-1	30-38	Same horizons as above less than 0.3 mm fraction.	2.29	15.92	6.94
YM13f-2	38-51		2.01	16.54	8.22
YM13f-3	51-64		1.99	18.28	9.17
YM13f-4	64-76		2.01	18.30	9.08
YM13f-5	76-91		2.30	15.77	6.85
YM13f-6	91-107		3.14	14.10	4.49
Lower part					
YM13m-7	107-122	Mostly gravel with abundant caliche rinds less than 2 mm fraction.	2.90	16.15	5.58
YM13m-8	122-137		3.26	16.09	4.93
YM13m-9	137-152		2.60	15.95	6.13
YM13m-10	152-167		2.87	16.71	5.83
Ym13m-11	167-182		4.12	15.90	3.86
YM13f-7	107-122	Same horizons as above less than 0.25 mm fraction.	2.92	15.99	5.48
YM13f-8	122-137		3.51	14.15	4.03
YM13f-9	137-152		2.58	15.27	5.91
YM13f-10	152-167		2.90	16.22	5.60
YM13f-11	167-182		3.54	15.09	4.26

Table 2. Uranium and thorium concentration and Th/U ratio in Quaternary deposits

Sample	Depth (cm)	Description	U (ppm)	Th (ppm)	Th/U
YM14B section, Q2 sand and alluvium in Yucca Mountain Trench 14					
Upper unit					
YM14B-1	50-53	3Bt soil horizon in lower part of Q2s loose sand	2.31	15.84	6.86
YM14B-2	53-56		3.95	15.66	3.96
YM14B-3	56-59		2.36	15.65	6.63
YM14B-4	59-62		2.46	15.55	6.33
YM14B-5	62-65		2.46	15.46	6.28
YM14B-6	65-68		2.56	15.49	6.04
YM14B-7	68-71		2.82	15.35	5.45
YM14B-8	71-74		2.89	15.36	5.31
YM14B-9	74-77		3.30	14.77	4.48
YM14 section, Upper and lower B horizon in Yucca Mountain Trench 14					
Upper unit					
YM14-1	30-37	Unit consists of Q2s loose sand.	2.09	12.84	6.14
YM14-2	37-44		2.08	14.82	7.11
YM14-3	44-51		2.10	14.90	7.09
YM14-4	51-58		2.26	15.32	6.79
YM14-5	58-65		2.20	15.42	7.02
YM14-6	65-72		2.28	15.06	6.60
YM14-7	72-79		2.39	15.72	6.58
YM14-8	79-86		2.74	15.00	5.48
YM14-9	86-93		3.05	14.49	4.74
YM14 section, Q2c alluvium in Yucca Mountain Trench 14					
Middle unit					
YM14-10	90-100	Laminar carbonate K-horizon	4.63	12.50	2.70
YM14-11	100-115		4.44	9.90	2.24
YM14-12	115-130		5.60	6.12	1.09
YM14-13	130-138		5.83	5.73	.98
YM14-14	138-146		4.26	1.16	.27
Lower unit					
YM14-15	146-154	Sandy part Cca horizon	2.46	7.60	3.09
YM14-16	154-167		2.39	8.80	3.69
YM14-17	167-182		2.67	9.46	3.55
YM14-18	182-197	Gravelly sand, calcite cemented, unit with reworked carbonate stringers.	3.16	12.87	4.07
YM14-19	197-212		3.40	11.47	3.38
YM14-20	212-227		3.55	15.69	4.42
YM14-21	227-242		5.22	12.01	2.30
YM14-22	242-257		3.80	15.53	4.08.

Table 2. Uranium and thorium concentration and Th/U ratio in Quaternary deposits, (cont'd.)

Sample	Depth (cm)	Description	U (ppm)	Th (ppm)	Th/U
CBQ unit, alluvium in Charlie Brown Quarry, Shoshone, California.					
CBQ-1	8-23	All samples analyzed in section are fine- to medium-grained sand with silt and clay.	2.07	11.31	5.46
CBQ-2	23-38		2.46	11.07	4.51
CBQ-3	38-53		2.88	11.39	3.96
CBQ-4	53-68		2.99	10.74	3.60
CBQ-5	68-83		2.54	10.99	4.32
CBQ-6	83-98		2.88	9.08	3.16
CBQ-7	98-113		2.09	10.50	5.02
CBQ-8	113-128		2.78	10.11	3.64
FHA unit, altered volcanic ash, Fairbanks Hills, Nevada.					
A15-A	0-15	Ash mostly altered to clay	4.79	20.89	4.36
A15-B	15-20	Ash mostly altered to clay	3.72	22.61	6.09
A15-C	20-30	Slightly altered ash	4.01	16.50	4.12
A15-D	85-93	Slightly altered ash	7.17	28.9	4.03
A15-E	93-96	Ash altered to clay	4.41	35.2	7.96
S3 unit, Eleana pediment Trench.					
S3-A	10-20	All samples analyzed in this section were medium to coarse sand, with caliche.	2.90	8.50	2.93
S3-B	20-30		2.42	10.50	4.34
S3-C	30-40		3.57	8.62	2.42
S3-D	40-50		2.42	8.78	3.63
S3-E	50-60		2.25	8.83	3.92
S3-F	60-70		2.46	8.59	3.50
S3-G	70-80		2.33	8.37	3.59
S3-H	80-90		2.29	8.67	3.78

Table 3. Isotopic ratios of uranium and thorium required for U-trend plots

Sample	U ppm	$^{234}U/^{238}U$	$^{230}Th/^{238}U$	$^{238}U/^{232}Th$	$^{230}Th/^{232}Th$	$(^{238}U-^{230}Th)/^{238}U$	$(^{234}U-^{238}U)/^{238}U$
		Activity Ratios					
SFF unit (Fig. 6)							
SFF-1	2.12	1.014	1.438	0.492±0.026	0.708±0.020	-0.438±0.060	+0.014±0.032
SFF-2	1.97	1.032	1.416	.518± .027	.733± .023	- .416± .059	+ .032± .033
SFF-3	1.66	1.006	1.468	.485± .025	.712± .023	- .468± .062	+ .006± .032
SFF-4	1.60	.982	1.417	.497± .026	.704± .023	- .418± .060	- .018± .031
SFF-5	1.53	.998	1.324	.524± .027	.695± .022	- .324± .056	- .002± .032
FFPG unit (Fig. 7)							
FFPG-1	2.59	.980	1.389	.478± .025	.663± .021	- .389± .058	- .020± .031
FFPG-2	2.39	1.035	1.515	.465± .024	.705± .023	- .515± .064	+ .035± .033
FFPG-3	1.96	1.065	1.476	.502± .026	.742± .024	- .476± .062	+ .065± .034
FFPG-4	1.82	1.073	1.528	.490± .025	.739± .024	- .528± .064	+ .064± .034
FFPG-5	1.71	1.045	1.549	.462± .024	.716± .023	- .549± .065	+ .045± .033
FFPG-6	1.75	1.032	1.532	.482± .025	.738± .024	- .532± .064	+ .032± .033
FFPG-7	1.78	1.064	1.550	.463± .024	.718± .023	- .550± .065	+ .064± .034
FFPG-8	1.72	1.047	1.549	.464± .024	.716± .023	- .549± .065	+ .047± .034
FFPG-9	1.59	1.053	1.603	.450± .023	.722± .023	- .603± .067	+ .053± .034
FFPG-10	1.62	1.029	1.585	.441± .023	.698± .022	- .585± .066	+ .029± .033
S1 unit (Fig. 8)							
S1-A	1.73	.972	1.561	.481± .025	.751± .024	- .561± .066	- .028± .031
S1-B	1.69	.991	1.680	.452± .024	.759± .024	- .680± .071	- .009± .032
S1-C	1.68	.992	1.687	.444± .023	.749± .024	- .687± .071	- .008± .032
S1-D	1.55	1.027	1.649	.438± .023	.722± .023	- .649± .069	+ .027± .033
S1-E	1.47	.993	1.699	.423± .022	.720± .023	- .699± .071	- .007± .032
S1-F	1.43	1.010	1.691	.442± .023	.748± .024	- .691± .071	+ .010± .032
F2 unit (Fig. 9)							
F2-1	1.54	1.086	1.019	.676± .035	.689± .019	- .019± .043	+ .086± .035
F2-2	1.50	1.085	1.051	.702± .037	.738± .021	- .051± .044	+ .085± .035
F2-3	1.47	1.084	1.026	.716± .037	.735± .021	- .026± .043	+ .084± .035
F2-4	1.50	1.104	.954	.767± .040	.737± .020	+ .046± .040	+ .104± .035
F2-5	1.46	1.080	.978	.770± .040	.753± .021	+ .022± .041	+ .080± .035
F2-6	1.39	1.088	1.010	.701± .036	.707± .020	- .010± .042	+ .088± .035
F2-7	1.22	1.051	1.091	.647± .034	.707± .020	- .091± .046	+ .051± .034
F2-8	1.29	1.040	1.058	.665± .035	.704± .020	- .058± .044	+ .041± .033

Table 3. Isotopic ratios of uranium and thorium required for U-trend plots, (cont'd.)

Sample	U ppm	Activity Ratios $^{234}U/^{238}U$	$^{230}Th/^{238}U$	$^{238}U/^{232}Th$	$^{230}Th/^{232}Th$	$(^{238}U-^{230}Th)/^{238}U$	$(^{234}U-^{238}U)/^{238}U$
F3 unit (Fig. 10)							
F3-1	1.37	1.041	1.013	.718±0.037	.727±0.020	- .013±0.043	+ .041±0.033
F3-2	1.40	1.079	1.002	.746± .039	.748± .039	- .002± .042	+ .079± .035
F3-3	1.37	1.061	1.018	.824± .043	.838± .043	- .018± .043	+ .061± .034
F3-4	1.58	1.058	1.095	.875± .045	.958± .027	- .095± .046	+ .058± .034
F3-5	1.54	1.064	.969	.637± .033	.618± .017	+ .031± .041	+ .064± .034
F3-6	1.62	1.060	.971	.712± .037	.691± .019	+ .029± .041	+ .060± .034
F3-7	1.53	1.036	1.041	.660± .034	.688± .019	- .041± .044	+ .036± .033
F3-8	1.57	1.095	1.104	.655± .034	.723± .020	- .104± .046	+ .095± .035
F3-9	1.48	1.008	1.137	.587± .031	.667± .019	- .137± .048	+ .008± .032
F3-10	1.55	1.014	1.136	.662± .034	.752± .021	- .136± .048	+ .014± .032
F3-11	1.42	1.012	1.141	.608± .032	.694± .019	- .141± .048	+ .012± .032
F3-12	1.49	1.001	1.161	.644± .033	.644± .021	- .161± .049	+ .001± .032
RV1 section (Fig. 11)							
RV1-A	2.18	1.055	1.503	.509± .026	.765± .021	- .503± .063	+ .055± .034
RV1-B	2.63	1.104	1.192	.634± .033	.756± .021	- .192± .050	+ .104± .035
RV1-C	4.95	1.288	.567	1.851± .096	1.049± .029	+ .433± .024	+ .288± .041
RV1-D	2.83	1.166	.864	.903± .047	.780± .022	+ .136± .036	+ .166± .037
RV1-E	2.46	1.075	.906	.743± .039	.673± .019	+ .094± .038	+ .075± .034
RV1-F	2.13	1.065	.945	.708± .037	.669± .019	+ .055± .040	+ .065± .034
RV1-G	2.25	1.050	.948	.686± .036	.651± .018	+ .052± .040	+ .050± .034
RV1-H	2.13	1.029	.984	.660± .034	.650± .018	+ .016± .041	+ .019± .033
RV1-I	2.25	1.031	.991	.680± .035	.674± .019	+ .009± .042	+ .031± .033
RV1 section (Fig. 12)							
RV1-J	1.99	1.047	1.566	.455± .024	.713± .020	- .566± .066	+ .047± .033
RV1-K	1.88	1.025	1.483	.457± .024	.677± .019	- .483± .062	+ .025± .032
RV1-L	1.78	1.005	1.504	.438± .023	.658± .018	- .504± .063	+ .005± .032
RV1-M	1.82	.998	1.519	.432± .022	.656± .018	- .519± .064	- .002± .032
RV1-N	1.70	1.005	1.518	.416± .022	.631± .018	- .518± .064	+ .005± .032
RV1-O	1.87	1.027	1.393	.458± .024	.638± .018	- .393± .059	+ .027± .033
RV1 section (Fig. 13)							
RV1-P	2.22	1.141	1.096	.572± .030	.627± .018	- .096± .046	+ .141± .037
RV1-Q	2.15	1.111	1.131	.551± .029	.623± .017	- .131± .047	+ .111± .036
RV1-R	2.06	1.061	1.227	.506± .026	.621± .017	- .227± .052	+ .061± .034
RV1-S	1.97	1.040	1.233	.504± .026	.621± .017	- .233± .052	+ .040± .033
RV1-T	2.05	1.040	1.194	.527± .027	.629± .018	- .194± .050	+ .040± .033
RV1-U	2.11	1.065	1.155	.551± .029	.636± .018	- .155± .049	+ .065± .034
RV1-V	2.57	1.127	.982	.758± .039	.744± .021	+ .018± .041	+ .127± .036
RV1-W	2.27	1.096	1.000	.694± .036	.694± .019	+ .000± .042	+ .096± .035
RV1-X	2.25	1.105	.983	.727± .038	.714± .020	+ .017± .041	+ .105± .035
RV1-Y	2.61	1.171	.863	.875± .045	.755± .021	+ .137± .036	+ .171± .037
RV1-Z	2.85	1.261	.750	1.066± .055	.800± .022	+ .250± .032	+ .261± .040

Table 3. Isotopic ratios of uranium and thorium required for U-trend plots, (cont'd.)

Sample	U ppm	$^{234}U/^{238}U$	$^{230}Th/^{238}U$	$^{238}U/^{232}Th$	$^{230}Th/^{232}Th$	$(^{238}U-^{230}Th)/^{238}U$	$(^{234}U-^{238}U)/^{238}U$
		Activity Ratios					
307 unit (Fig. 14)							
307-A	2.00	1.033	1.395	.518±0.027	.722±0.020	- .395±0.059	+ .033±0.033
307-B	2.10	1.064	1.329	.502± .026	.668± .019	- .329± .056	+ .064± .034
307-C	2.01	1.036	1.318	.477± .025	.629± .018	- .318± .055	+ .036± .033
307-D	2.05	1.062	1.183	.550± .029	.651± .018	- .183± .050	+ .062± .034
307-E	3.23	1.092	.891	.704± .037	.627± .018	+ .109± .038	+ .092± .035
307-F	2.64	1.168	.824	.944± .049	.778± .022	+ .176± .035	+ .168± .037
307-G	2.40	1.230	.822	1.017± .053	.836± .023	+ .178± .035	+ .230± .039
RV2 section (Fig. 15							
RV2-1	2.15	1.057	1.314	.506± .026	.664± .019	- .314± .055	+ .057± .034
RV2-2	1.99	1.062	1.331	.491± .026	.654± .018	- .331± .056	+ .062± .034
RV2-3	1.97	1.069	1.324	.477± .025	.631± .018	- .324± .056	+ .069± .034
RV2-4	1.92	1.038	1.351	.464± .024	.627± .018	- .351± .057	+ .038± .033
RV2-5	1.82	1.019	1.452	.444± .023	.645± .018	- .452± .061	+ .019± .033
RV2-6	1.88	1.012	1.363	.456± .024	.622± .017	- .363± .057	+ .012± .032
RV2-7	1.86	1.021	1.331	.478± .025	.636± .018	- .331± .056	+ .021± .033
RV2-8	2.02	1.054	1.222	.529± .027	.646± .018	- .222± .051	+ .054± .034
RV2-9	2.16	1.059	.986	.682± .035	.672± .019	+ .014± .041	+ .059± .034
RV2-10	2.28	1.062	.984	.732± .038	.720± .020	+ .016± .041	+ .062± .034
RV2-11	2.47	1.102	.963	.779± .041	.750± .021	+ .037± .040	+ .102± .035
RV2-12	2.24	1.049	.971	.687± .036	.667± .019	+ .029± .041	+ .049± .034
RV2-13	2.77	1.072	.946	.873± .045	.826± .023	+ .054± .040	+ .072± .034
RV2-14	2.52	1.070	.949	.828± .043	.786± .022	+ .051± .040	+ .070± .034
RV2-15	2.70	1.084	.958	.867± .045	.831± .023	+ .042± .040	+ .084± .035
RV2-16	2.33	1.053	.956	.744± .039	.712± .020	+ .044± .040	+ .053± .034
Q2E unit (Fig. 16)							
Q2E-1	1.90	.978	1.283	.465± .024	.596± .017	- .283± .054	- .022± .031
Q2E-2	1.83	.996	1.246	.461± .024	.575± .016	- .246± .052	- .004± .032
Q2E-3	1.84	.982	1.253	.479± .025	.600± .017	- .253± .053	- .018± .031
Q2E-4	2.21	.972	1.112	.567± .029	.630± .018	- .112± .047	- .028± .031
Q2S unit (Fig. 17)							
Q2S-1	1.74	.981	1.254	.484± .025	.607± .017	- .254± .053	- .109± .031
Q2S-2	1.71	.979	1.270	.468± .024	.595± .017	- .270± .054	- .021± .031
Q2S-3	1.69	.995	1.231	.485± .025	.597± .017	- .231± .052	- .005± .032
Q2S-4	1.68	1.013	1.198	.501± .026	.600± .017	- .198± .050	+ .013± .032
Q2S-5	1.72	.984	1.217	.493± .026	.600± .017	- .217± .051	- .016± .031
Q2S-6	1.68	.997	1.207	.501± .026	.605± .017	- .207± .051	- .003± .032
Q2S-7	1.90	.984	1.189	.524± .027	.623± .017	- .189± .050	- .016± .031
Q2S-8	1.91	.994	1.172	.521± .027	.611± .017	- .172± .049	- .006± .032
Q2S-9	2.13	.992	1.126	.547± .028	.616± .017	- .126± .047	- .008± .032

Table 3. Isotopic ratios of uranium and thorium required for U-trend plots, (cont'd.)

		Activity Ratios					
Sample	U ppm	$^{234}U/^{238}U$	$^{230}Th/^{238}U$	$^{238}U/^{232}Th$	$^{230}Th/^{232}Th$	$(^{238}U-^{230}Th)/^{238}U$	$(^{234}U-^{238}U)/^{238}U$
			S9 unit (Fig. 18)				
S9-A	2.24	.983	1.462	.450± .023	.658± .018	- .462± .061	- .017± .031
S9-B	2.10	1.030	1.373	.464± .024	.645± .018	- .373± .058	+ .030± .033
S9-C	2.41	1.045	1.066	.534± .028	.570± .016	- .066± .045	+ .045± .033
S9-D	2.52	1.108	.979	.617± .032	.604± .017	+ .021± .041	+ .108± .036
S9-E	3.07	1.217	.721	.947± .049	.682± .019	+ .279± .030	+ .217± .039
S9-F	2.75	1.085	.978	.661± .034	.646± .018	+ .022± .041	+ .085± .035
S9-G	3.18	1.067	.927	.734± .038	.681± .019	+ .073± .039	+ .067± .034
S9-H	2.93	1.032	.998	.673± .035	.672± .019	+ .002± .042	+ .032± .033
			JD unit (Fig. 19)				
JD-1	3.24	1.137	1.079	.946± .049	1.020± .029	- .079± .045	+ .137± .036
JD-2	3.11	1.116	1.059	.785± .041	.831± .023	- .059± .044	+ .116± .036
JD-3	3.68	1.125	1.074	.958± .050	1.029± .029	- .074± .045	+ .125± .036
JD-4	3.33	1.106	1.027	.839± .044	.861± .024	- .027± .043	+ .106± .036
JD-5	2.91	1.056	1.061	.731± .038	.776± .022	- .061± .045	+ .056± .034
JD-6	2.97	1.010	1.024	.698± .036	.715± .020	- .024± .043	+ .010± .032
JD-7	3.30	1.047	1.069	.791± .041	.845± .024	- .069± .045	+ .047± .034
JD-8	3.69	1.076	1.051	.865± .045	.909± .025	- .051± .044	+ .076± .034
			SCf1m unit (Fig. 20)				
SCF1m-1	2.63	1.038	1.386	.510± .027	.707± .020	- .386± .058	+ .038± .033
SCF1m-2	2.76	1.044	1.274	.556± .029	.708± .020	- .274± .053	+ .044± .033
SCF1m-3	2.86	1.024	1.213	.561± .029	.680± .019	- .213± .051	+ .024± .033
SCF1m-4	2.58	1.035	1.232	.530± .028	.653± .018	- .232± .052	+ .035± .033
SCF1m-5	2.61	1.039	1.111	.575± .030	.639± .018	- .111± .047	+ .039± .033
SCF1m-6	2.62	1.048	1.096	.570± .030	.625± .018	- .096± .046	+ .048± .034
SCF1m-7	2.69	1.019	1.069	.573± .030	.613± .017	- .069± .045	+ .019± .033
SCF1m-8	2.69	.995	1.092	.569± .030	.621± .017	- .092± .046	- .005± .032
			SCF1f unit (Fig. 20)				
SCF1f-1	2.52	1.047	1.442	.501± .026	.723± .020	- .442± .061	+ .047± .034
SCF1f-2	2.61	1.106	1.447	.534± .028	.772± .022	- .447± .061	+ .106± .035
SCF1f-3	2.57	1.113	1.465	.515± .027	.754± .021	- .465± .062	+ .113± .036
SCF1f-4	2.59	1.108	1.440	.502± .026	.723± .020	- .440± .060	+ .108± .035
SCF1f-5	2.69	1.137	1.349	.502± .026	.677± .019	- .349± .057	+ .137± .036
SCF1f-6	2.58	1.130	1.215	.535± .028	.649± .018	- .215± .051	+ .130± .036
SCF1f-7	2.53	1.075	1.171	.518± .027	.607± .017	- .171± .049	+ .075± .034
SCF1f-8	2.39	1.063	1.227	.470± .024	.577± .016	- .227± .052	+ .063± .034

Table 3. Isotopic ratios of uranium and thorium required for U-trend plots, (cont'd.)

Sample	U ppm	Activity Ratios $^{234}U/^{238}U$	$^{230}Th/^{238}U$	$^{238}U/^{232}Th$	$^{230}Th/^{232}Th$	$(^{238}U-^{230}Th)/^{238}U$	$(^{234}U-^{238}U)/^{238}U$
				SCF2m unit (Fig. 21)			
SCF2m-1	3.77	1.343	1.286	.804±0.042	1.033±0.029	- .286±0.054	+ .343±0.043
SCF2m-2	4.50	1.393	1.036	.987± .051	1.022± .029	- .036± .044	+ .393± .045
SCF2m-3	4.31	1.455	1.165	1.063± .055	1.239± .035	- .165± .049	+ .455± .047
SCF2m-4	4.55	1.604	1.205	1.492± .078	1.797± .050	- .205± .051	+ .604± .051
SCF2m-5	4.08	1.541	1.275	1.206± .063	1.537± .043	- .275± .054	+ .541± .049
SCF2m-6	3.58	1.322	1.303	.755± .039	.984± .028	- .303± .055	+ .322± .042
SCF2m-7	3.72	1.320	1.205	.732± .038	.882± .025	- .205± .051	+ .320± .042
SCF2m-8	4.47	1.393	1.024	.871± .045	.892± .025	- .024± .043	+ .393± .045
SCF2m-9	4.51	1.411	1.048	.932± .049	.977± .027	- .048± .044	+ .411± .045
				SCF2f unit (Fig. 21)			
SCF2f-1	3.67	1.378	1.318	.807± .042	1.063± .030	- .318± .055	+ .378± .044
SCF2f-2	4.55	1.489	1.029	1.086± .056	1.117± .031	- .029± .043	+ .489± .048
SCF2f-3	4.42	1.549	1.195	1.187± .062	1.419± .040	- .195± .050	+ .549± .050
SCF2f-4	4.48	1.639	1.225	1.525± .079	1.868± .052	- .225± .051	+ .639± .052
SCF2f-5	4.25	1.604	1.325	1.398± .073	1.853± .052	- .325± .056	+ .604± .051
SCF2f-6	4.13	1.550	1.549	.919± .048	1.423± .040	- .549± .065	+ .550± .050
SCF2f-7	4.76	1.560	1.415	.954± .050	1.351± .038	- .415± .059	+ .560± .050
SCF2f-8	6.36	1.677	1.166	1.202± .062	1.402± .039	- .166± .049	+ .677± .054
SCF2f-9	4.76	1.512	1.097	1.003± .052	1.100± .031	- .097± .046	+ .512± .048
				SCF3 unit (Fig. 22)			
SCF3-1	2.58	1.042	1.301	.531± .028	.690± .019	- .301± .055	+ .042± .033
SCF3-2	2.73	1.023	1.234	.543± .028	.670± .019	- .234± .052	+ .023± .033
SCF3-3	2.79	1.030	1.124	.571± .030	.642± .018	- .124± .047	+ .030± .033
SCF3-4	2.75	1.033	1.149	.556± .029	.638± .018	- .149± .048	+ .033± .033
SCF3-5	2.80	1.020	1.102	.567± .030	.625± .018	- .102± .046	+ .020± .033
				SCF4 unit (Fig. 23)			
SCF4-1	3.61	1.383	1.204	.849± .044	1.022± .029	- .204± .051	+ .383± .044
SCF4-2	3.40	1.318	1.184	.799± .042	.946± .026	- .184± .050	+ .318± .042
SCF4-3	3.28	1.315	1.164	.734± .038	.855± .024	- .164± .049	+ .315± .042
SCF4-4	3.01	1.265	1.139	.750± .039	.854± .024	- .139± .048	+ .265± .040
SCF4-5	3.51	1.345	.976	.814± .042	.795± .022	+ .024± .041	+ .345± .043
SCF4-6	3.95	1.414	.840	.869± .045	.730± .020	+ .160± .035	+ .414± .045
SCF4-7	3.69	1.302	.877	.767± .040	.673± .019	+ .123± .037	+ .302± .042
SCF4-8	3.67	1.376	.825	.888± .046	.733± .021	+ .175± .035	+ .376± .044
				TSV 396m (Fig. 24)			
396m-A	4.07	1.258	1.008	0.846± .044	0.852± .024	-0.008± .042	+0.258± .040
396m-B	2.90	1.274	.908	1.104± .057	1.003± .028	+ .092± .038	+ .274± .041
396m-C	3.25	1.197	1.129	.840± .044	.948± .027	- .129± .047	+ .197± .038
396m-D	5.55	1.254	1.044	1.581± .082	1.652± .046	- .044± .044	+ .254± .040
396m-E	2.85	1.271	1.031	1.803± .094	1.859± .052	- .031± .043	+ .271± .041
396m-F	2.92	1.240	1.053	2.680± .139	2.822± .079	- .053± .044	+ .240± .040

Table 3. Isotopic ratios of uranium and thorium required for U-trend plots

Sample	U ppm	$^{234}U/^{238}U$	$^{230}Th/^{238}U$	$^{238}U/^{232}Th$	$^{230}Th/^{232}Th$	$(^{238}U-^{230}Th)/^{238}U$	$(^{234}U-^{238}U)/^{238}U$
		Activity Ratios					
TSV 396f (Fig. 24)							
396f-A	4.12	1.259	.980	.888± .046	.870± .024	+ .020± .041	+ .259± .040
396f-B	4.57	1.296	.866	1.151± .060	.996± .028	+ .134± .036	+ .296± .041
396f-C	3.82	1.192	1.083	.881± .046	.954± .027	- .083± .045	+ .193± .038
396f-D	5.46	1.253	1.041	1.434± .075	1.494± .042	- .041± .044	+ .253± .040
396f-E	6.69	1.270	1.015	1.803± .094	1.830± .051	- .015± .043	+ .270± .041
396f-F	7.16	1.267	1.027	2.590± .131	2.661± .075	- .027± .043	+ .267± .041
CF1 unit (Fig. 25)							
CF1-1	2.16	1.061	1.475	.450± .023	.664± .019	- .475± .062	+ .061± .034
CF1-2	2.20	1.069	1.567	.484± .025	.758± .021	- .567± .066	+ .069± .034
CF1-3	2.32	1.104	1.343	.485± .025	.651± .018	- .343± .056	+ .104± .035
CF1-4	2.50	1.117	1.236	.517± .027	.640± .018	- .236± .052	+ .117± .036
CF1-5	2.47	1.127	1.263	.510± .027	.643± .018	- .263± .053	+ .127± .036
CF1-6	2.46	1.148	1.249	.519± .027	.648± .018	- .249± .052	+ .148± .037
CF1-7	2.35	1.135	1.289	.503± .026	.648± .018	- .289± .054	+ .135± .036
CF1-8	2.31	1.118	1.272	.502± .026	.638± .018	- .272± .053	+ .118± .036
CF6 unit (Fig. 26)							
CF6-1	2.65	1.142	1.277	.509± .026	.650± .018	- .277± .054	+ .142± .037
CF6-2	2.70	1.142	1.288	.503± .026	.648± .018	- .288± .054	+ .142± .037
CF6-3	2.24	1.146	1.280	.505± .026	.647± .018	- .280± .054	+ .146± .037
CF6-4	2.51	1.135	1.231	.537± .028	.661± .019	- .231± .052	+ .135± .036
CF6-5	2.59	1.103	1.293	.508± .026	.657± .018	- .293± .054	+ .103± .035
CF2m unit (Fig. 27)							
CF2m-1	3.83	1.237	.950	.821± .043	.780± .022	+ .050± .040	+ .237± .039
CF2m-2	4.23	1.272	.850	1.000± .052	.850± .024	+ .150± .036	+ .272± .041
CF2m-3	3.91	1.267	.892	.899± .047	.801± .022	+ .108± .038	+ .267± .040
CF2m-4	3.23	1.124	1.001	.690± .036	.691± .019	- .001± .042	+ .124± .036
CF2m-5	3.28	1.126	1.004	.725± .038	.728± .020	- .004± .042	+ .125± .036
CF2m-6	3.29	1.117	1.052	.680± .035	.715± .020	- .052± .045	+ .117± .035
CF2m-7	3.28	1.150	1.051	.768± .040	.808± .023	- .051± .045	+ .150± .037
CF2f unit (Fig. 27)							
CF2f-1	3.54	1.287	.978	.840± .044	.822± .023	+ .022± .041	+ .287± .041
CF2f-2	4.31	1.322	.848	1.030± .053	.873± .024	+ .152± .036	+ .322± .042
CF2f-3	3.79	1.305	.923	.982± .051	.907± .025	+ .077± .039	+ .305± .042
CF2f-4	3.43	1.247	.950	.848± .044	.805± .023	+ .050± .040	+ .247± .040
CF2f-5	2.90	1.164	1.038	.680± .035	.706± .020	- .038± .044	+ .164± .037
CF2f-6	2.81	1.146	1.086	.595± .031	.646± .018	- .086± .046	+ .146± .037
CF2f-7	2.85	1.152	1.062	.725± .038	.770± .022	- .062± .045	+ .152± .037

Table 3. Isotopic ratios of uranium and thorium required for U-trend plots

		Activity Ratios					
Sample	U ppm	$^{234}U/^{238}U$	$^{230}Th/^{238}U$	$^{238}U/^{232}Th$	$^{230}Th/^{232}Th$	$(^{238}U-^{230}Th)/^{238}U$	$(^{234}U-^{238}U)/^{238}U$
			YM2m section (Fig. 28)				
YM2m-1	2.42	1.051	1.369	0.460± .024	0.630± .018	-0.369± .057	+0.051± .034
YM2m-2	2.35	1.076	1.431	.434± .023	.621± .017	- .431± .060	+ .076± .034
YM2m-3	2.21	1.078	1.416	.393± .020	.556± .016	- .416± .059	+ .078± .034
YM2m-4	2.72	1.159	1.124	.510± .027	.573± .016	- .124± .047	+ .159± .037
YM2m-5	3.83	1.251	.831	.746± .039	.619± .017	+ .169± .035	+ .251± .040
YM2m-6	3.31	1.130	1.034	.597± .031	.617± .017	- .034± .043	+ .130± .036
YM2m-7	3.43	1.133	1.014	.636± .033	.645± .018	- .014± .043	+ .133± .036
YM2m-8	3.54	1.160	1.006	.794± .041	.799± .022	- .006± .042	+ .160± .037
YM2m-9	4.12	1.184	.887	.845± .044	.749± .021	+ .113± .037	+ .184± .038
YM2m-10	3.43	1.199	.925	.868± .045	.803± .022	+ .075± .039	+ .199± .038
			YM2f section (Fig. 28)				
YM2f-1	2.23	1.059	1.402	.455± .024	.638± .018	- .402± .059	+ .059± .034
YM2f-2	2.17	1.104	1.413	.428± .022	.605± .017	- .413± .059	+ .104± .035
YM2f-3	2.08	1.089	1.428	.387± .020	.553± .015	- .428± .060	+ .089± .035
YM2f-4	2.53	1.215	1.137	.527± .027	.599± .017	- .137± .048	+ .215± .039
YM2f-5	3.68	1.283	.884	.738± .038	.652± .018	+ .116± .037	+ .382± .041
YM2f-6	3.09	1.186	1.018	.649± .034	.661± .018	- .018± .043	+ .186± .038
YM2f-7	3.39	1.201	.994	.768± .040	.763± .021	+ .006± .042	+ .201± .038
YM2f-8	3.46	1.194	.999	.876± .046	.876± .025	+ .001± .042	+ .194± .038
YM2f-9	4.06	1.270	.880	1.012± .053	.890± .025	+ .120± .037	+ .270± .041
YM2f-10	3.64	1.233	.911	.907± .047	.826± .023	+ .089± .038	+ .233± .039
			YM13m section (Fig. 29)				
YM13m-1	2.18	1.007	1.589	.442± .023	.702± .020	- .589± .067	+ .007± .032
YM13m-2	1.93	.989	1.769	.309± .016	.547± .015	- .769± .074	- .011± .032
YM13m-3	1.97	1.014	1.755	.338± .018	.593± .017	- .755± .074	+ .014± .032
YM13m-4	1.97	1.012	1.671	.334± .017	.559± .016	- .671± .070	+ .012± .032
Ym13m-5	2.54	1.122	1.406	.460± .024	.647± .018	- .406± .059	+ .122± .036
YM13m-6	3.29	1.164	1.125	.669± .035	.752± .021	- .125± .047	+ .164± .037
YM13m-7	2.90	1.095	1.146	.554± .029	.635± .018	- .146± .048	+ .095± .035
YM13m-8	3.26	1.146	.969	.627± .033	.607± .017	+ .031± .041	+ .146± .037
YM13m-9	2.60	1.056	1.070	.505± .026	.540± .015	- .070± .045	+ .056± .034
YM13m-10	2.87	1.096	.977	.530± .028	.518± .015	+ .023± .041	+ .096± .035
YM13m-11	4.12	1.168	.865	.800± .042	.692± .019	+ .135± .036	+ .168± .037
			YM13f section (Fig. 29)				
YM13f-1	2.29	.999	1.486	.438± .023	.650± .018	- .486± .062	- .001± .032
YM13f-2	2.01	1.017	1.729	.369± .019	.638± .018	- .729± .072	+ .017± .033
YM13f-3	1.99	.966	1.722	.331± .017	.570± .016	- .722± .072	- .034± .031
YM13f-4	2.01	.992	1.681	.334± .017	.562± .016	- .681± .071	- .008± .032
YM13f-5	2.30	1.091	1.491	.443± .023	.660± .018	- .491± .063	+ .091± .035
YM13f-6	3.14	1.186	1.203	.676± .035	.814± .023	- .203± .051	+ .186± .038

Table 3. Isotopic ratios of uranium and thorium required for U-trend plots

Sample	U ppm	$^{234}U/^{238}U$	$^{230}Th/^{238}U$	$^{238}U/^{232}Th$	$^{230}Th/^{232}Th$	$(^{238}U-^{230}Th)/^{238}U$	$(^{234}U-^{238}U)/^{238}U$
		Activity Ratios					
YM13f section (Fig. 29)							
YM13f-7	2.92	1.126	1.128	.544±0.029	.625±0.017	- .128±0.047	+ .126±0.036
YM13f-8	3.51	1.211	.895	.753± .039	.673± .018	+ .011± .042	+ .211± .039
YM13f-9	2.58	1.078	1.105	.513± .026	.567± .016	- .105± .041	+ .078± .034
YM13f-10	2.90	1.122	.980	.552± .029	.541± .038	+ .020± .041	+ .122± .036
YM13f-11	3.54	1.130	1.084	.724± .038	.786± .022	+ .084± .046	+ .130± .036
YM14B upper unit (Fig. 30)							
YM14B-1	2.31	1.060	1.608	.450± .023	.724± .020	- .608± .068	+ .060± .034
YM14B-2	3.95	1.207	.990	.779± .041	.772± .022	+ .010± .042	+ .207± .039
YM14B-3	2.36	1.078	1.695	.466± .024	.790± .022	- .695± .071	+ .078± .034
YM14B-4	2.46	1.082	1.617	.488± .025	.790± .022	- .617± .068	+ .082± .035
YM14B-5	2.46	1.089	1.625	.493± .026	.800± .022	- .625± .068	+ .089± .035
YM14B-6	2.56	1.083	1.588	.512± .027	.812± .023	- .588± .067	+ .083± .035
YM14B-7	2.82	1.119	1.529	.567± .029	.867± .024	- .529± .064	+ .119± .036
YM14B-8	2.89	1.127	1.498	.583± .030	.870± .024	- .498± .063	+ .127± .036
YM14B-9	3.30	1.140	1.428	.690± .036	.986± .028	- .428± .063	+ .140± .036
YM14 upper unit (Fig. 31)							
YM14-1	2.09	1.024	1.452	0.503± .026	0.730± .020	-0.452± .061	+0.024± .033
YM14-2	2.08	1.002	1.569	.435± .023	.682± .019	- .569± .066	+ .002± .032
YM14-3	2.10	1.040	1.566	.436± .023	.683± .019	- .566± .066	+ .040± .033
YM14-4	2.26	1.041	1.591	.456± .024	.725± .020	- .591± .067	+ .041± .033
YM14-5	2.20	1.050	1.553	.440± .023	.684± .019	- .553± .065	+ .050± .034
YM14-6	2.28	1.048	1.539	.468± .024	.720± .020	- .539± .065	+ .048± .034
YM14-7	2.39	1.079	1.674	.470± .024	.787± .022	- .674± .070	+ .079± .035
YM14-8	2.74	1.088	1.620	.565± .029	.914± .026	- .620± .068	+ .088± .035
YM14-9	3.05	1.184	1.465	.655± .034	.960± .027	- .465± .062	+ .184± .038
YM14 section (Fig. 31)							
YM14-10	4.63	1.314	.881	1.144± .059	1.009± .028	+ .119± .037	+ .314± .042
YM14-11	4.44	1.246	.758	1.378± .072	1.044± .029	+ .242± .032	+ .246± .040
YM14-12	5.60	1.262	.894	2.829± .147	2.530± .071	+ .106± .038	+ .262± .040
YM14-13	5.83	1.265	.906	3.149± .164	2.852± .080	+ .094± .038	+ .265± .040
YM14-14	4.26	1.362	.938	11.29± .59	10.60± .30	+ .062± .039	+ .362± .044
YM14-15	2.46	1.101	.988	1.000± .052	.988± .028	+ .012± .041	+ .101± .035
YM14-16	2.39	1.053	.963	.838± .044	.807± .023	+ .037± .040	+ .053± .034
YM14-17	2.67	.972	.958	.872± .045	.835± .023	+ .042± .040	- .028± .031
YM14-18	3.16	.949	.980	.759± .039	.743± .021	+ .020± .041	- .051± .030
YM14-19	3.40	.968	.986	.916± .048	.903± .025	+ .014± .041	- .032± .031
YM14-20	3.55	.952	.997	.700± .036	.697± .020	+ .004± .042	- .048± .030
YM14-21	5.22	.936	.999	1.345± .069	1.345± .038	+ .001± .042	- .064± .030
YM14-22	3.80	.906	.947	.757± .039	.717± .020	+ .053± .040	- .094± .029

Table 3. Isotopic ratios of uranium and thorium required for U-trend plots

Sample	U ppm	Activity Ratios					
		$^{234}U/^{238}U$	$^{230}Th/^{238}U$	$^{238}U/^{232}Th$	$^{230}Th/^{232}Th$	$(^{238}U-^{230}Th)/^{238}U$	$(^{234}U-^{238}U)/^{238}U$
CBQ unit (Fig. 32)							
CBQ-1	2.07	1.045	1.147	.555±0.020	.637±0.020	- .147±0.048	+ .045±0.033
CBQ-2	2.46	1.121	.996	.673± .035	.671± .021	+ .005± .042	+ .121± .036
CBQ-3	2.88	1.191	.888	.766± .040	.680± .022	+ .112± .037	+ .191± .038
CBQ-4	2.99	1.205	.827	.884± .044	.698± .022	+ .173± .035	+ .205± .039
CBQ-5	2.54	1.151	.987	.702± .037	.693± .022	+ .013± .042	+ .151± .037
CBQ-6	2.85	1.199	.955	.844± .044	.806± .026	+ .045± .044	+ .199± .038
CBQ-7	2.09	1.116	1.073	.604± .031	.648± .021	- .073± .045	+ .116± .036
CBQ-8	2.78	1.189	.975	.833± .043	.812± .026	+ .025± .043	+ .189± .038
FHA unit (Fig. 33)							
A15-A	4.79	1.295	1.189	.697± .036	.828± .023	- .189± .050	+ .189± .038
A15-B	3.72	1.268	1.220	.499± .026	.609± .017	- .220± .051	+ .268± .041
A15-C	4.01	1.346	.826	.737± .038	.609± .017	+ .174± .035	+ .346± .043
A15-D	7.17	1.367	1.239	.753± .039	.933± .026	- .239± .052	+ .367± .044
A15-E	4.41	1.346	1.542	.381± .020	.588± .016	- .542± .065	+ .346± .043
S3 unit (Fig. 34)							
S3-A	2.90	1.241	1.209	1.035± .054	1.251± .035	- .209± .051	+ .241± .040
S3-B	2.42	1.215	1.524	.679± .036	1.065± .030	- .524± .064	+ .215± .039
S3-C	3.57	1.176	1.180	1.257± .065	1.483± .042	- .180± .050	+ .176± .038
S3-D	2.42	1.161	1.248	.837± .044	1.044± .029	- .248± .052	+ .161± .037
S3-E	2.25	1.156	1.129	.744± .040	.874± .024	- .129± .047	+ .156± .037
S3-F	2.46	1.189	1.031	.868± .045	.895± .025	- .031± .043	+ .189± .038
S3-G	2.33	1.173	1.032	.845± .044	.868± .024	- .032± .043	+ .173± .038
S3-H	2.29	1.187	1.249	.803± .042	1.003± .028	- .249± .052	+ .187± .038

Table 4. Uranium-trend model parameters and ages of deposition units in NTS area.

Unit	Description of Deposit	U-trend slope	X intercept	Half period of F(O) (Ka)	Age Ka
39	FFPG unit,eolian surface Frenchman Flat Trench	+0.276	-0.721	73	30±30
40	S1 unit, alluvium, upper part, Frenchman Flat Trench	+ .706	- .682	74	80±60
41	F2 unit, buried B horizon Frenchman Flat Trench	+ .417	- .208	400	200±80
42	F3 unit, alluvium lower part, Frenchman Flat Trench	+ .331	- .196	440	190±70
43	RV1 section, (A-D) unit Rock Valley Trench 1	+ .238	- .671	74	31±10
44	RV1 section, (E-I) unit, Rock Valley Trench 1	+ .590	- .039	660	310±40
45	RV1 section, (J-O) unit, Rock Valley Trench 1	+ .219	- .539	82	37±24
46	RV1 section, (P-U) unit, Rock Valley Trench 1	+ .759	- .273	250	180±40
47	RV1 section (V-Z) unit, Rock Valley Trench 1	+ .628	- .157	500	270±30
48	TSV 307 unit, upper part Rock Valley Trench 2	+ .249	- .496	86	38±10
49	RV2 section, upper part, Rock Valley Trench 2	+ .250	- .500	84	36±20
50	RV2 section, lower part Rock Valley Trench 2	+2.121	- .004	700	390±100
51	Q2S unit, sand sheet, Jackass Flat Engine Test Trench	+ .428	- .210	400	160±90
52	S9 unit, alluvium, upper part, Jackass Divide Trench	+ .545	- .112	560	270±35
53	JD unit, alluvium, lower part Jackass Divide Trench	-3.87	- .033	660	430±40

Table 4. Uranium-trend model parameters and ages of deposition units (cont.)

Unit	Description of Deposit	U-trend slope	X intercept	Half period of F(O) (Ka)	Age Ka
54	SCF4 section, lower unit (upper part) South Crater Flat Trench	-1.78	+ .008	730	400±50
55	SCF4 section, lower unit (lower part) South Crater Flat Trench	-2.38	- .002	730	480±60
56	TSV 396 unit, carbonate enriched zone Crater Flat Trench 1	+ .400	- .648	76	48±20
57	CF1 unit, upper unit Crater Flat Trench 3	+ .313	- .674	74	40±10
58	CF6 unit, lower B horizon Crater Flat Trench 3	+1.42	- .290	210	190±50
59	CF2 unit, lower unit Crater Flat Trench 3	+ .985	- .191	440	270±30
60	YM2 section, upper unit Yucca Mountain Trench 2	+ .401	- .603	77	47±18
61	YM2 section, lower unit Yucca Mountain Trench 2	+ .594	- .287	220	145±25
62	YM-13 section, upper unit Yucca Mountain Trench 13	- .326	+ .723	74	41±10
63	YM13 section, lower unit Yucca Mountain Trench 13	+ .600	- .197	430	240±50
64	YM14B section, lower B horizon upper & lower B horizons Yucca Mountain Trench 14	+ .315 +1.58	- .881 - .612	72 77	38±10 55±20
65	YM14M section, carbonate enriched zone Yucca Mountain Trench 14	- .523	+ .675	74	270±90
66	YM14L section, sandy horizon Yucca Mountain Trench 14	-4.61	+ .040	660	420±50
67	YM14G section, gravel horizon Yucca Mountain Trench 14	-1.26	- .027	680	480±90
68	CBQ unit, alluvium, Shoshone, CA Charlie Brown Quarry	+ .522	- .266	270	160±25
69	FHA unit, altered ash Fairbanks Hills, NV	- .303	+1.17	70	> 600
70	S3 unit, QTA terrace Eleana Pediment	- .176	+2.22	70	> 800

Table 5. Summary of stratigraphic units and their U-trend ages in the NTS area

Stratigraphic unit	Sample Suite	Sample location	U-trend Age (Ka)	Comments
Q2	FFPG	Frenchman Flat	30 ± 30	Clayey silt of eolian deposit
Q2a	RV1-AD	Rock Valley	31 ± 10	Slope wash
	RV1-JO	Rock Valley	37 ± 24	Buried B-horizon
	TSV-307	Rock Valley	38 ± 10	Gravel alluvium
	RV2U	Rock Valley	36 ± 20	Buried B-horizon
	CF1	Crater Flat	40 ± 10	Pebbly fan gravel
	YM2U	Yucca Mountain	47 ± 18	Buried B-horizon
	YM13U	Yucca Mountain	41 ± 10	Buried B-horizon
	YM14B	Yucca Mountain	38 ± 10	Buried B-horizon
	YM14U	Yucca Mountain	55 ± 20	Buried B-horizon
Q2b	S1	Frenchman Flat	80 ± 60δ	Poor age, unit recollected as F2/3
	F2	Frenchman Flat	200 ± 80	Buried B-horizon
	F3	Frenchman Flat	190 ± 70	Pebbly fan gravel
	RV1-PU	Rock Valley	180 ± 40	Calcareous B-horizon
	CF6	Crater Flat	190 ± 50	Buried B-horizon
	YM2L	Yucca Mountain	145 ± 25	Gravel alluvium
	CBQ	Shoshone, CA	160 ± 25	Pebbly alluvium
Q2c Younger unit	RV1-EI	Rock Valley	310 ± 40	Alluvium
	RV1-VZ	Rock Valley	270 ± 30	K-horizon
	S9	Jackass Divide	270 ± 35	Alluvium
	CF2	Crater Flat	270 ± 30	Gravel alluvium
	YM13L	Yucca Mountain	240 ± 50	Gravel alluvium
Q2c Older unit	RV2L	Rock Valley	390 ± 100	Gravel alluvium
	JD	Jackass Divide	430 ± 40	Gravel alluvium
	SCF4	South Crater Flat	440 ± 60	Average age of two different facies in alluvium deposit
Q2s	Q2S	Jackass Flat	160 ± 90	Large error-higher limit age range suggested
	YM14M	Yucca Mountain	270 ± 90	Laminar carbonate--indicates time of calcium carbonate development
	YM14L	Yucca Mountain	420 ± 50	Cca-horizon in sand deposit
	YM14G	Yucca Mountain	480 ± 90	Basalt gravel in sand deposit.
Q2e	FHA	Fairbanks Hills	>600	Poor plot, exceeds time range of method
QTa	S3	Eleana Pediment	>800	Exceeds time range of method

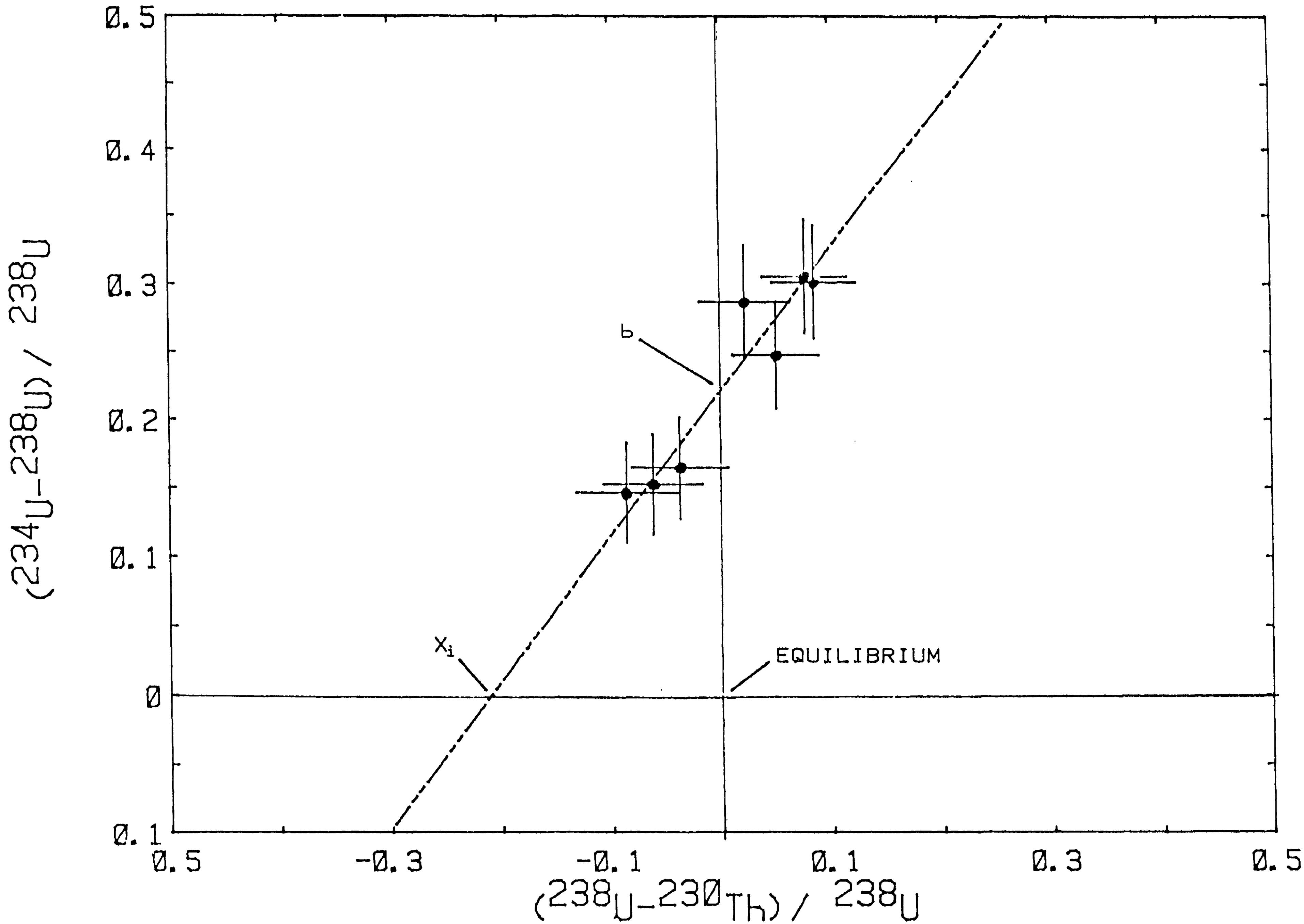

Figure 1. Uranium-trend plot of CF2 alluvium in Crater Flat Trench 3. All samples plotted in terms of activity ratios.

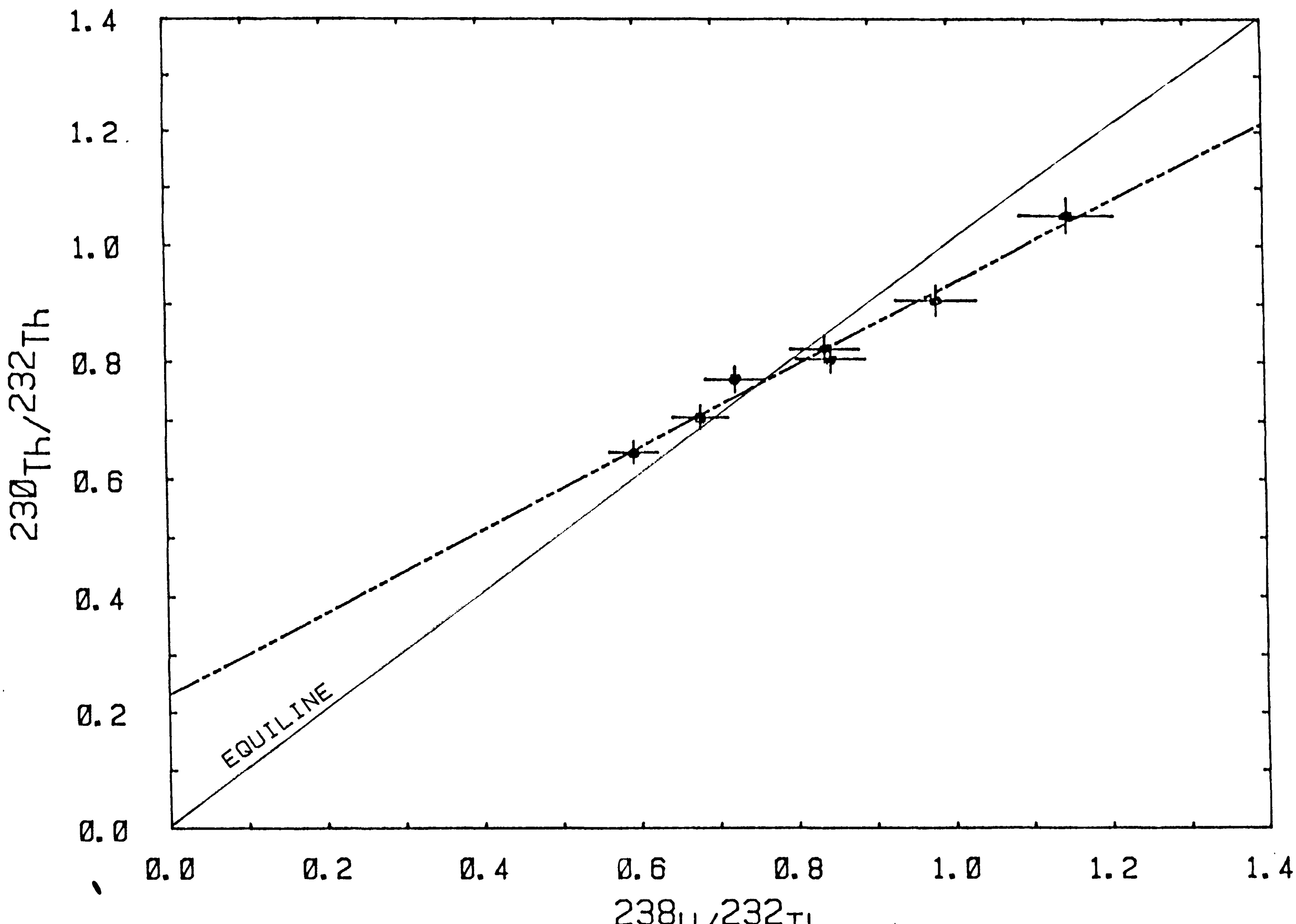

Figure 2. Thorium plot of CF2 alluvium in Crater Flat Trench 3. All samples plotted in terms of activity ratios.

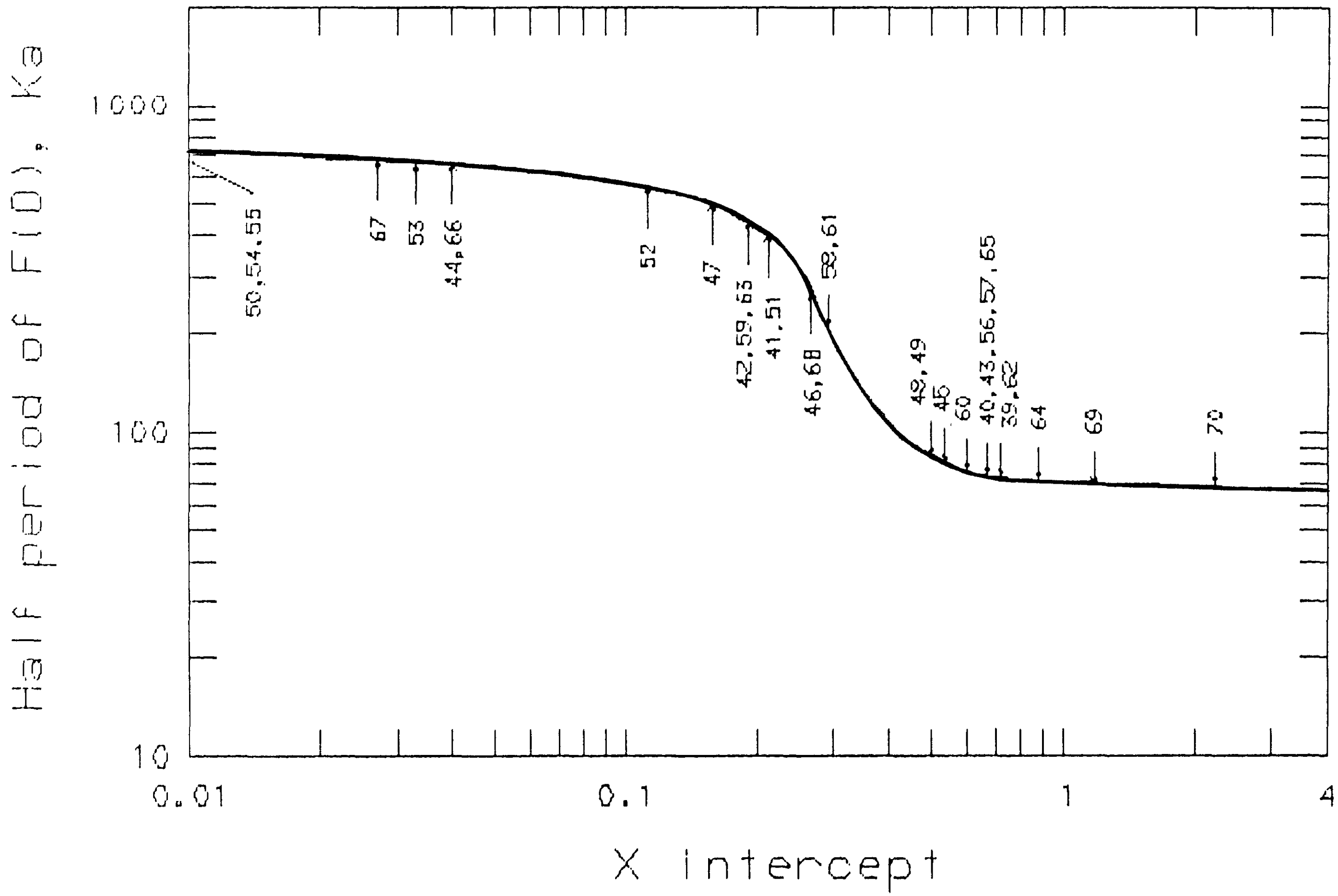

Figure 3. Calibration curve for determination of F(O) from X-intercept value. Indices on curve show unit number from Tables 3 and 4.

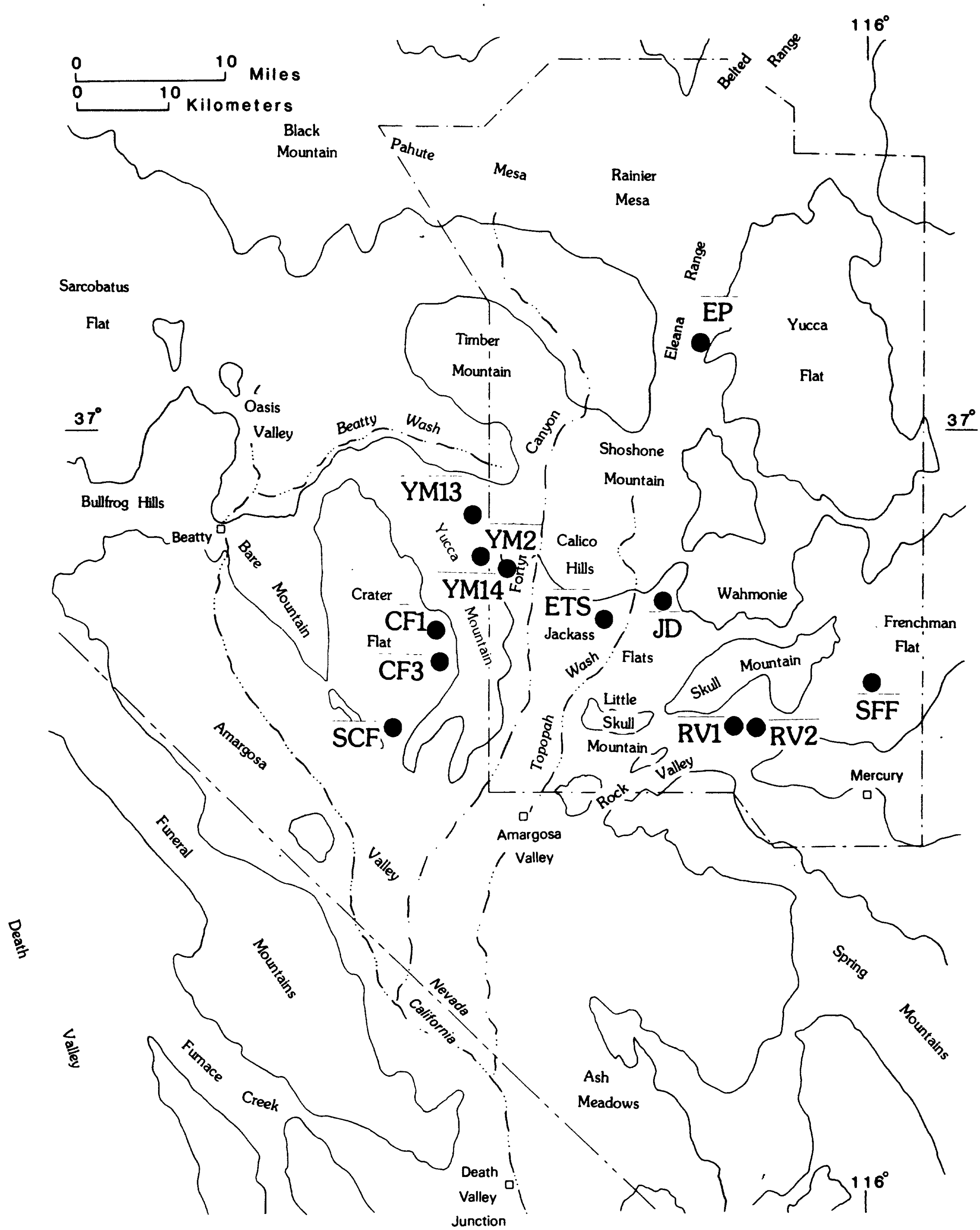

Figure 4. Location of sampling sites (see Table 1) for U-trend dating in the Nevada Test Site area.

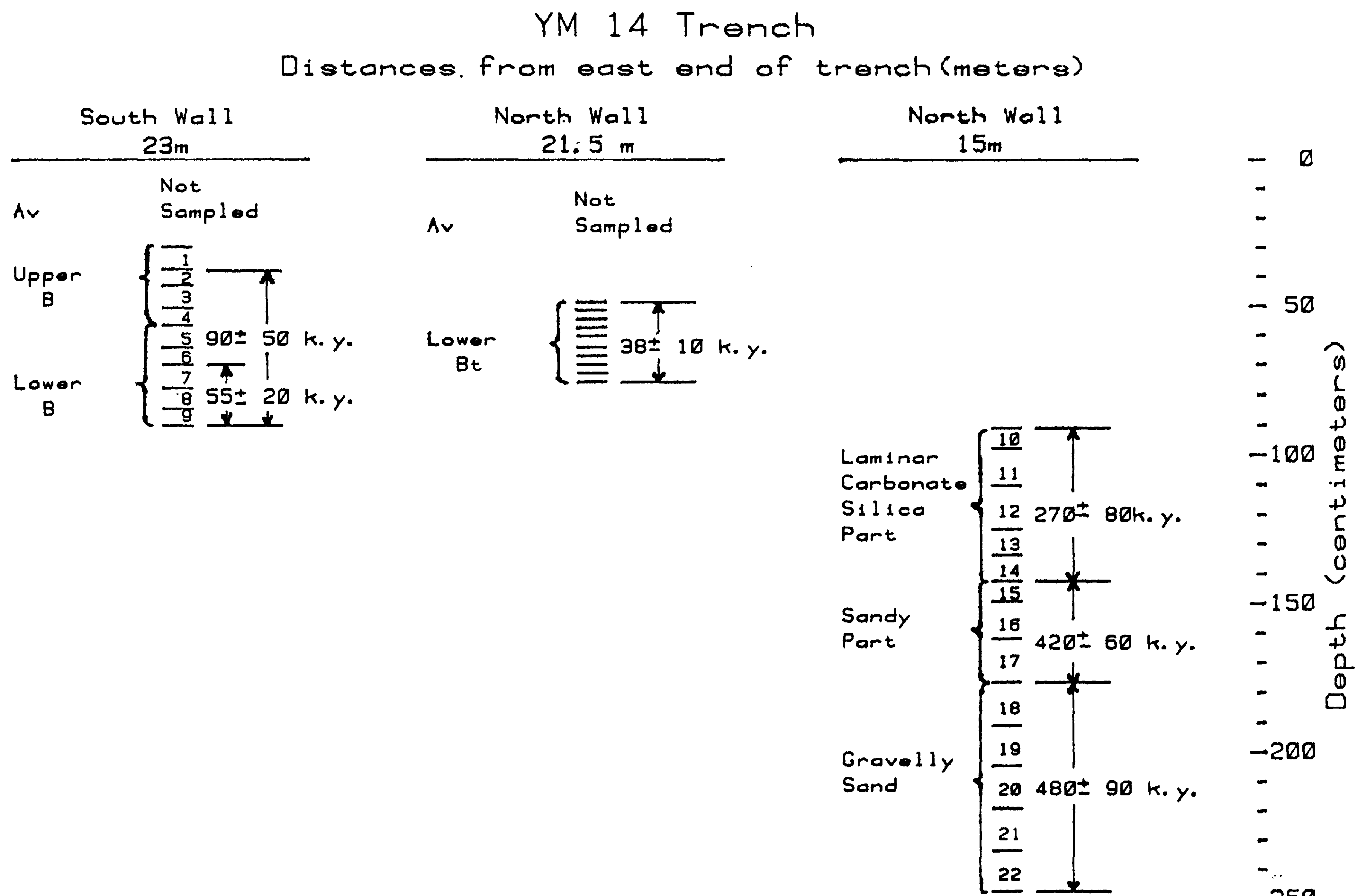

Figure 5. Sample sites in Yucca Mountain Trench 14.

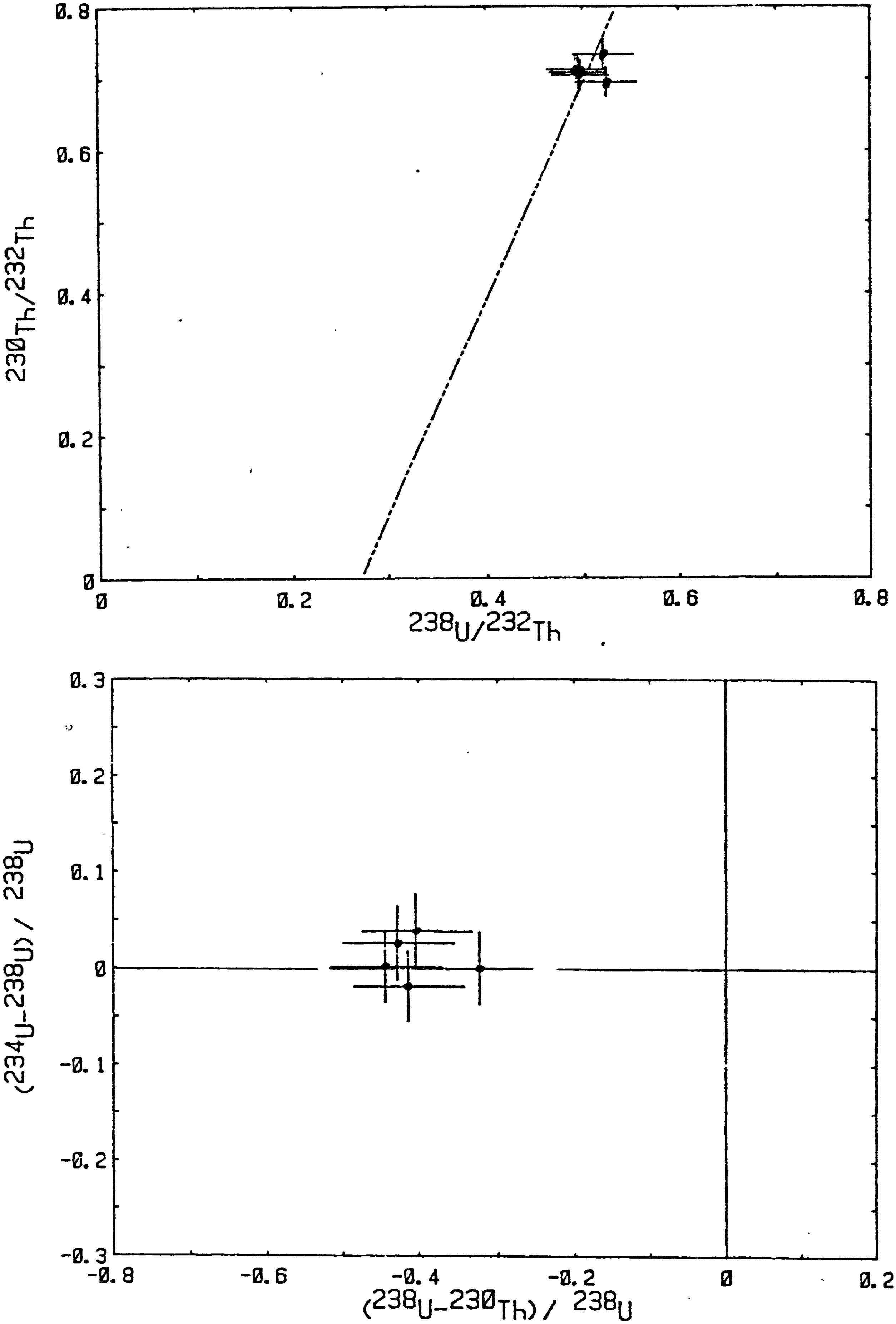

Figure 6. Plots of SFF unit, eolian sand, Frenchman Flat Trench. No age could be calculated because of the circular array of data points.

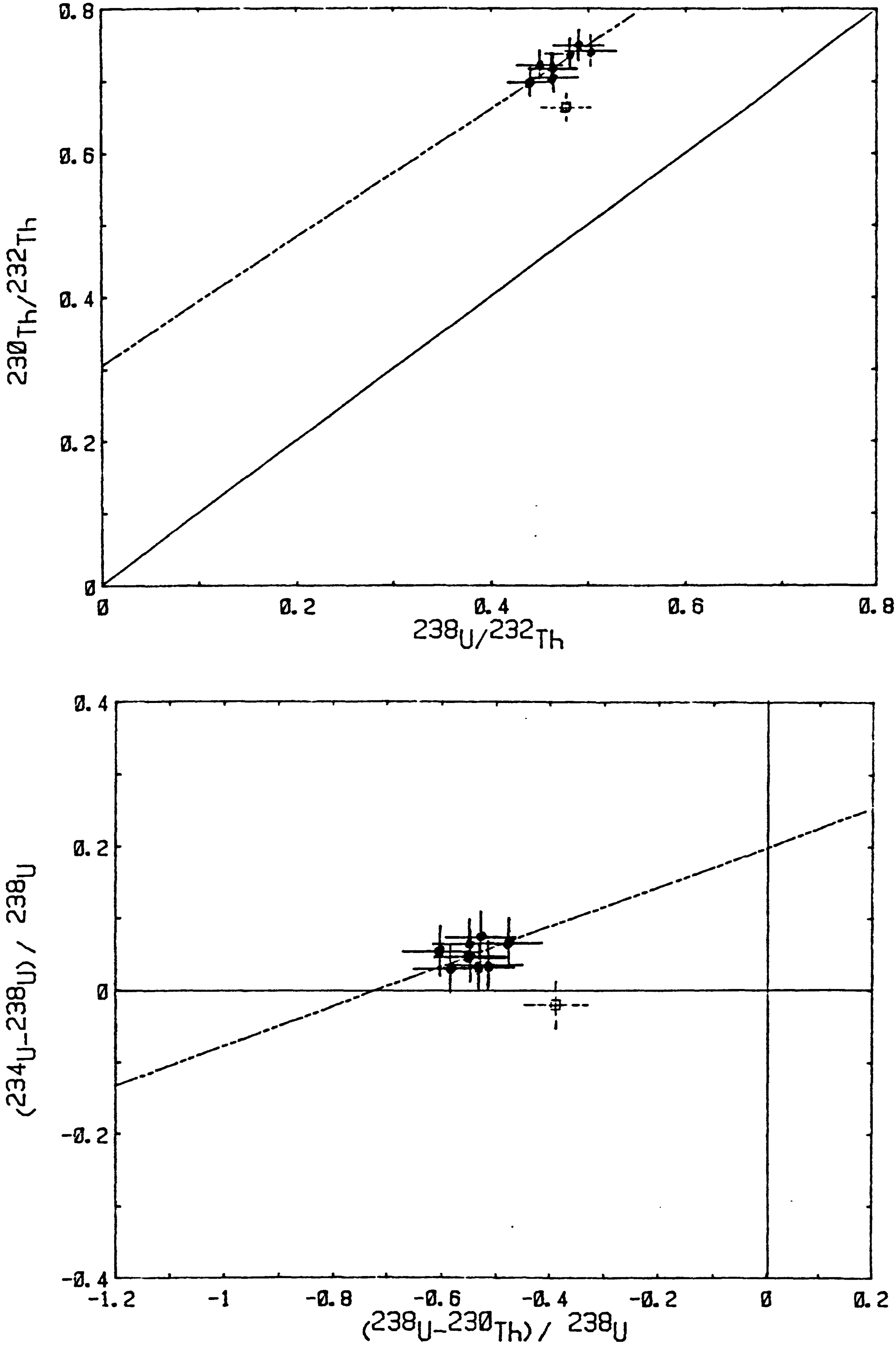

Figure 7. Plots of FFPG unit, eolian sand in Frenchman Flat Trench. The uppermost sample, □, is not included in U-trend slope because it may contain material from overlying deposit.

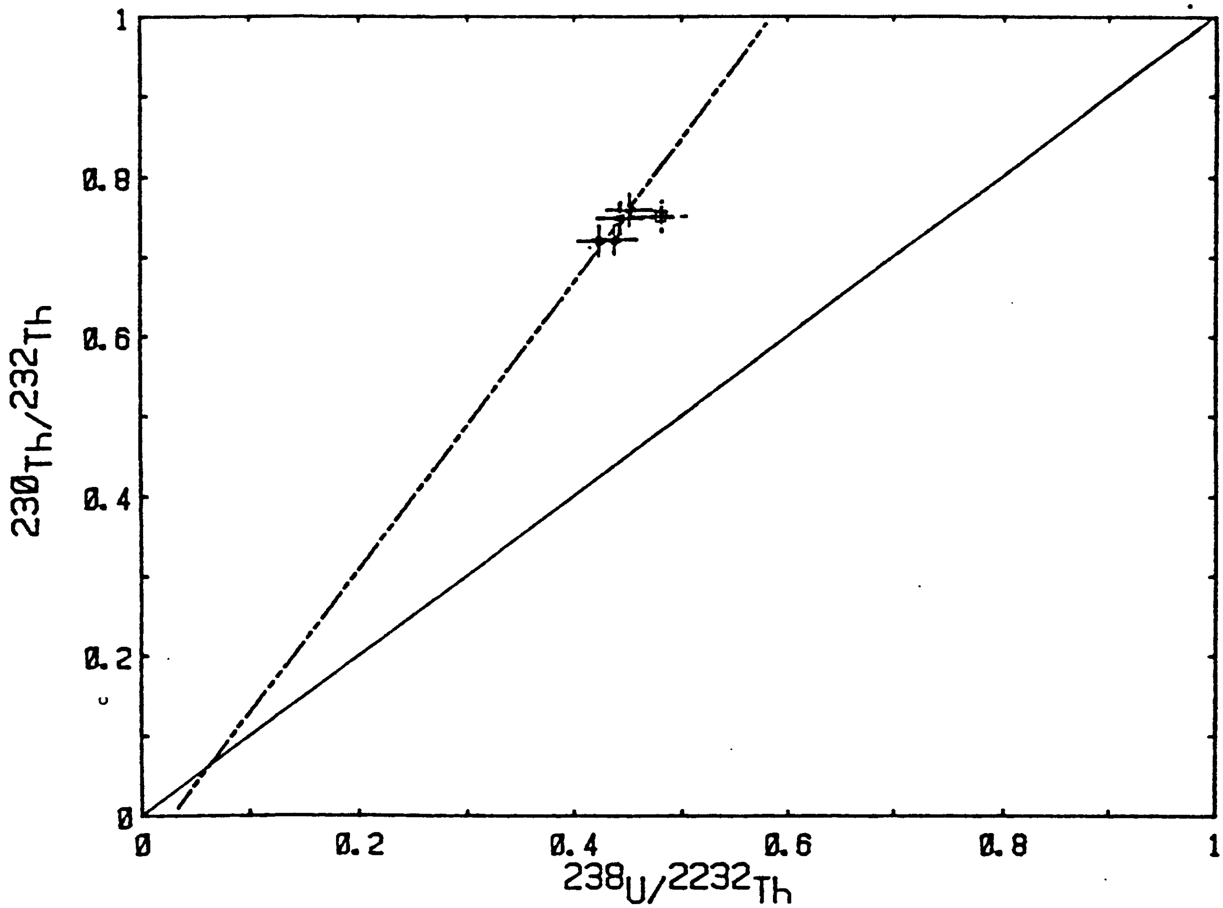

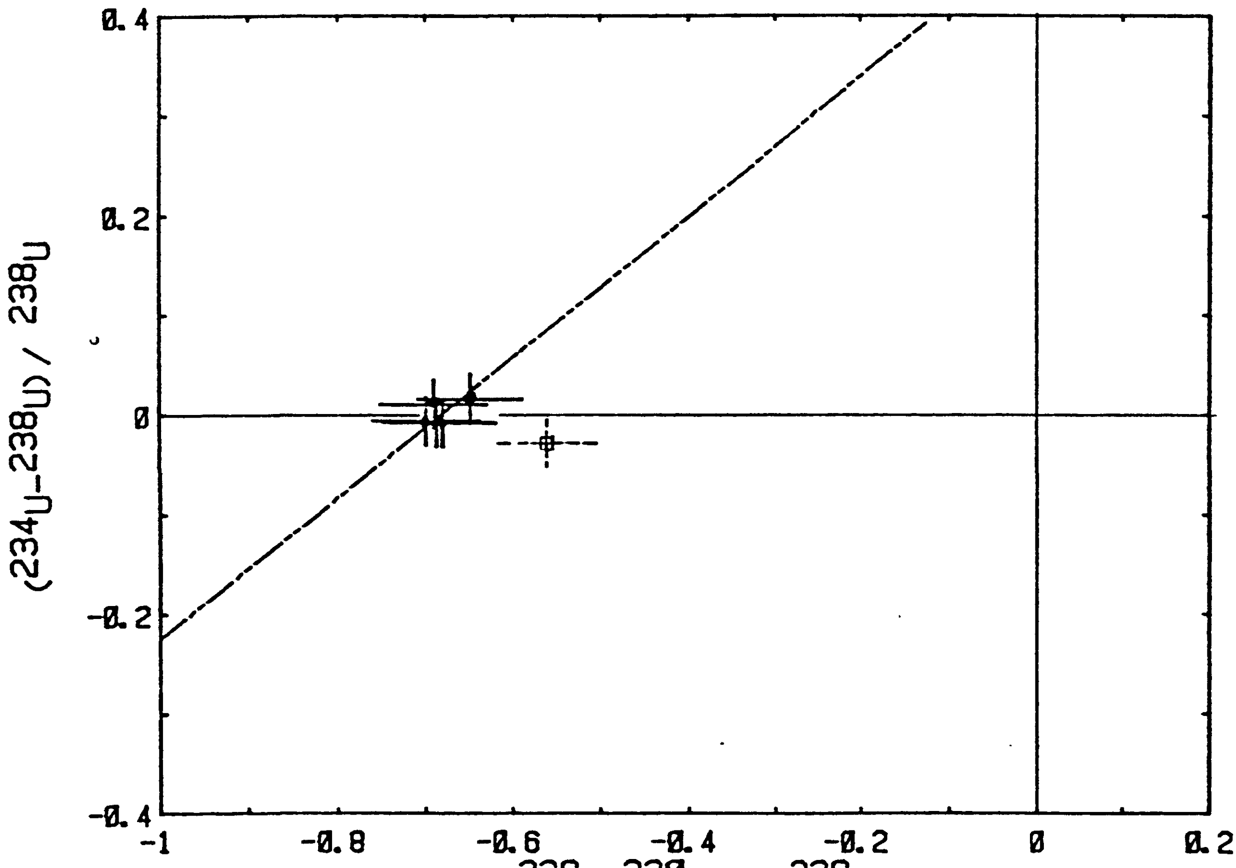

Figure 8. Plots of S1 unit, alluvium in Frenchman Flat Trench. The uppermost sample, □, is not included in the U-trend slope because it may contain material from the overlying deposit.

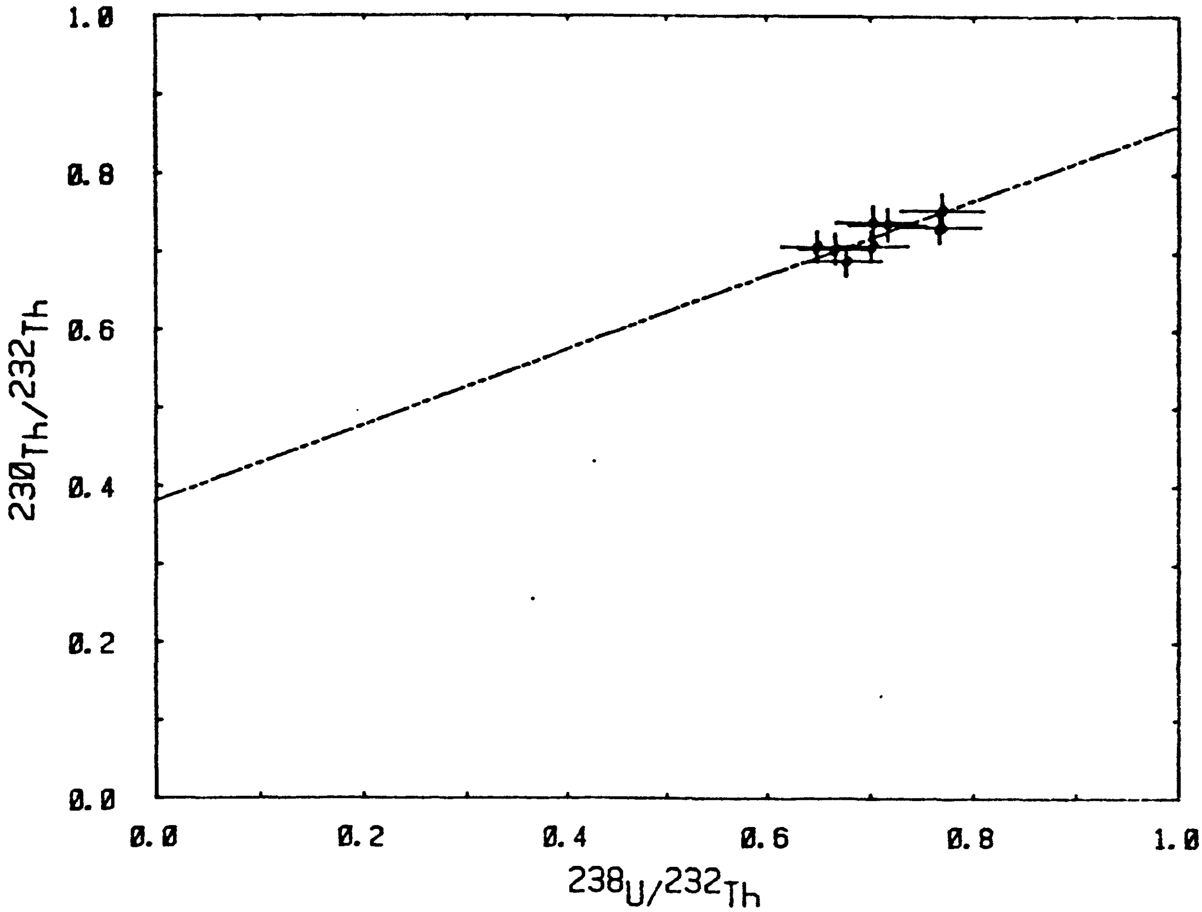

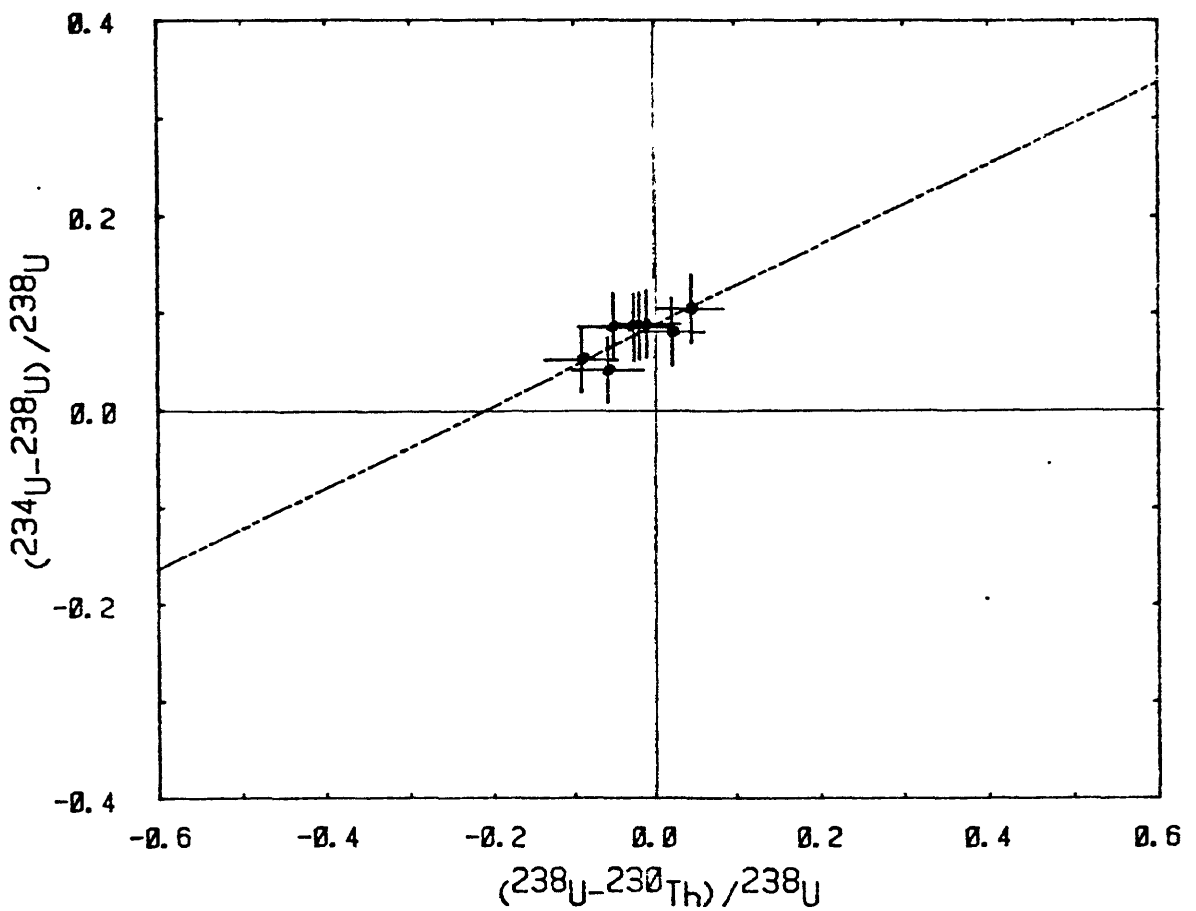

Figure 9. Plots of F2 unit, buried B horizon, Frenchman Flat Trench.

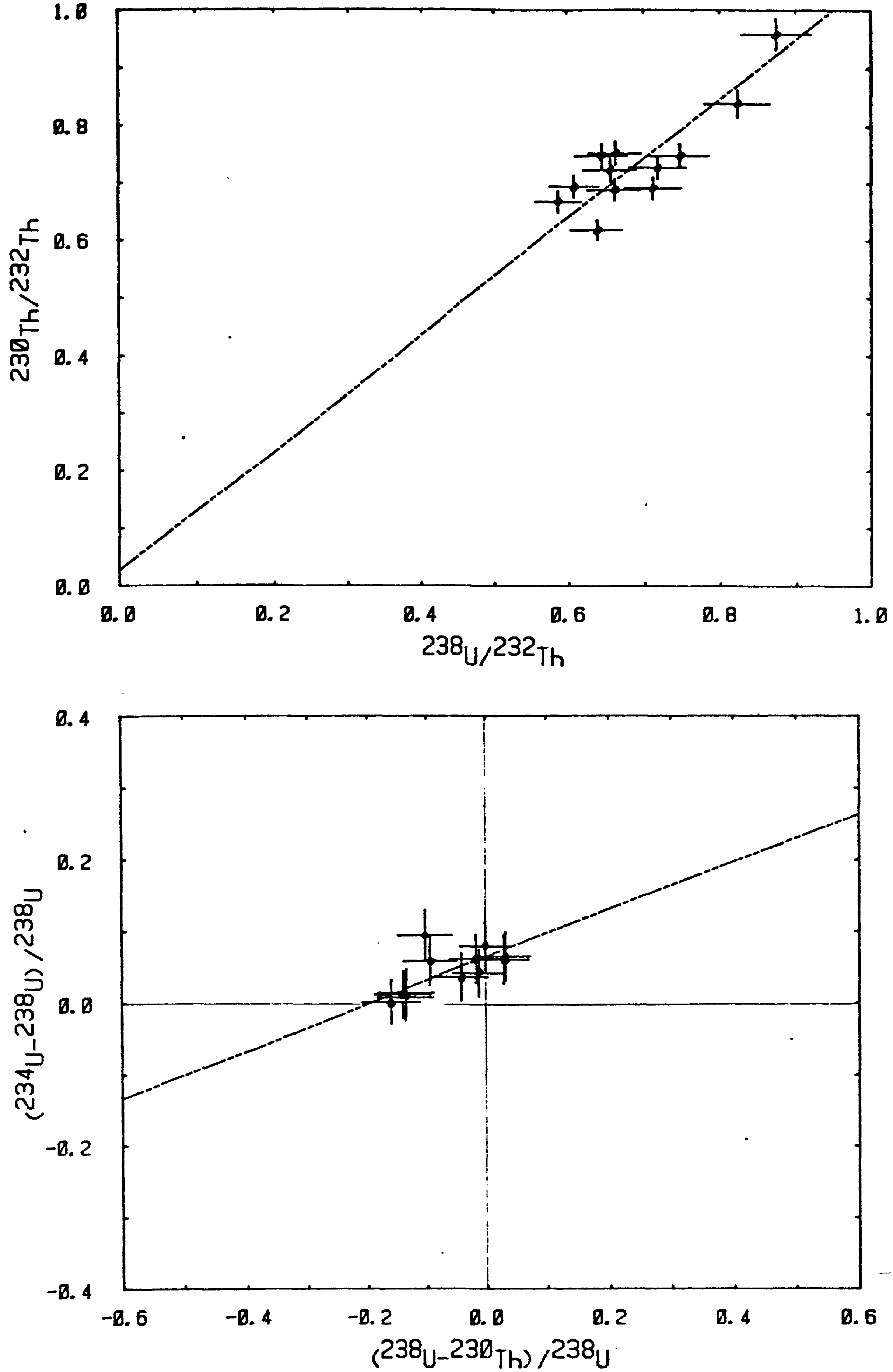

Figure 10. Plots of F3 unit, pebbly fan gravel, Frenchman Flat Trench.

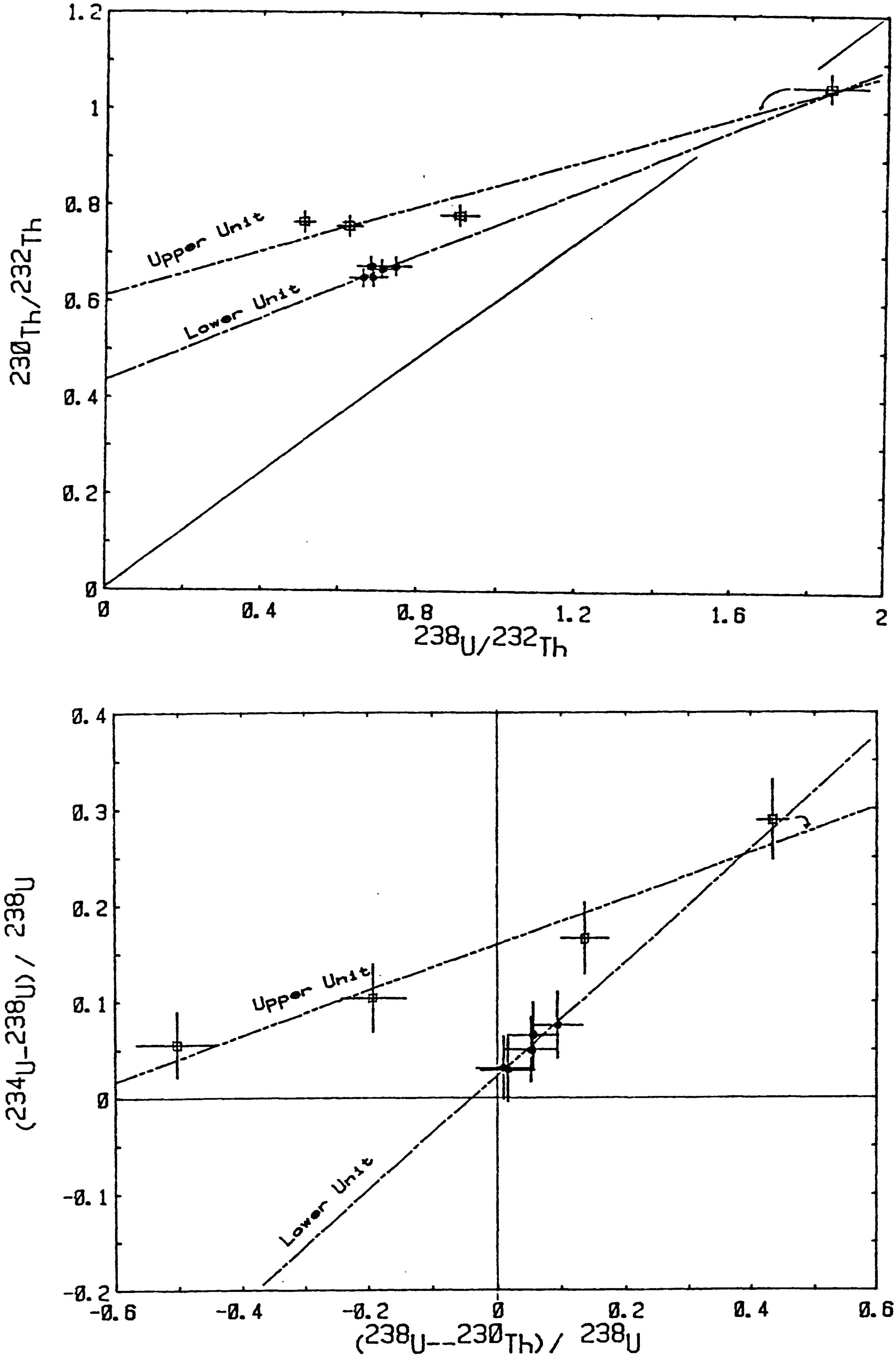

Figure 11. Plots of RV1 section, upper and lower alluvium in Rock Valley Fault Trench 1.

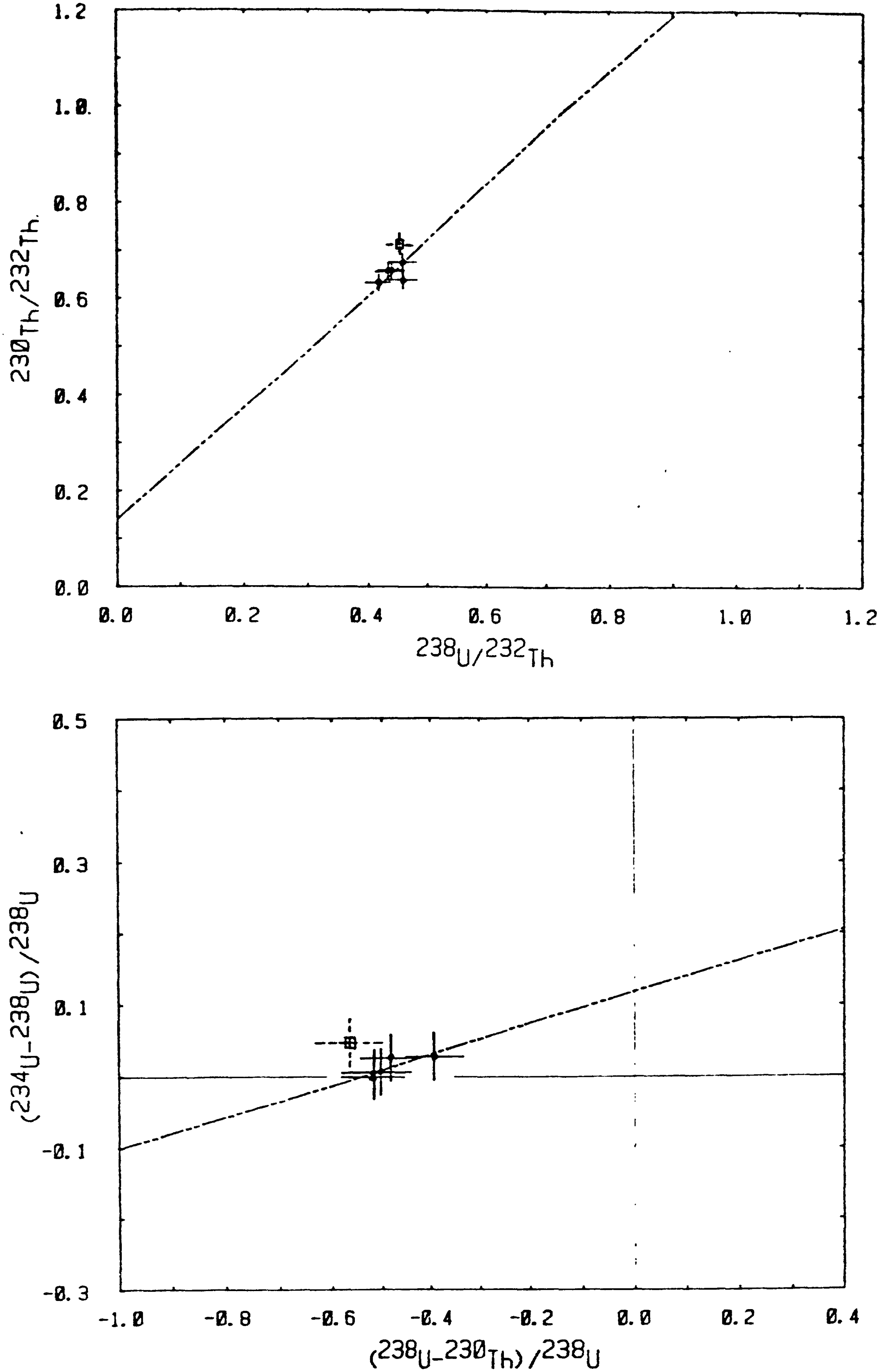

Figure 12. Plots of RV1(J-O) unit, buried B horizon, Rock Valley Trench 1. Upper Sample J, □, is not included in the U-trend slope.

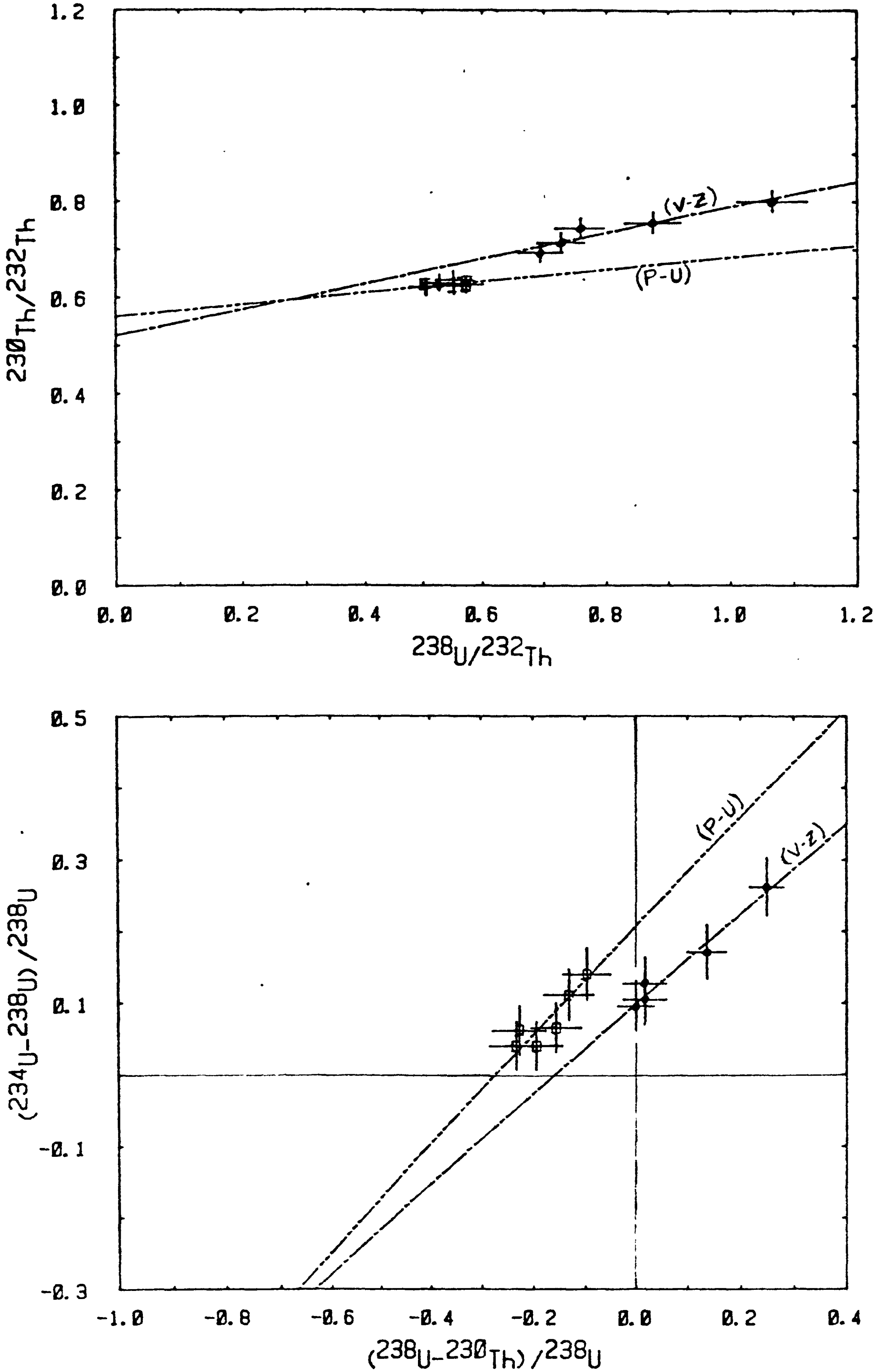

Figure 13. Plots of RV1 section, calcareous B horizon, □(P-U), and K horizon, ●(V-Z), in Rock Valley Trench 1.

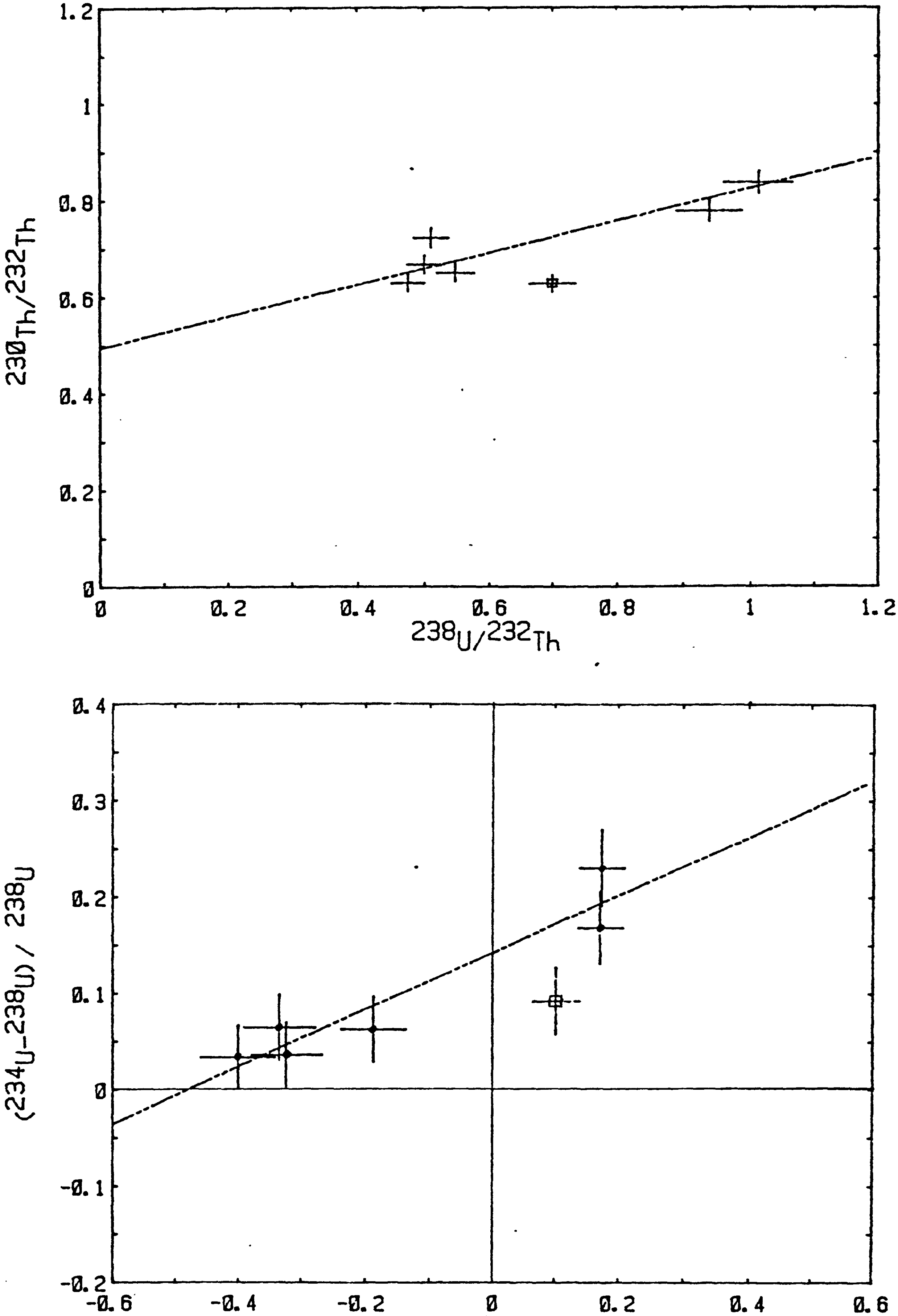

Figure 14. Plots of TSV307 unit, alluvium with caliche horizon in Rock Valley Fault Trench 2. Caliche horizon, □, is not included in U-trend slope.

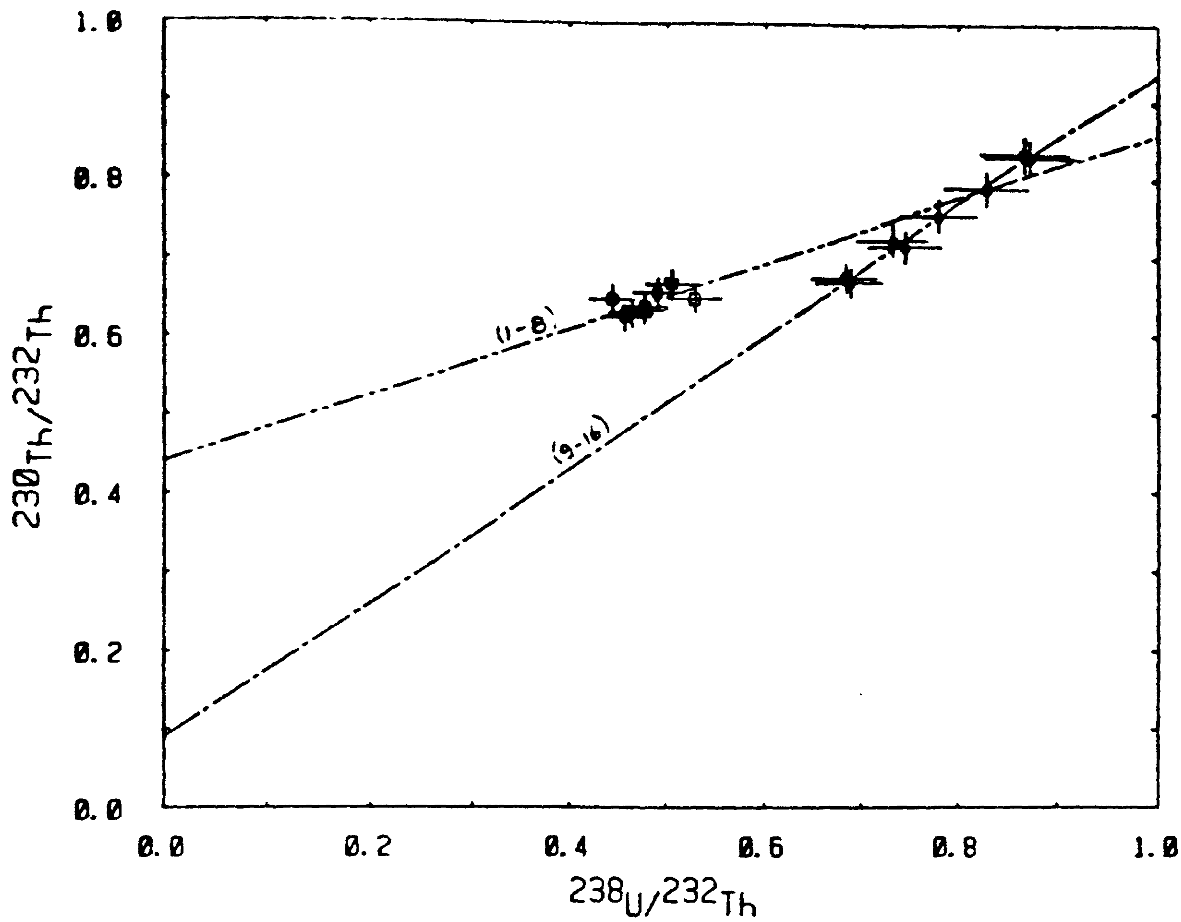

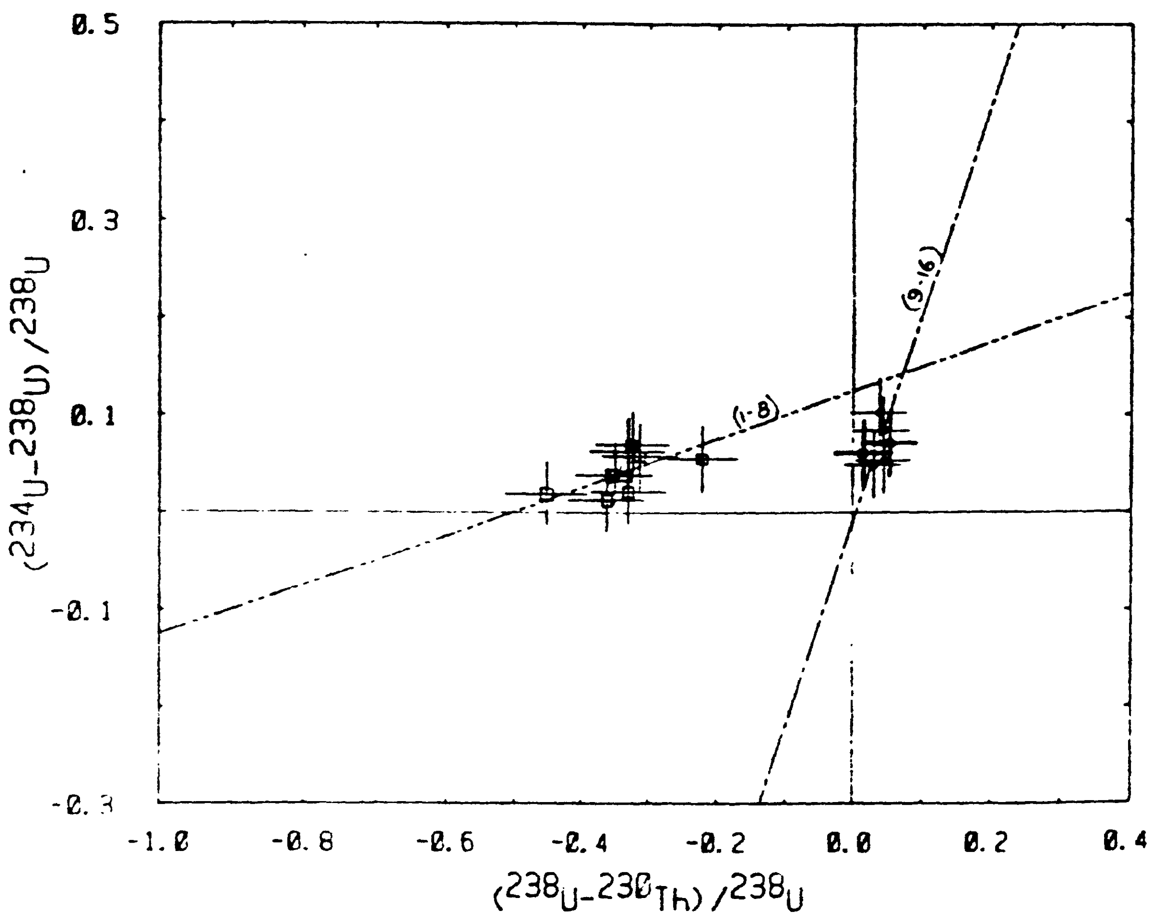

Figure 15. Plots of RV2 Section, buried B horizon □, and gravel alluvium ●, in Rock Valley Trench 2.

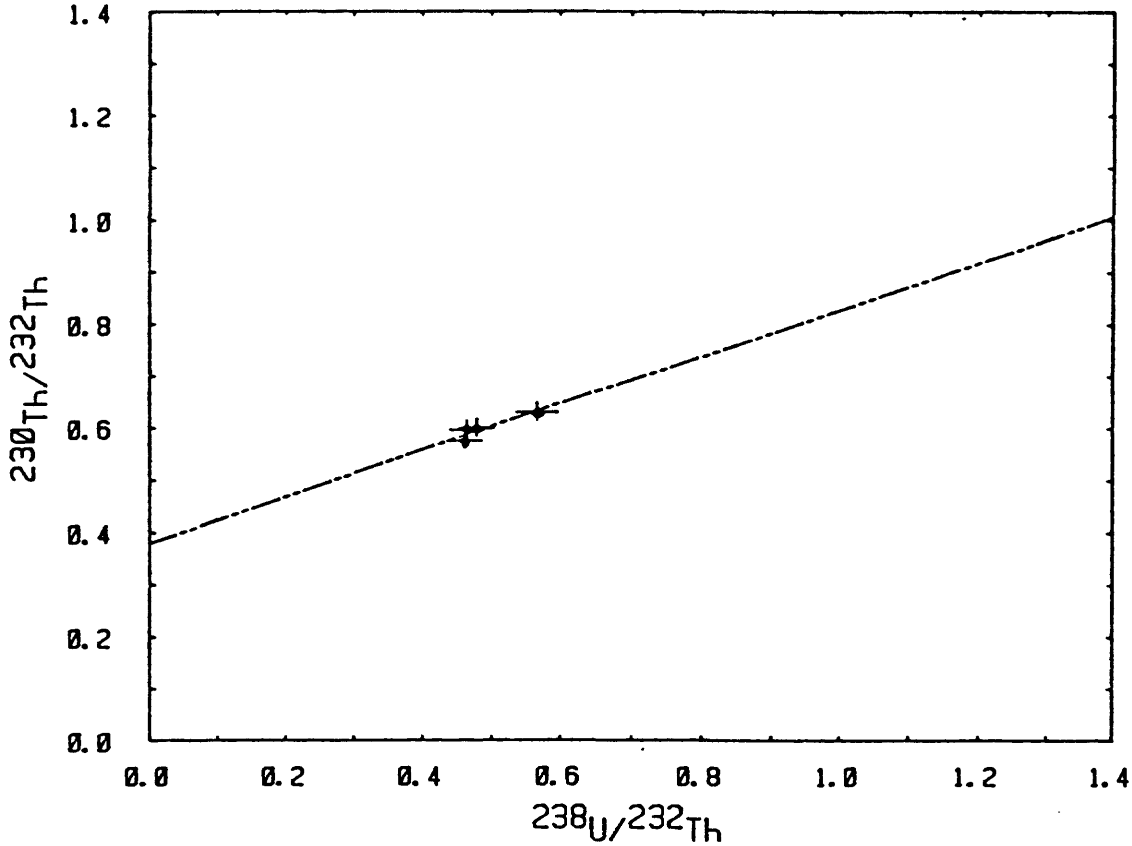

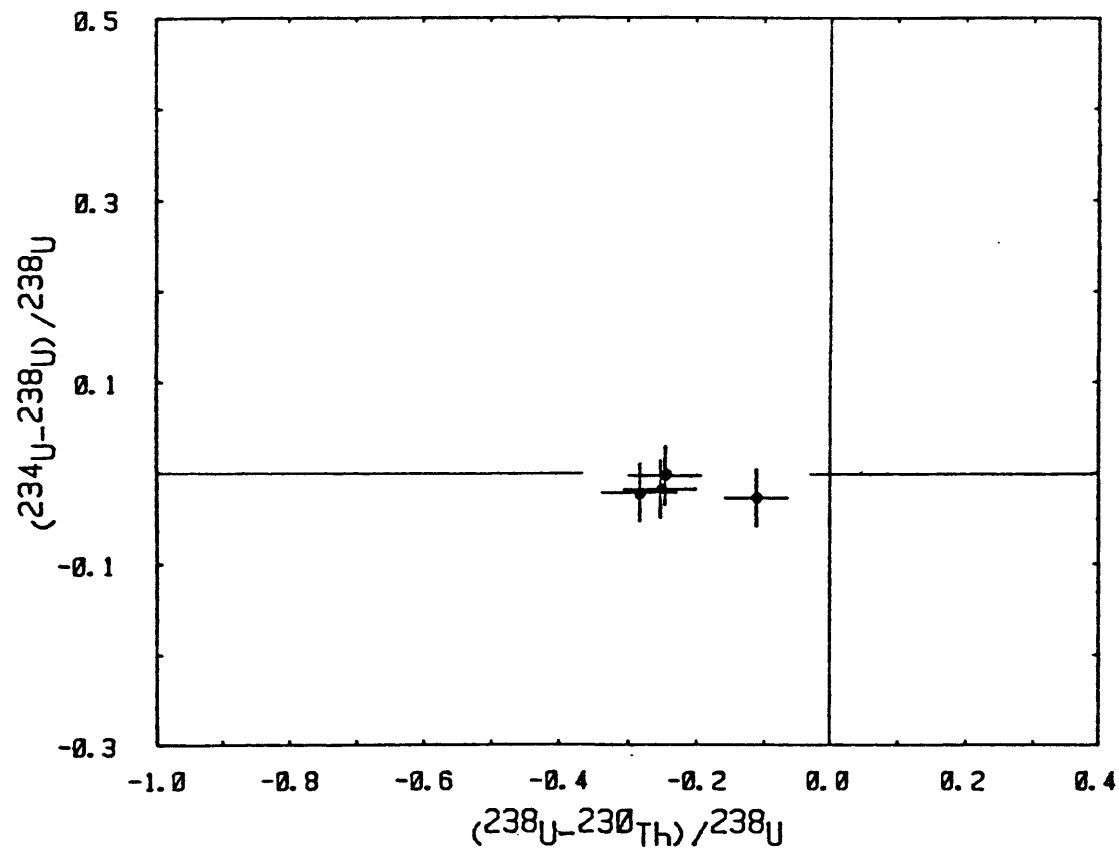

Figure 16. Plots of Q2E unit, sand sheet deposit in Jackass Flat Engine Test Stand Trench. The 4-sample profile was not datable.

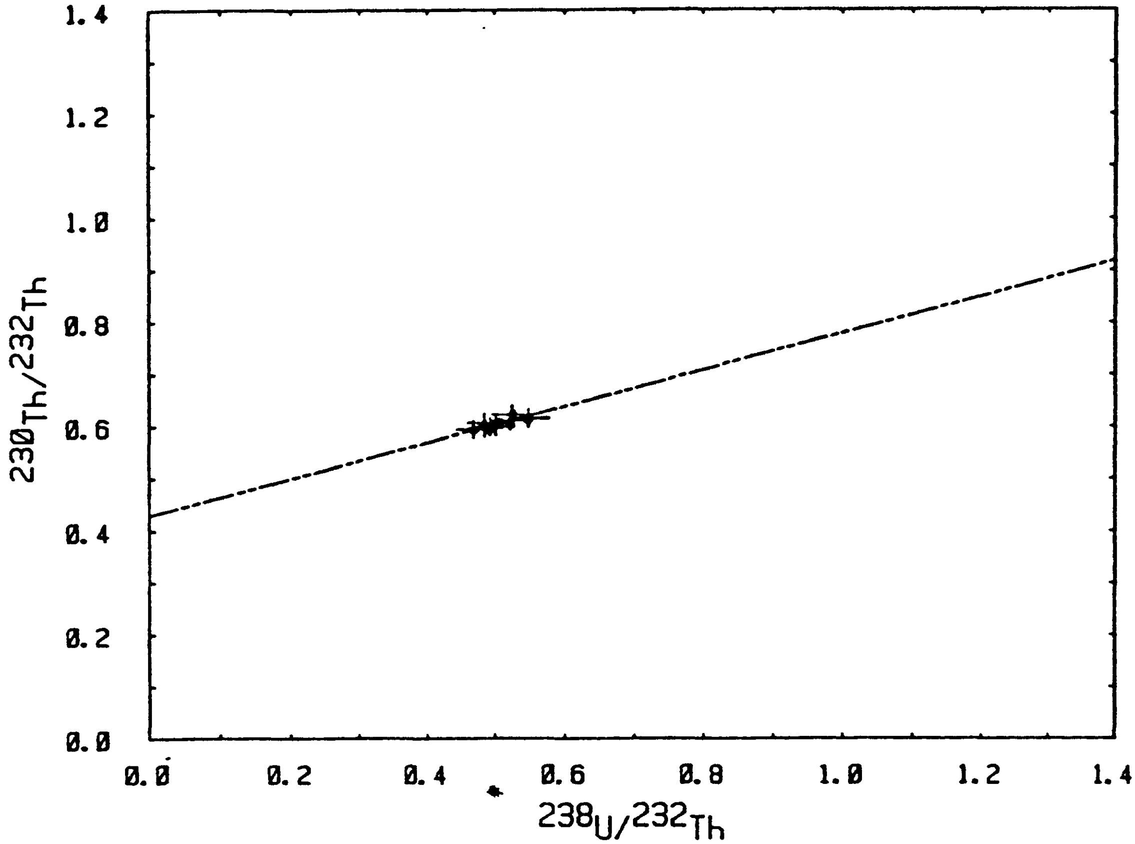

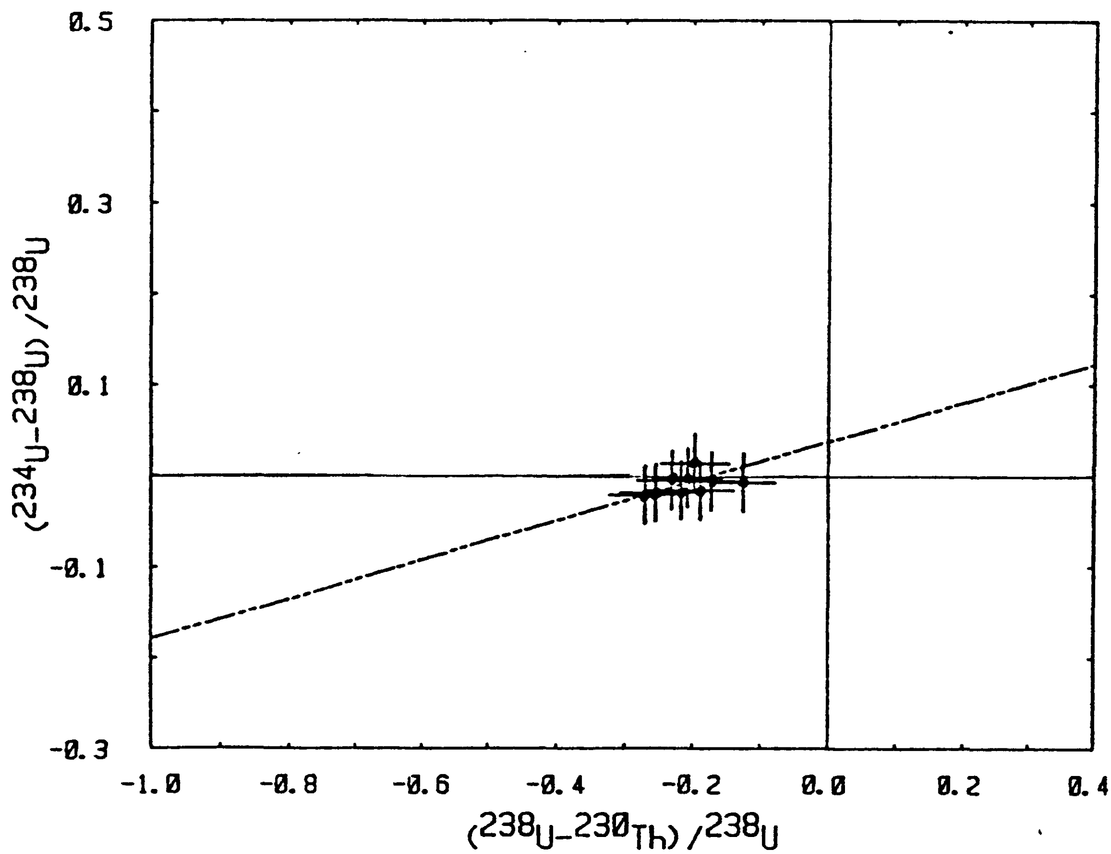

Figure 17. Plots of Q2S unit, sand sheet deposit in Jackass Flat Engine Test Stand Trench.

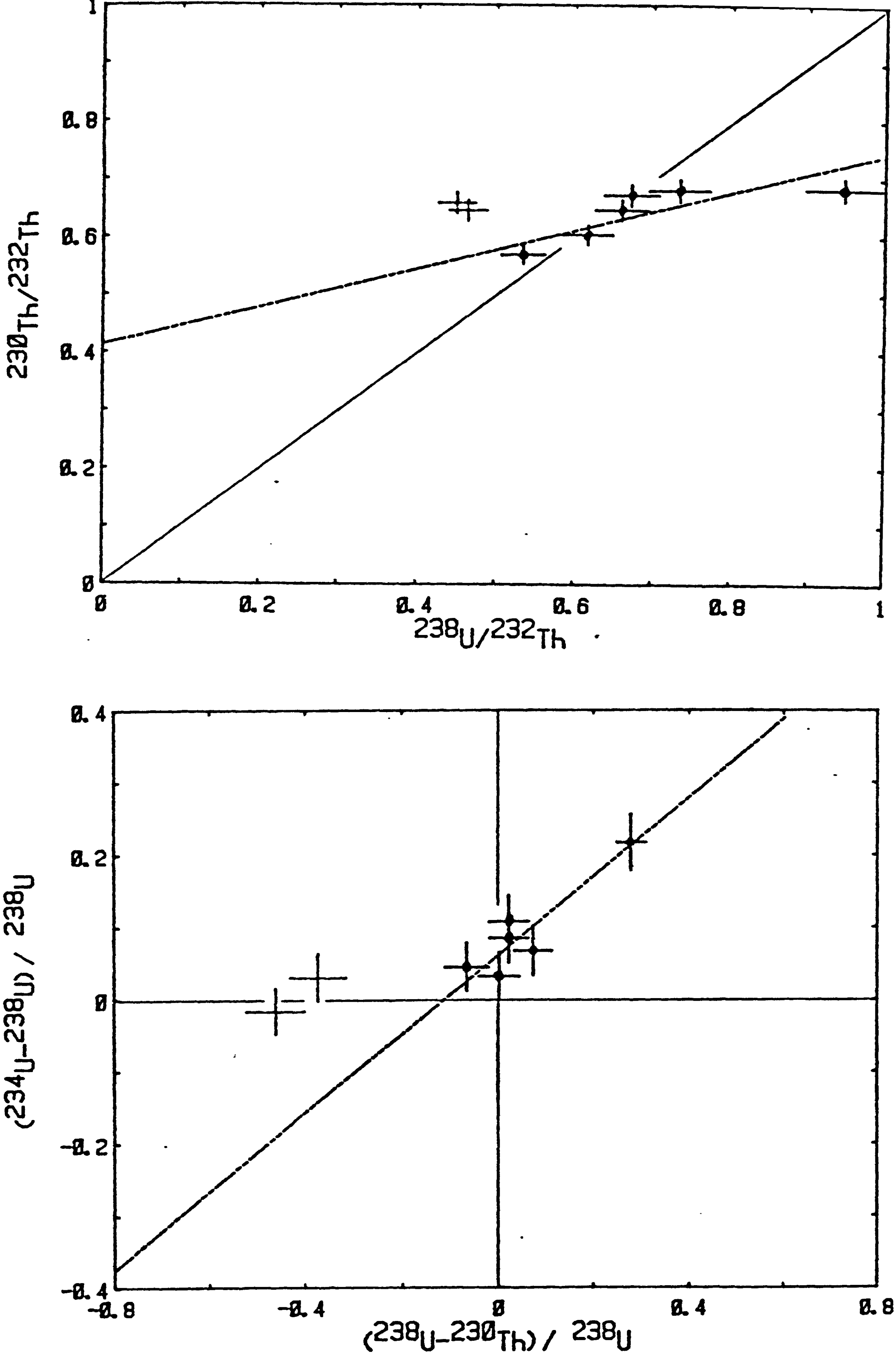

Figure 18. Plots of S9 unit, upper alluvium in Jackass Divide Trench. The upper two samples are not included in the U-trend slope because they do not fit with other samples on the thorium plot.

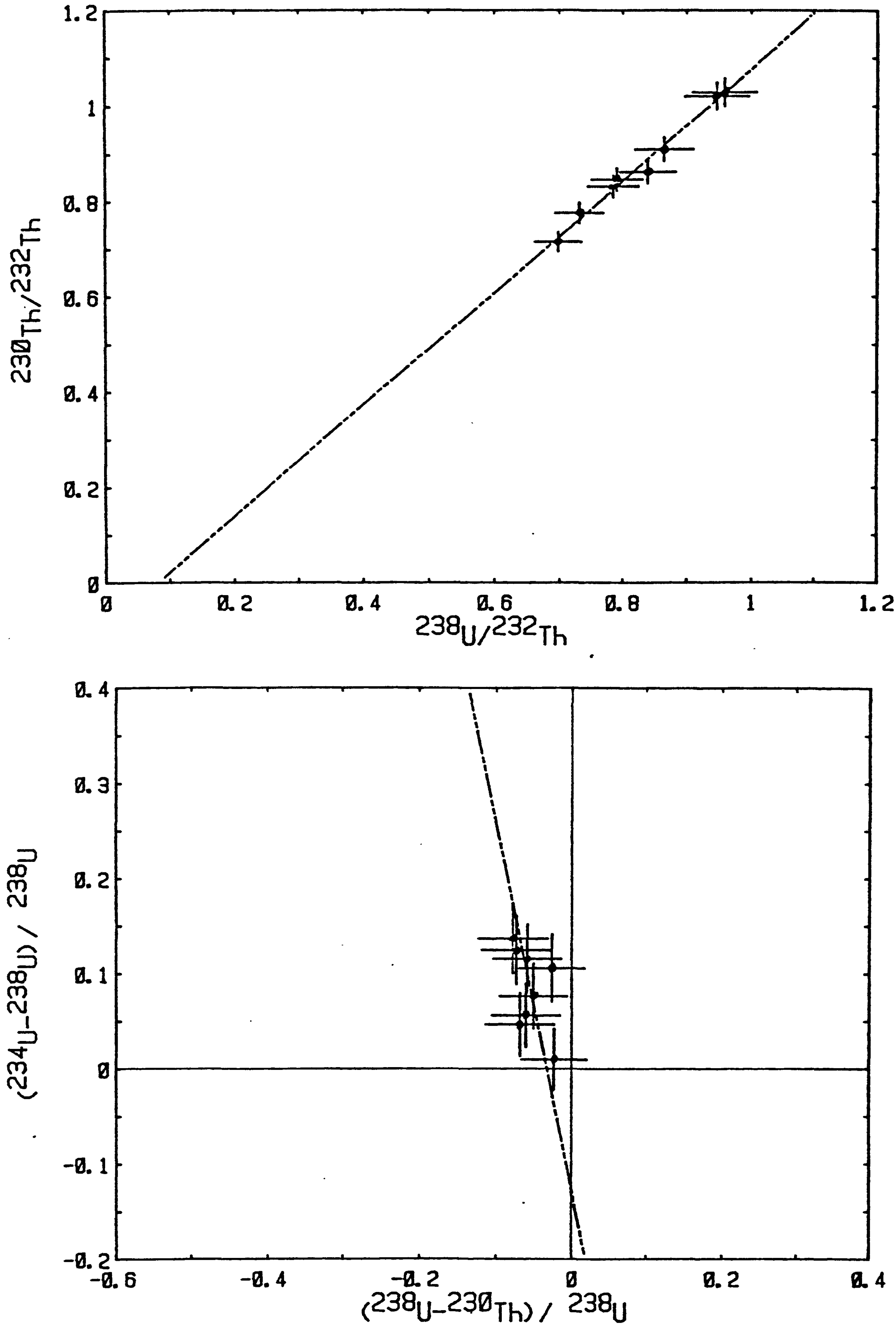

Figure 19. Plots of JD unit, lower alluvium in Jackass Divide Trench.

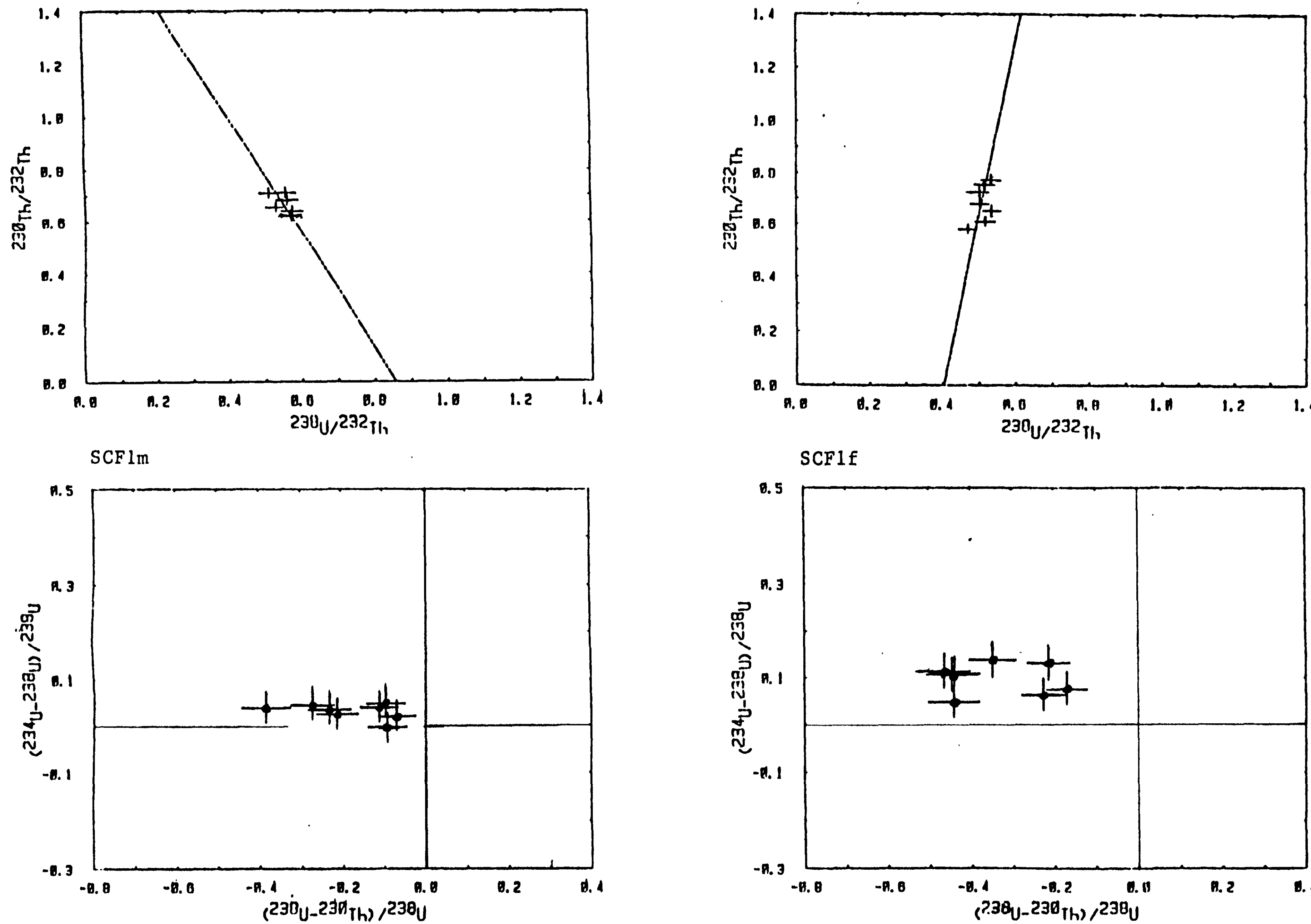

Figure 20. Plots of SCF1 unit, upper alluvium in South Crater Flat West Trench. SCF1m represents samples less than 2 mm size fraction and SCF1f represents samples less than 0.3 mm size fraction; neither fraction was datable by U-trend.

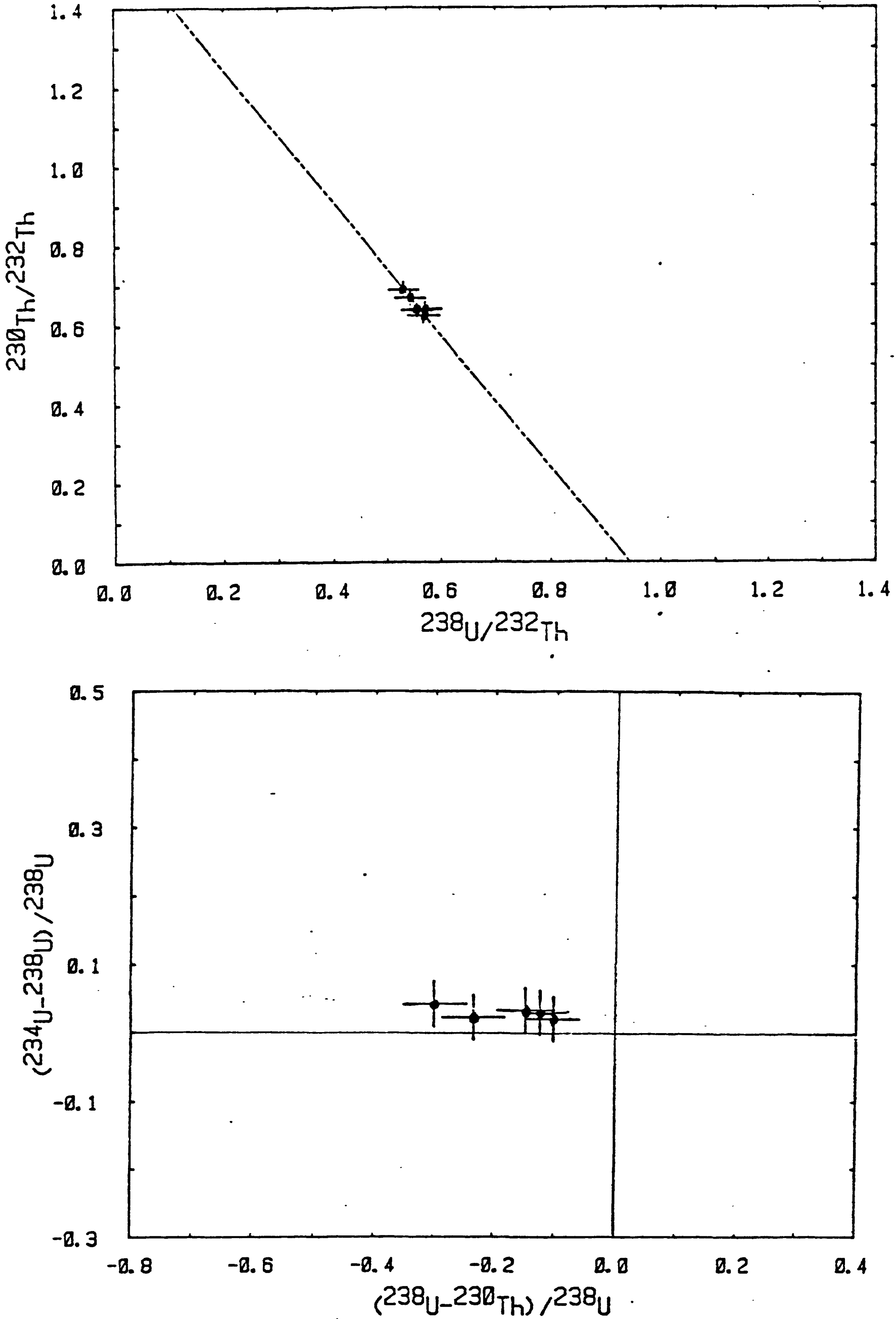

Figure 21. Plots of SCF3 unit, upper alluvium in South Crater Flat West Trench. This profile was not datable because of insufficient variation of $^{234}U/^{238}U$ ratios in 5 samples.

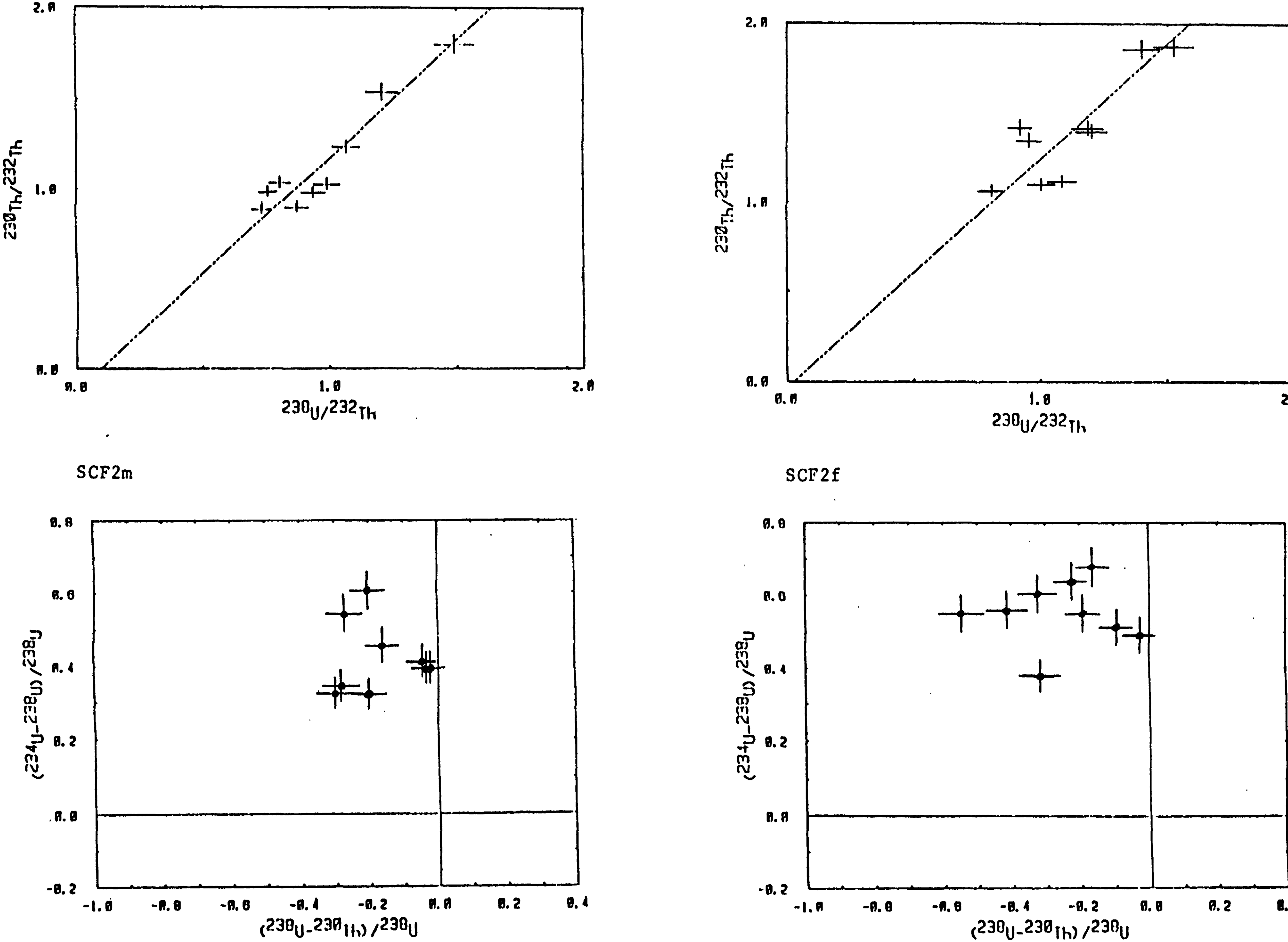

Figure 22. Plots of SCF2 unit, lower alluvium in South Crater Flat West Trench. SCF2m represents samples less than 2 mm size fraction, and SCF2f represents samples less than 0.3 mm size fraction; neither fraction was datable by U-trend.

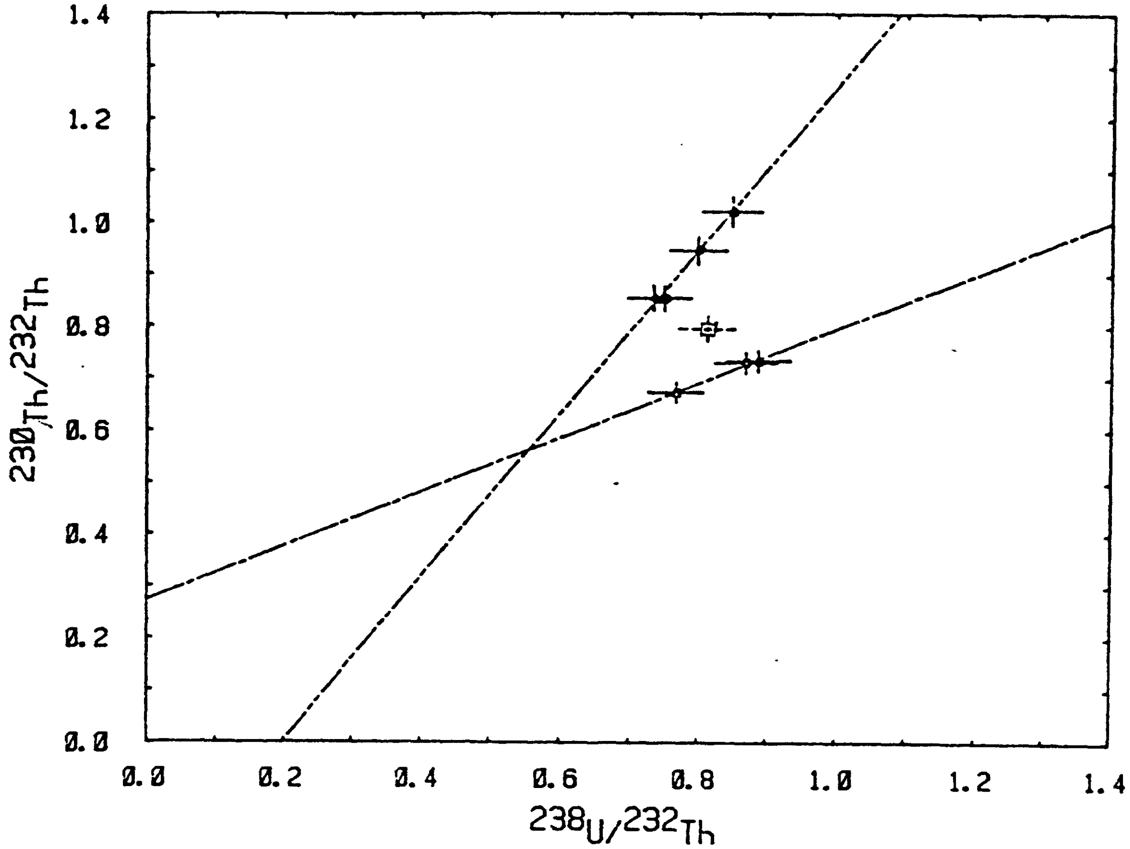

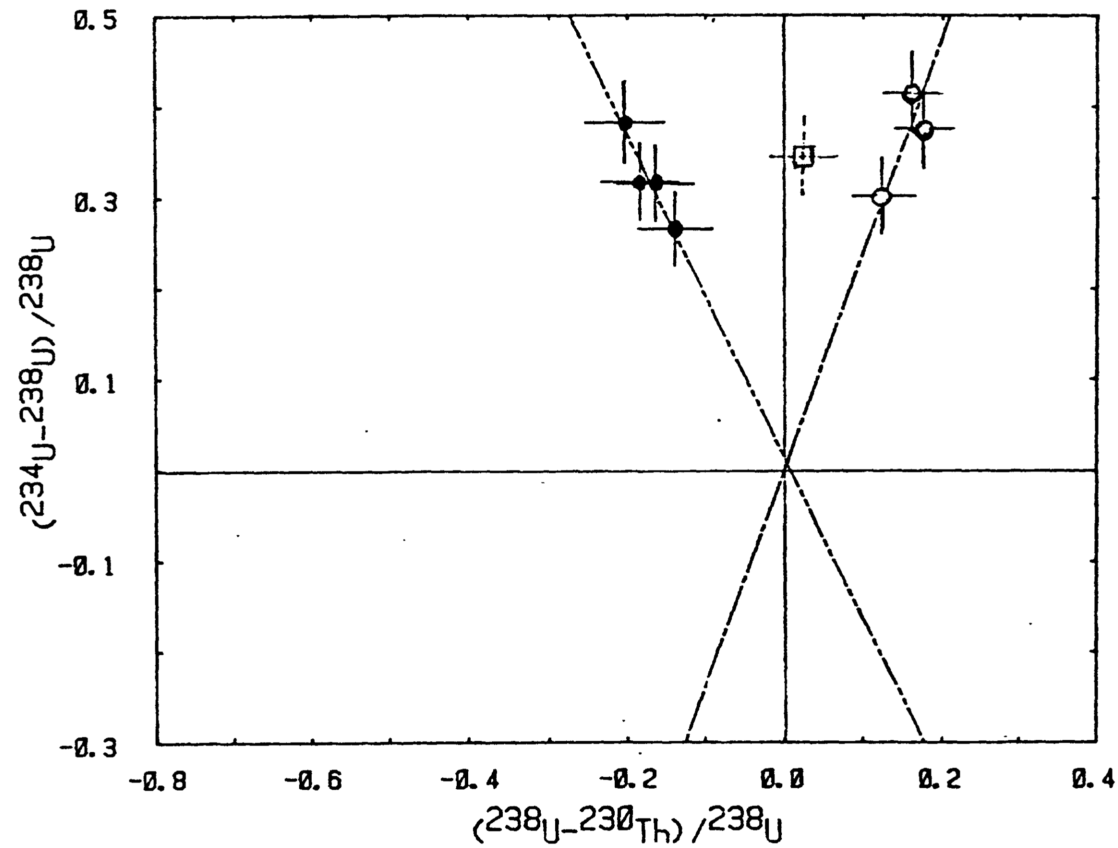

Figure 23. Plots of SCF4 section, lower alluvium in South Crater Flat West Trench. Sample SCF4-5, □, is a mixture of the upper faci s, ●, and lower facies, ○, in the unit.

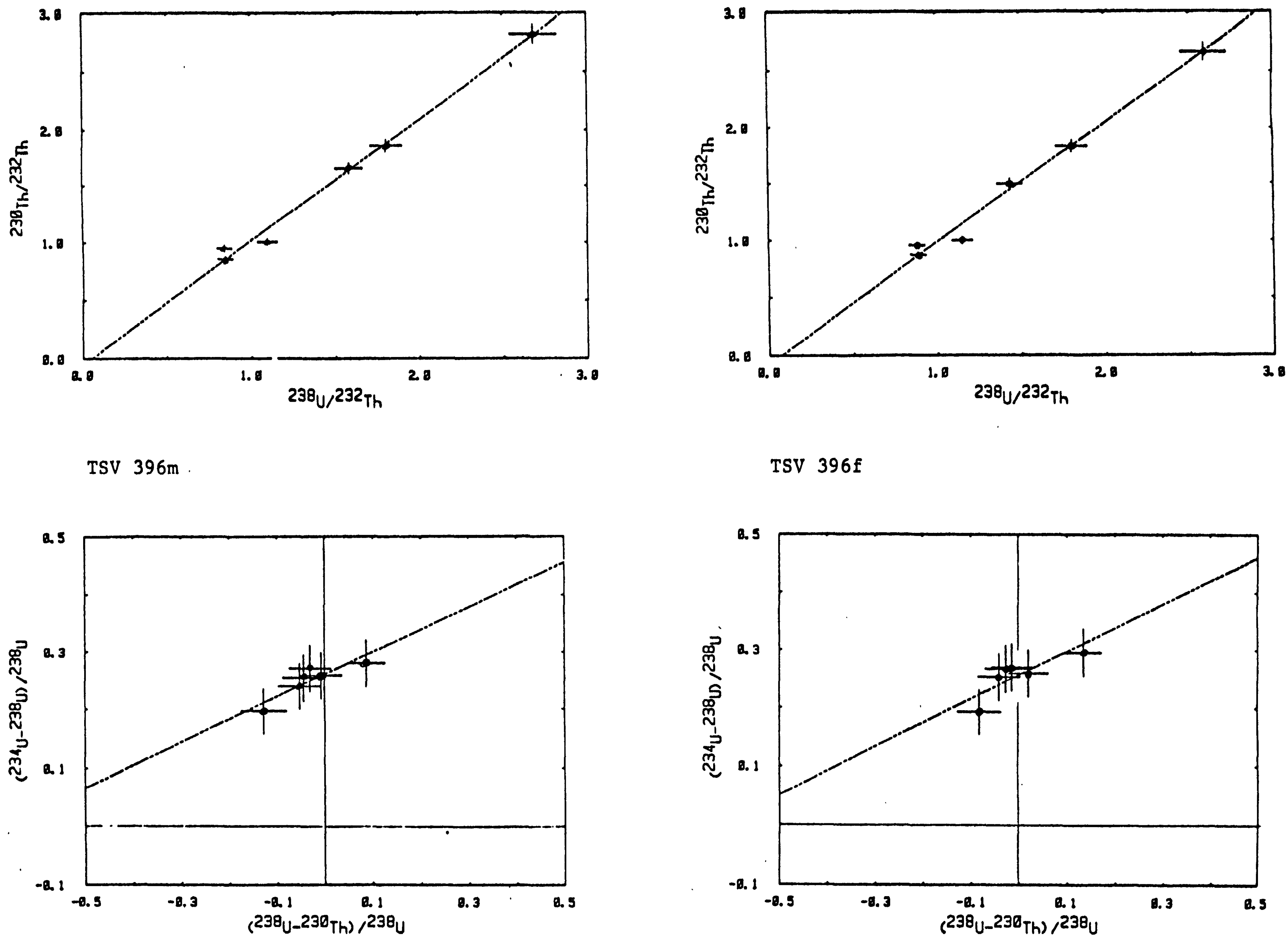

Figure 24. Plots of TSV 396 unit, carbonate-enriched zone in Crater Flat Trench 1. TSV 396m represents samples less than 2 mm size fraction, and TSV 396f represents samples less than 0.3 mm size fraction.

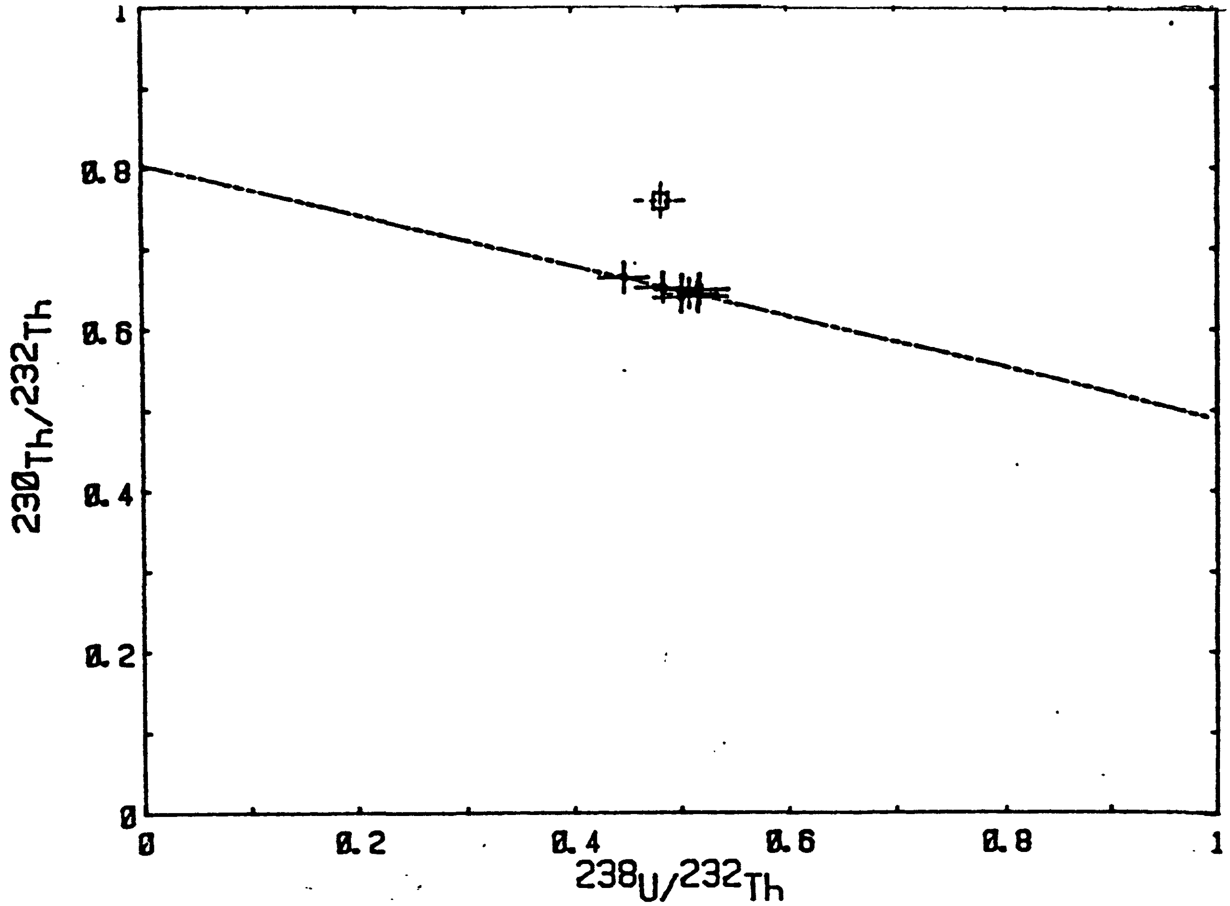

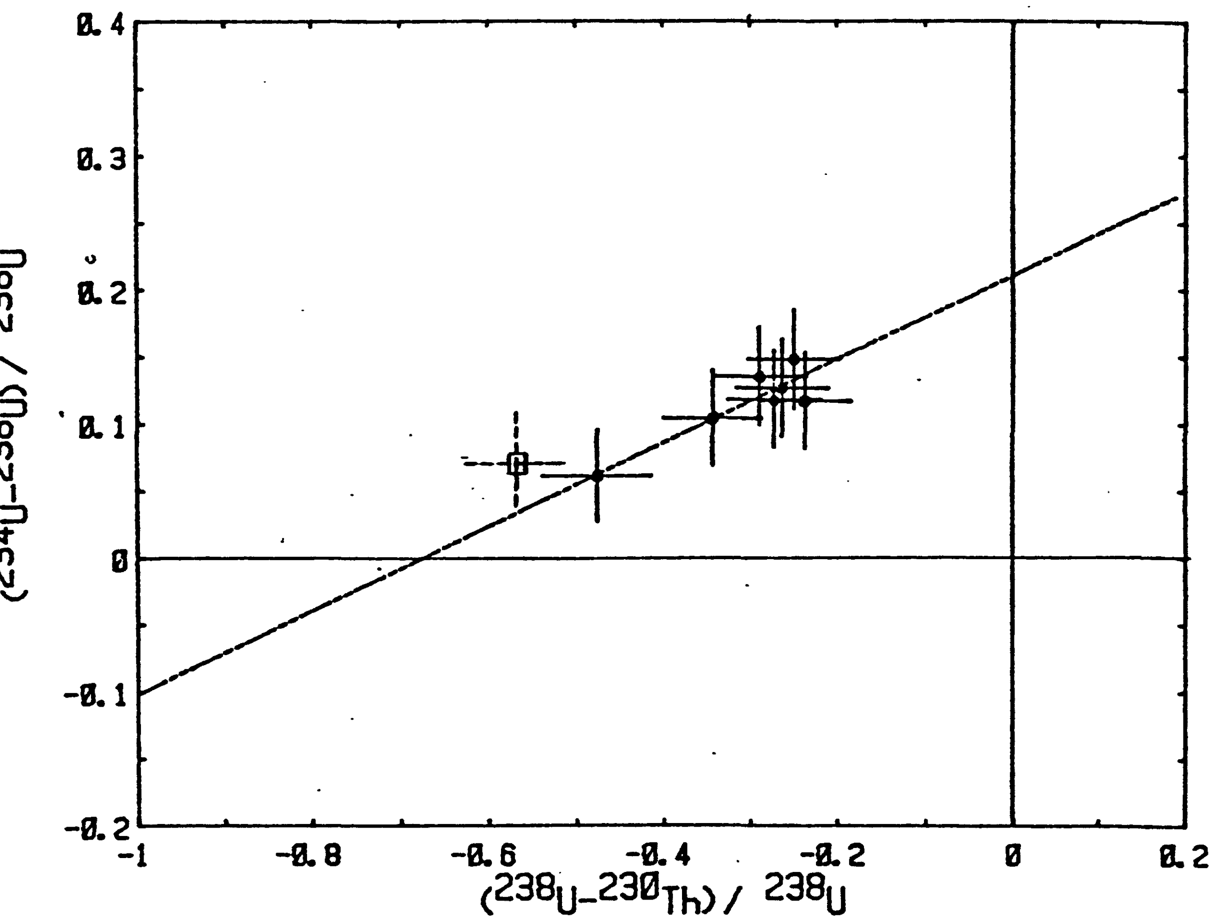

Figure 25. Plots of CF1 unit, upper alluvium in Crater Flat Trench 3. Sample CF1-2, □, is not included in U-trend slope because it does not fit on slope of the thorium plot.

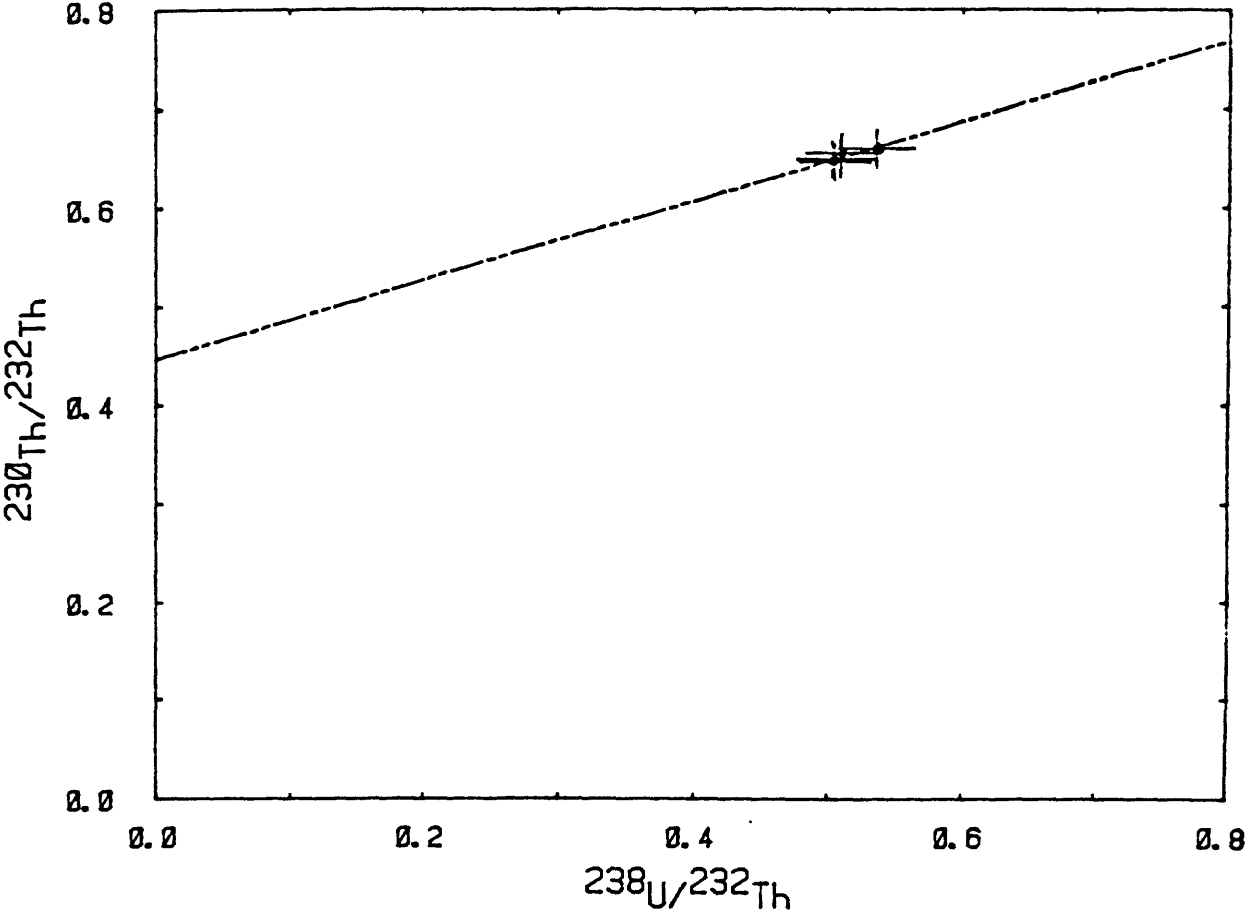

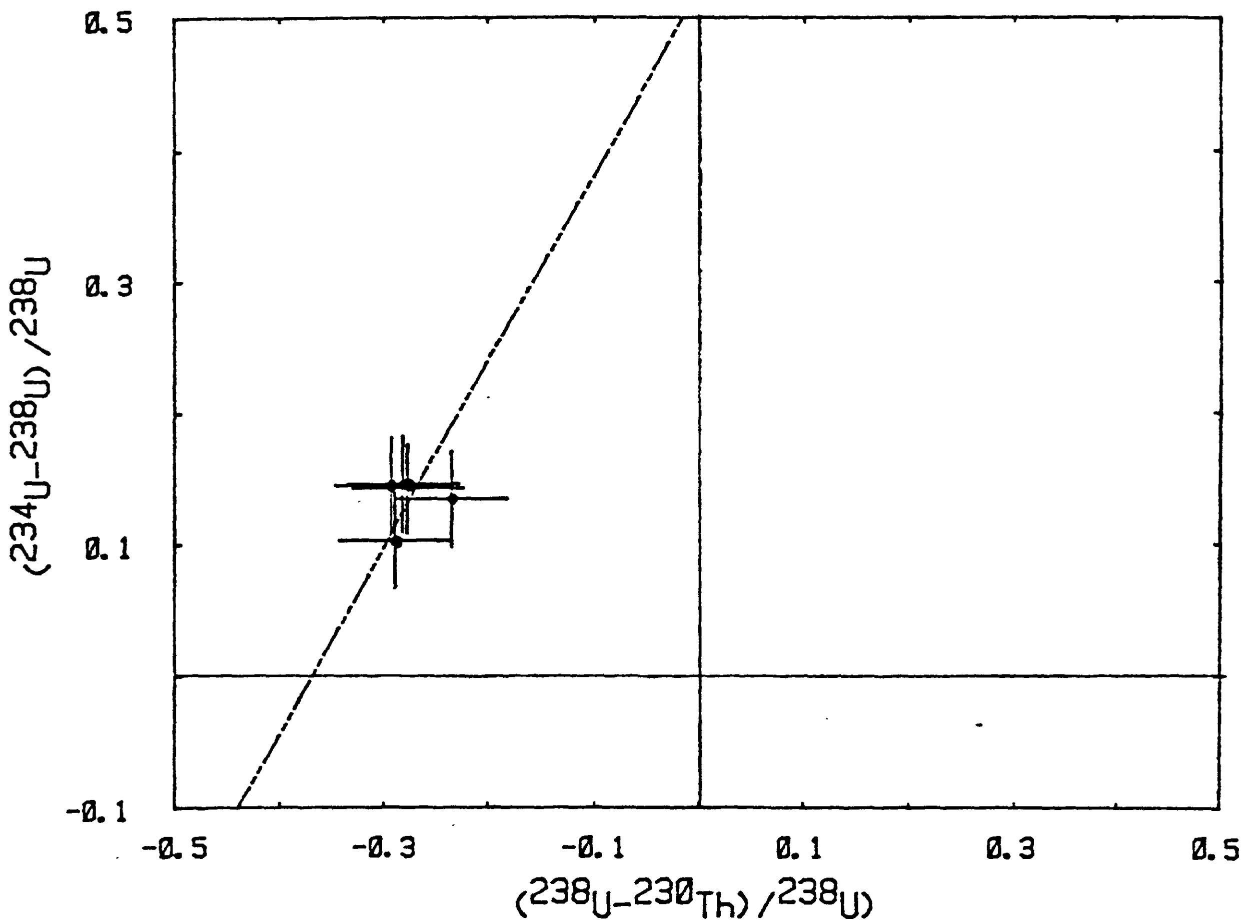

Figure 26. Plots of CF6 unit, lower B horizon exposed in Crater Flat Trench 3.

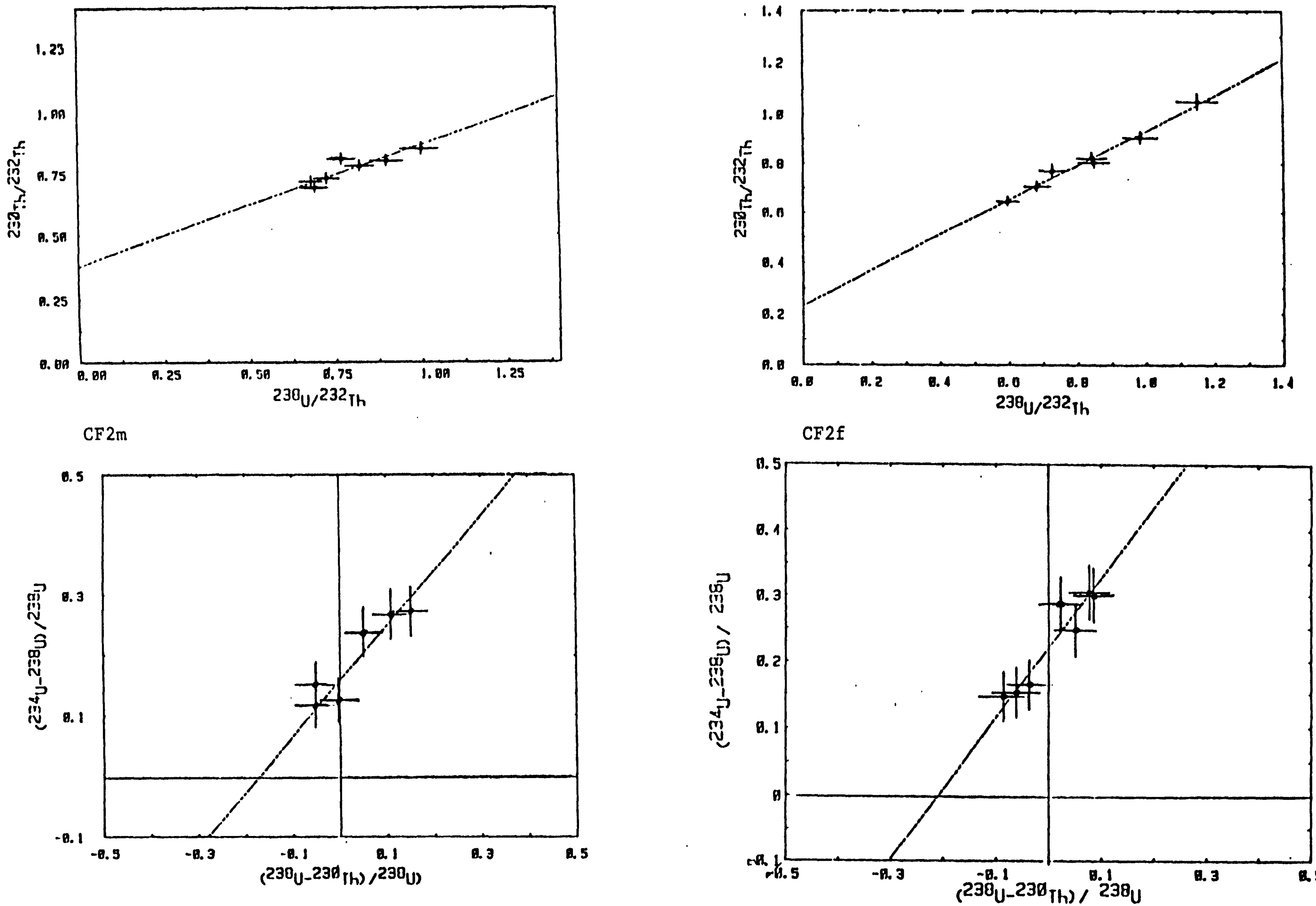

Figure 27. Plots of CF2 unit, lower alluvium in Crater Flat Trench 3. CF2m represents samples less than 2 mm size fraction and CF2f represents samples less than 0.3 mm size fraction.

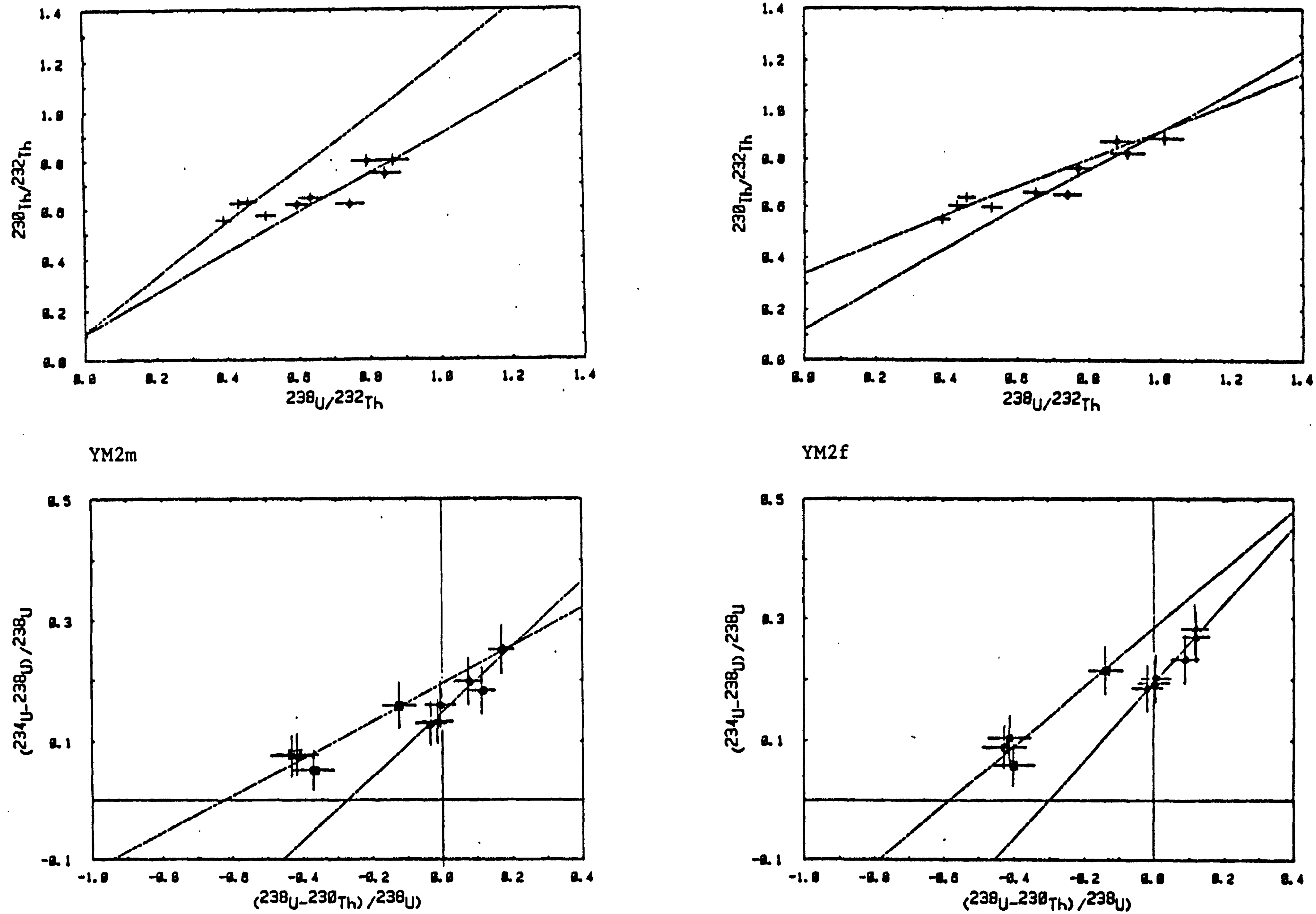

Figure 28. Plots of YM2 section, upper alluvium, □, and lower alluvium, ●, in Yucca Mountain Trench 2. YM2m represents samples less than 2 mm size fraction and YM2f represents samples less than 0.3 mm size fraction.

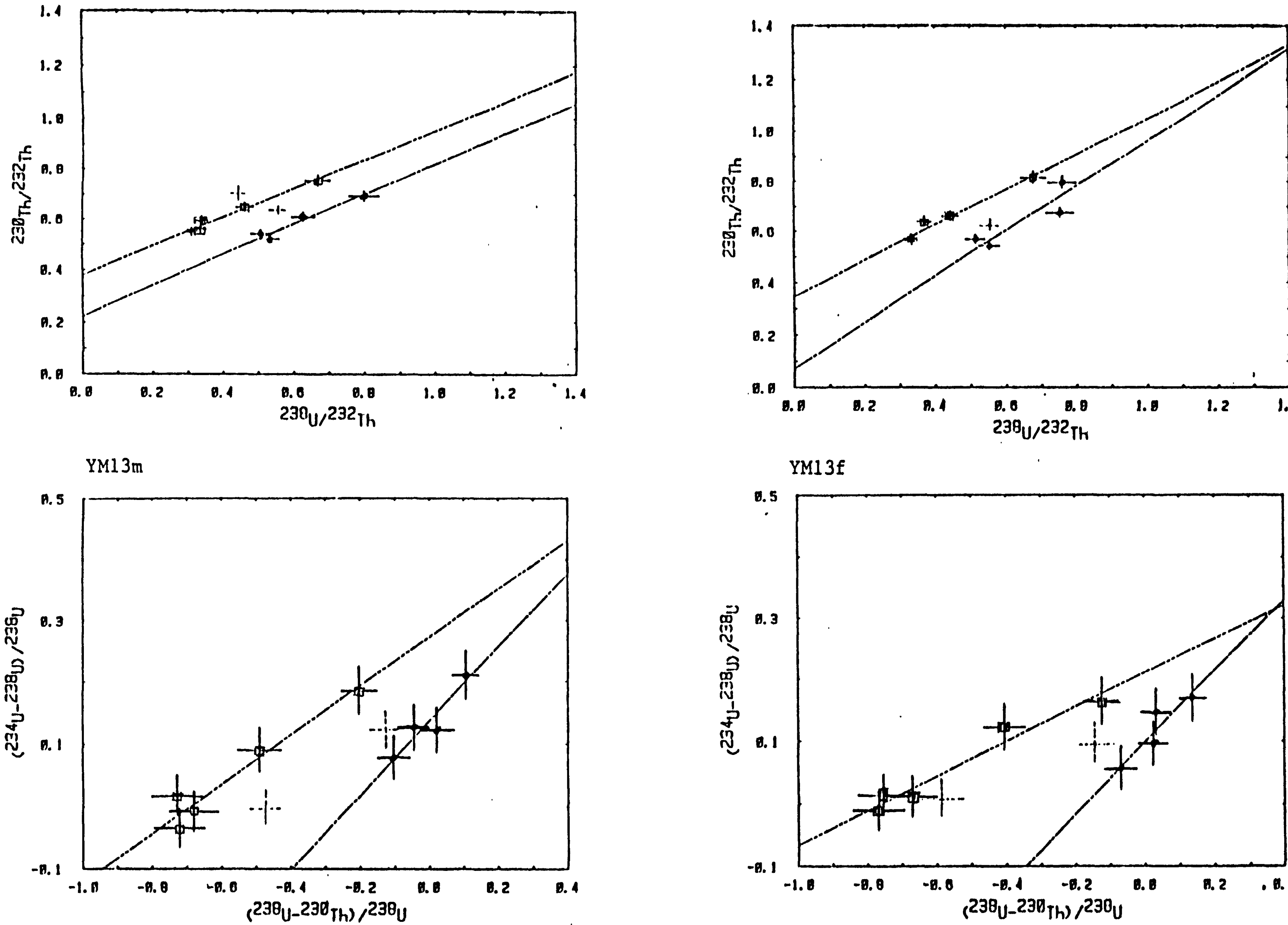

Figure 29. Plots of YM13 section, upper alluvium, □, and lower alluvium, ●, in Yucca Mountain Trench 13. Upper sample in each unit was not included in U-trend slope because of possible mixtures with material from overlying unit.

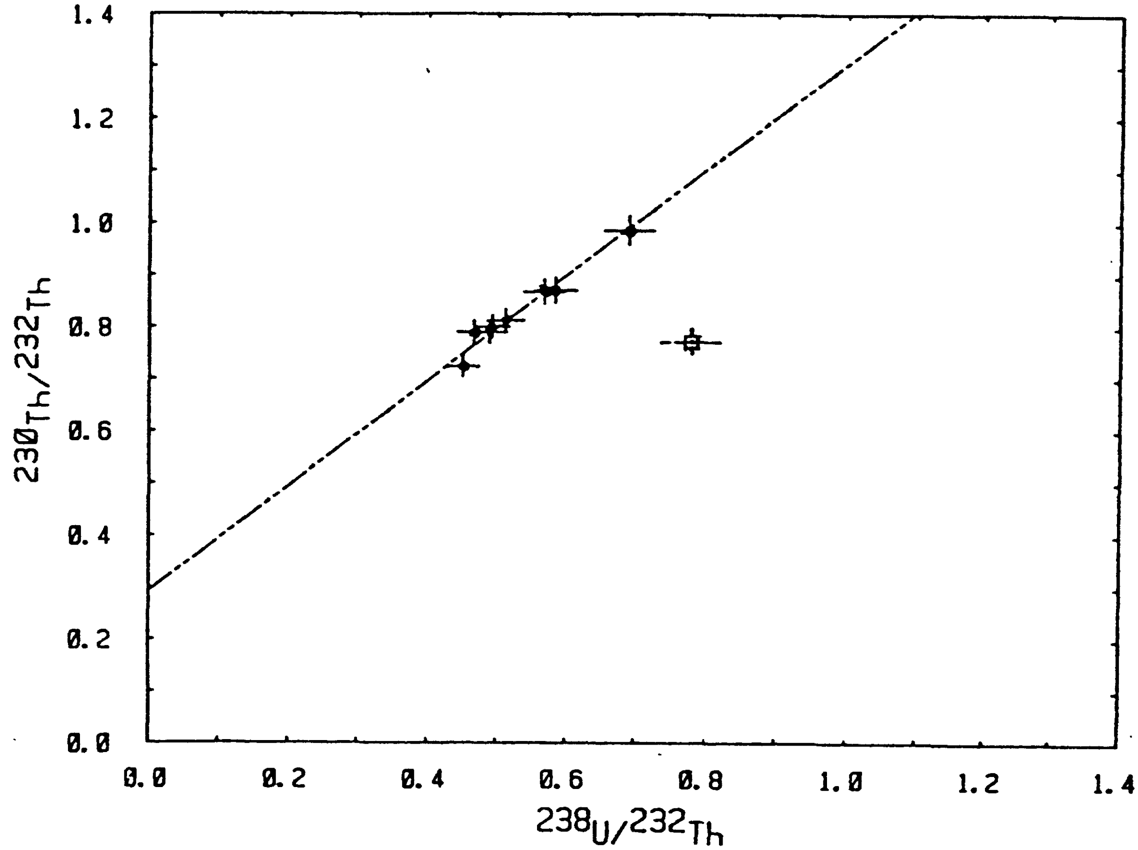

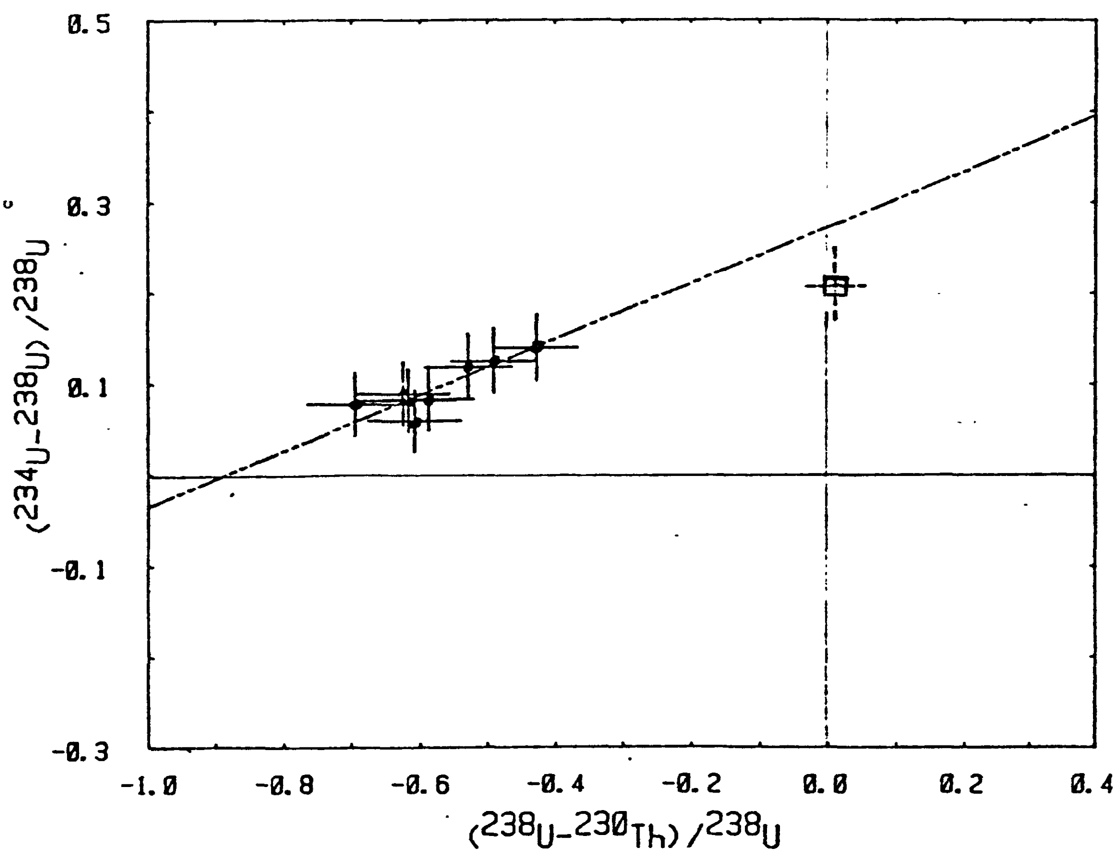

Figure 30. Plots of YM14B unit, lower B horizon exposed in Yucca Mountain Trench 14. Sample YM14B-2, □, is not included in U-trend slope because it does not fit on slope of thorium plot.

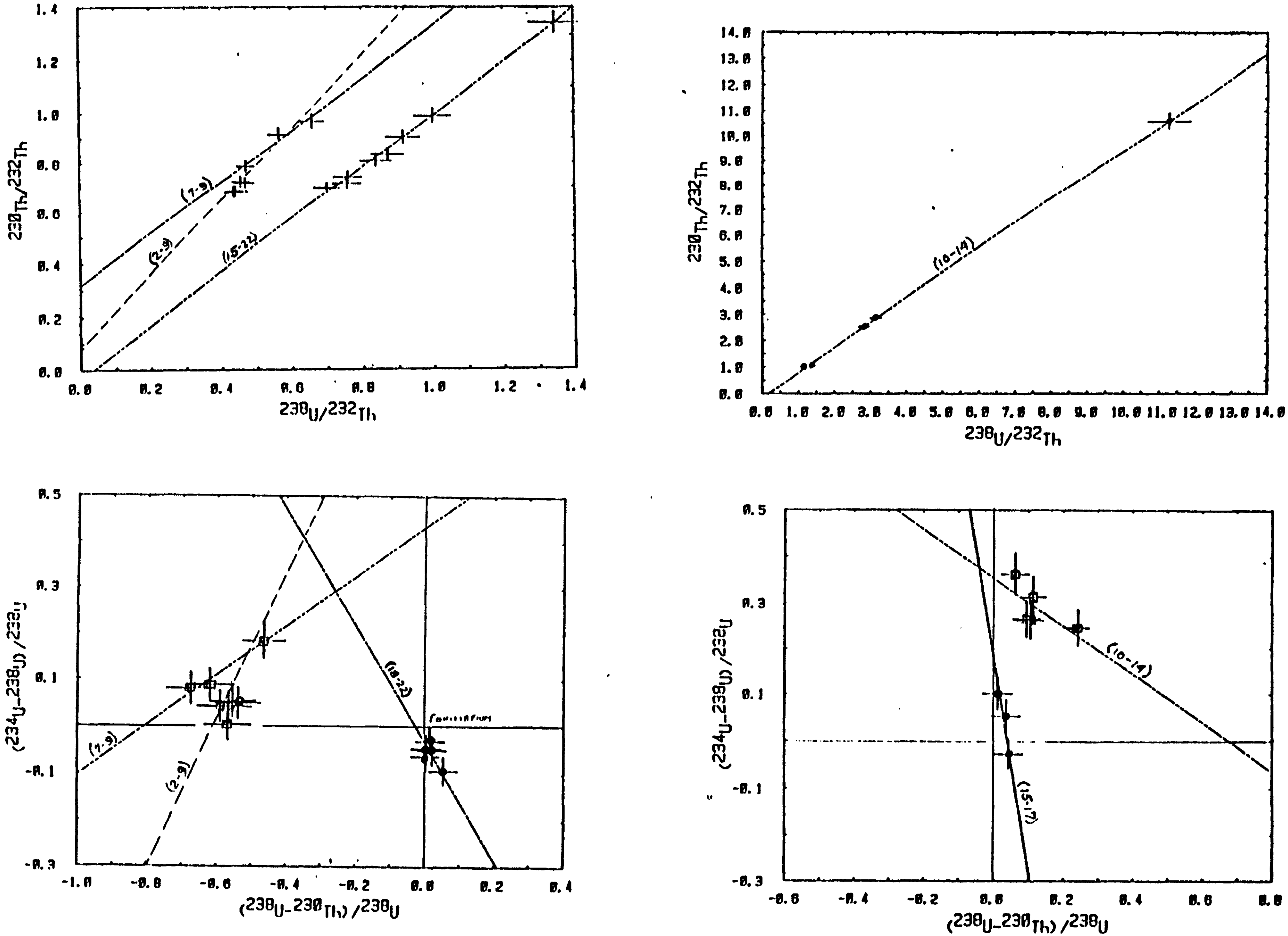

Figure 31. Plots of YM14 section, upper alluvium (2-9), laminar carbonate enriched zone (10-14), and lower alluvium (15-17) with gravel facies (18-22).

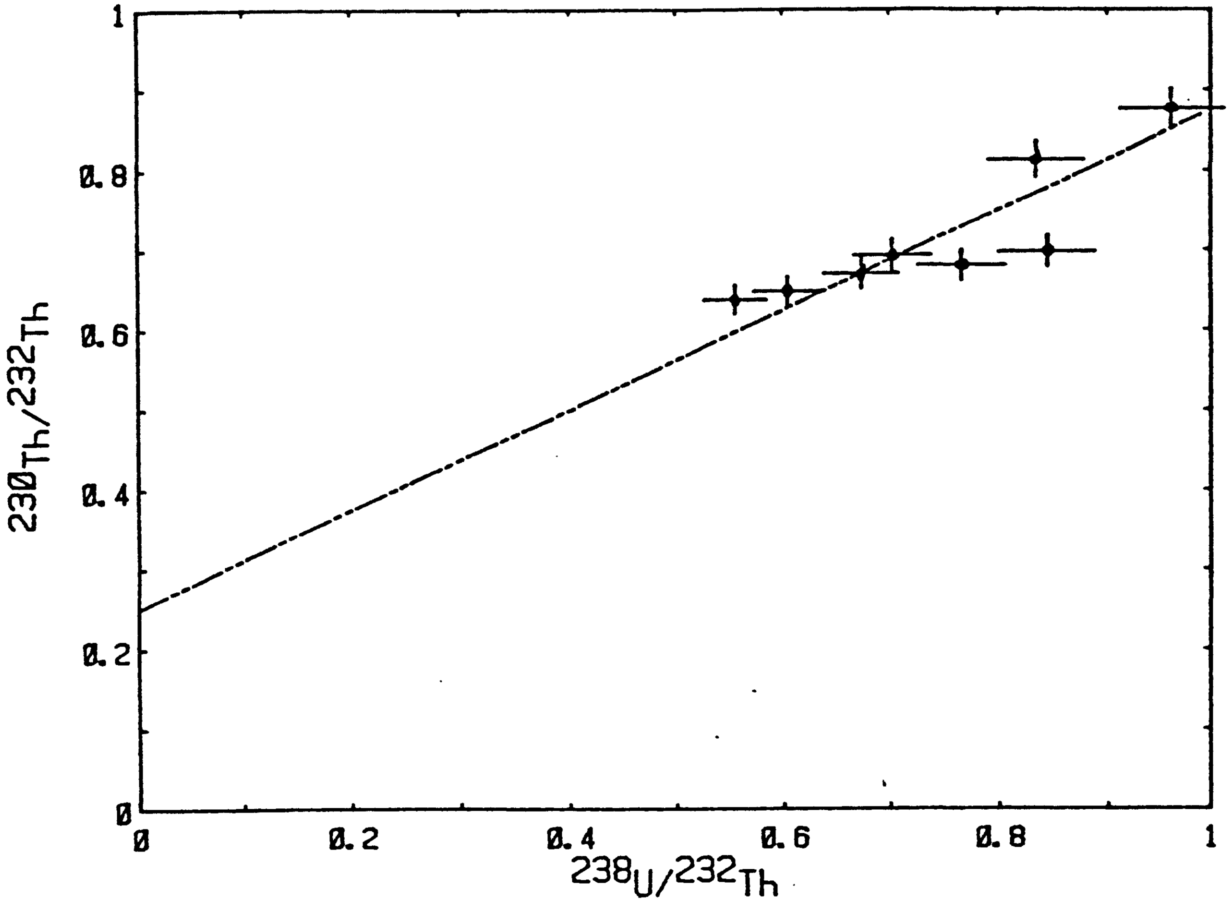

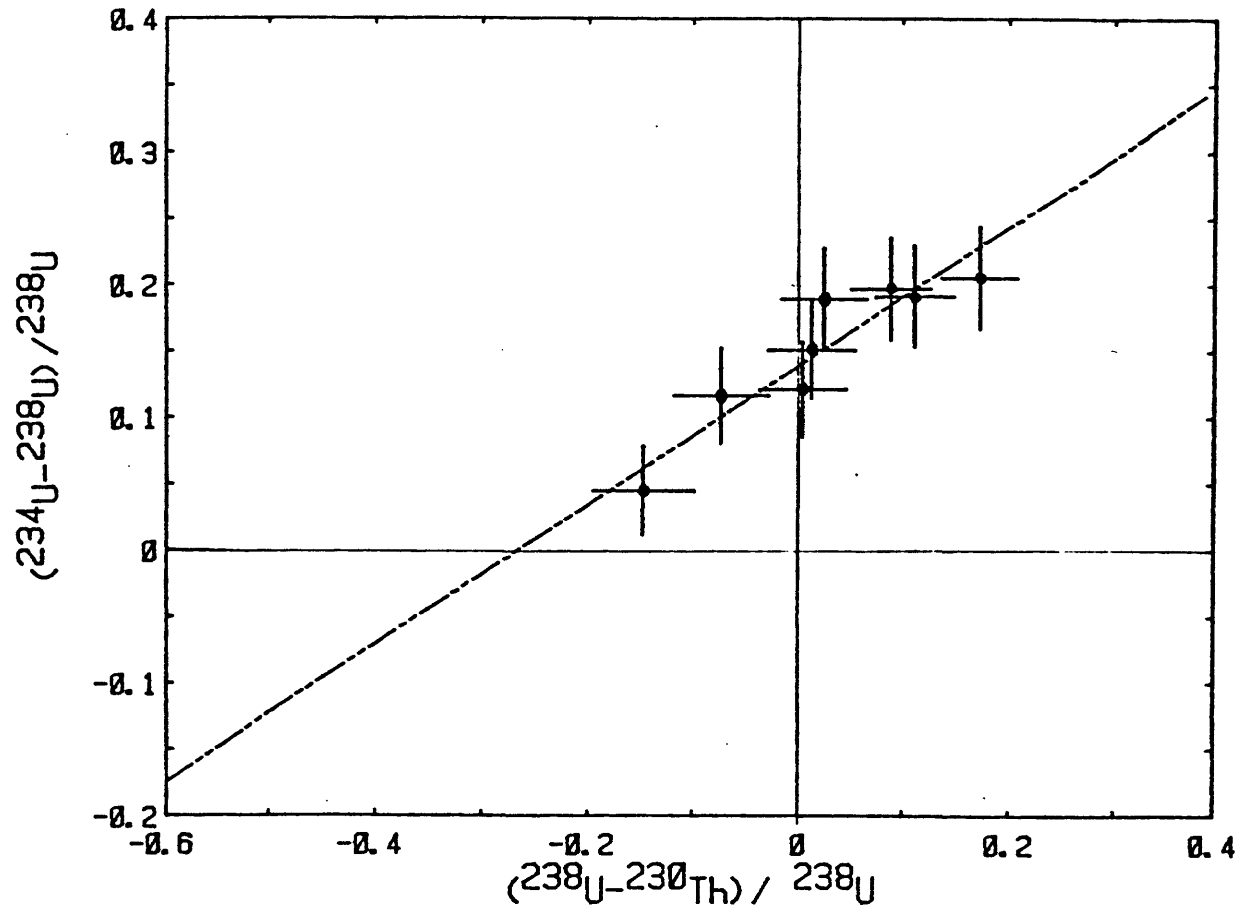

Figure 32. Plots of CBQ unit, alluvium in Charlie Brown Quarry, Shoshone, California.

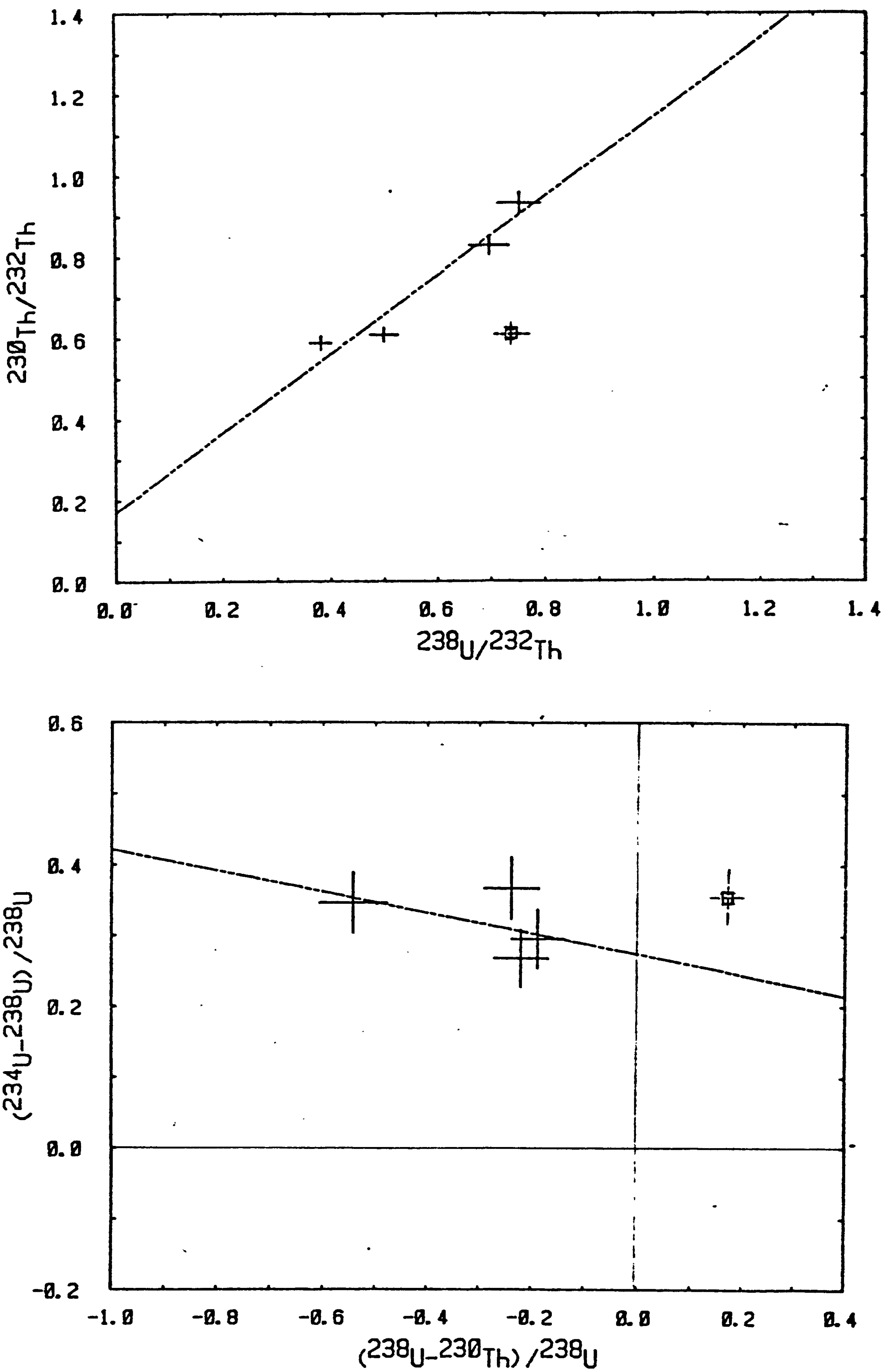

Figure 33. Plots of FHA unit, Bishop ash partially altered to clay exposed in gully at Fairbanks Hills, Nevada. Sample A-15C, □, is not included in U-trend slope because it does not fit on slope of the thorium plot.

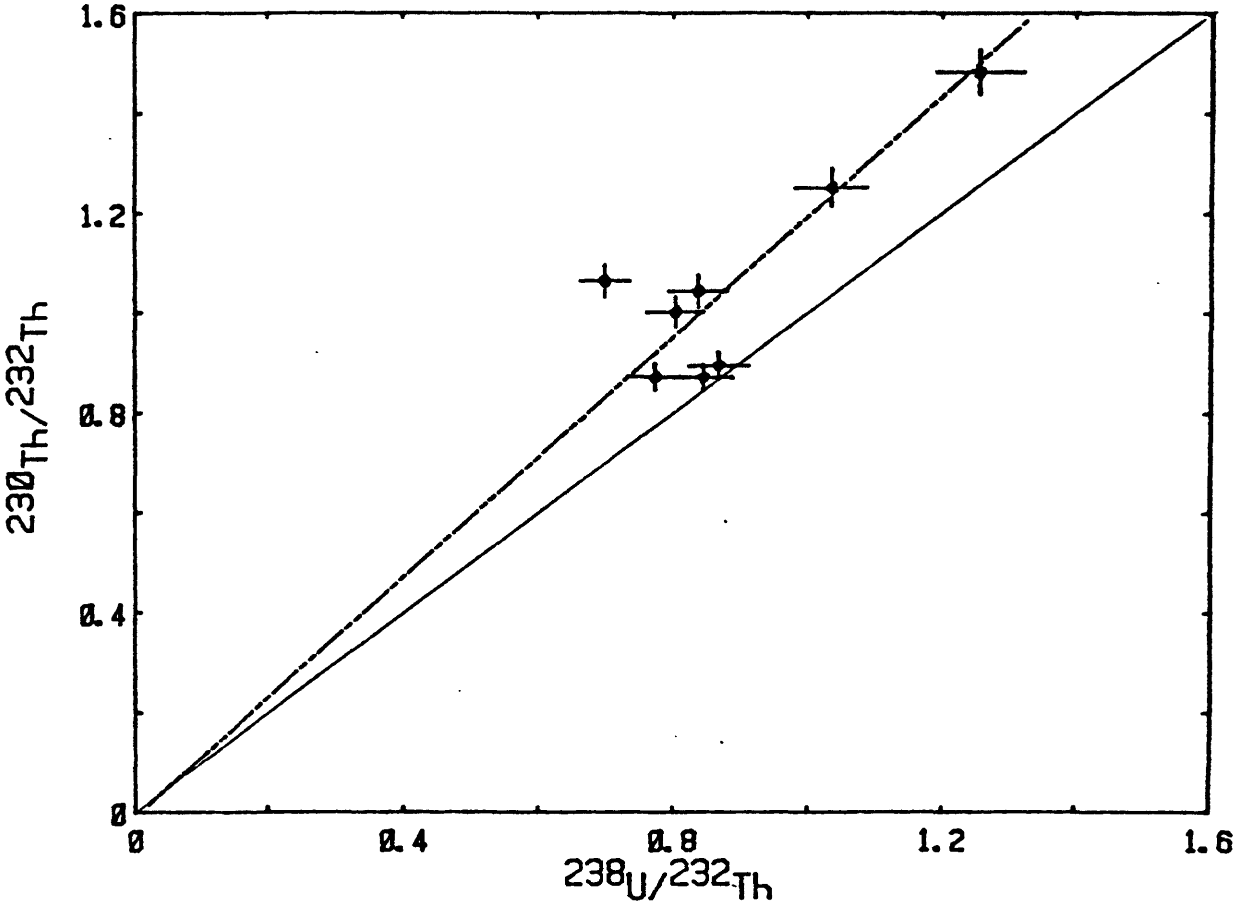

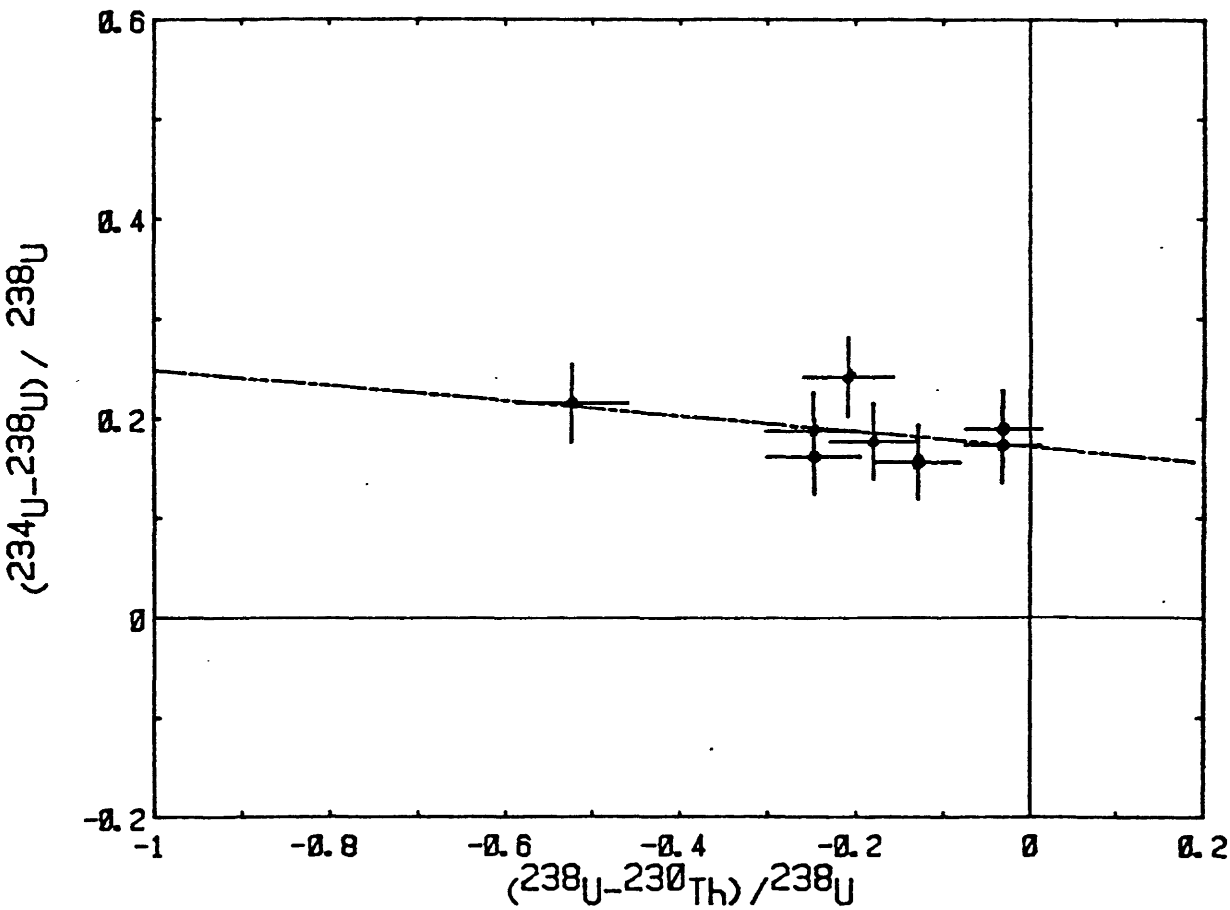

Figure 34. Plots of S3 unit, calcite-cemented alluvium in Eleana Pediment trench.

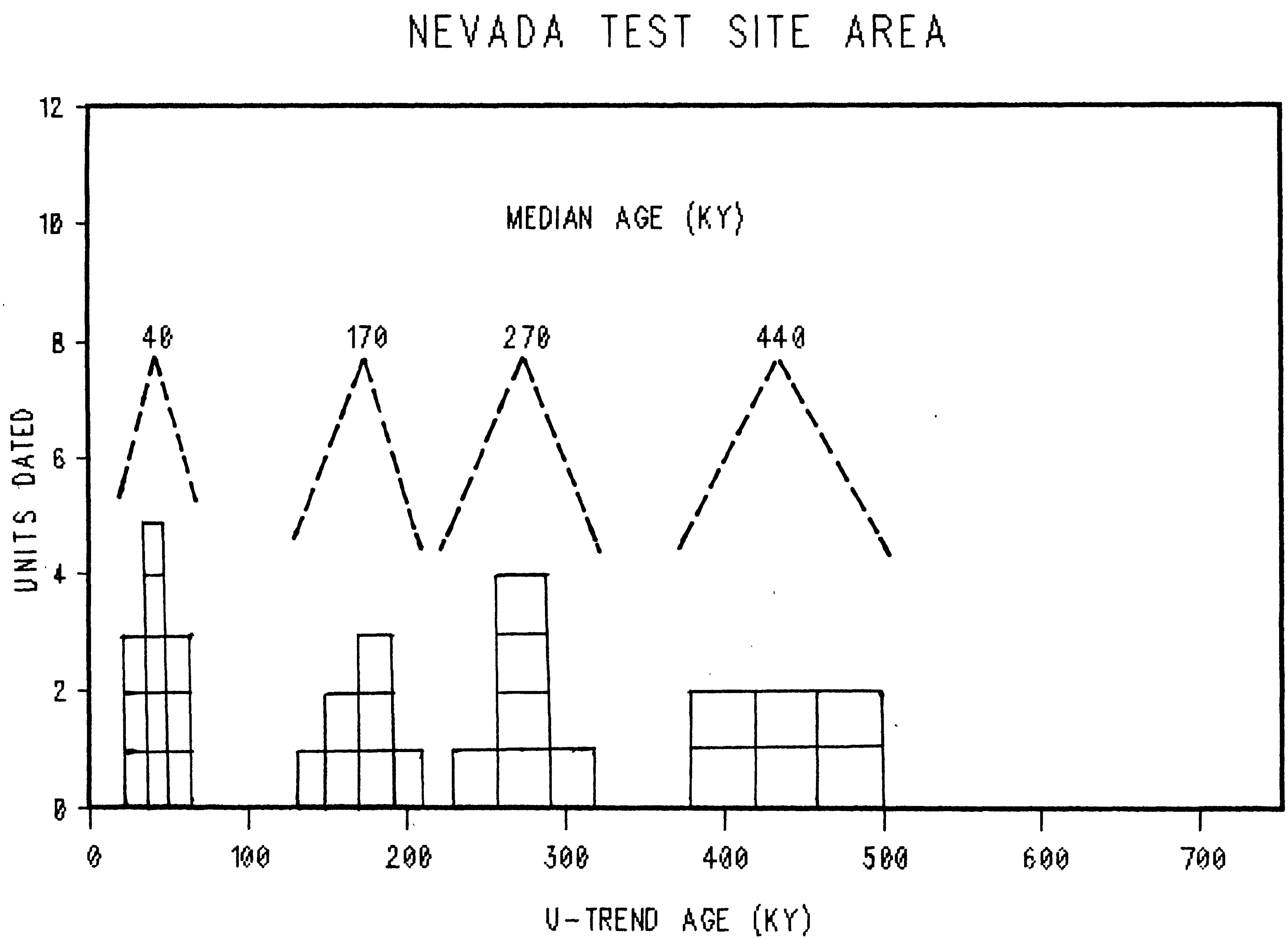

Figure 35. Histogram showing age groups of alluvial units analyzed from the Nevada Test Site area.